Oil/water separation study of dispersed oil in water using a recycled construction material in Vietnam

ベトナムにおけるリサイクル建設廃棄物を用いた水中分散油の油水分離研究

A dissertation submitted in partial fulfillment of the requirements for the degree
of

Doctor of Philosophy

in Civil and Environmental Engineering,
at

Graduate school of science and Engineering
Saitama University, Japan

by

Akihiro Matsuno
(20DE001)

Approved by
Prof. Ken Kawamoto, Academic supervisor and committee chairman
Prof. Takeshi Maki, Committee member
Assoc. Prof. Junji Yagisawa, Committee member
Assist. Prof. Kengo Nakamura, Committee member

March 2023

ACKNOWLEDGEMENT

In carrying out this research, I would like to thank Professor Ken Kawamoto of the Graduate school of science and Engineering, Saitama University, and Hanoi University of Civil Engineering. Thank you very much for his full support and advise. I thought it was a miracle that I was encouraged to continue my research without giving up even during the difficult times due to the COVID-19 crisis. Thank you very much Kawamoto sensei. I would also like to thank Prof. Takeshi Maki and Assoc. Prof. Junji Yagisawa of the Graduate school of science and Engineering Saitama University for their valuable advice.

I would also like to thank Assist. Prof. Kengo Nakamura and Previous Assist. Prof. Takeshi Saito (Now at AIST). In addition to their comments, I received encouragement for this research. Emeritus Professor Toshiko Komatsu, Saitama University, gave her knowledge on civil engineering, and their applications. Thank you for your help throughout. I would also like to thank Mr. Muhammad Junaid Zafar, of the Previous Master student of the Graduate school for helping me with various observations under severe conditions of COVID-19.

This research was carried out under the JST-JICA Science and Technology Cooperation Program for Global Issues ((No. JPMJSA1701): Representative Ken Kawamoto). We would like to express our gratitude to Dr. Nguyen Hoang Giang of Hanoi University of Civil Engineering for his cooperation.

I would also like to thank Dr. Akira Kato (Now at NIT, Tomakomai college) and other SATREPS members, and Kunihiro Kobayashi and the other members of the Soil science lab, the Graduate school of science and Engineering, Saitama University. It was a great encouragement for me to continue.

I would like to take this opportunity to express their heartfelt gratitude to all the people who have supported me in this research, including the people mentioned above. Finally, I would like to thank my family for supporting me.

TABLE OF CONTENTS

References

LIST OF TABLES

LIST OF FIGURES

Chapter 1 General introduction

1.1 Backgrounds

It is an international goal aiming for a sustainable and better world by 2030, described in the "2030 Agenda for Sustainable Development" adopted unanimously by member countries at the United Nations Summit in September 2015. It has Sustainable Development Goals (SDGs) and pledges to "leave no one behind" on earth (e.g, Sachs et al., 2022). Therefore, the SDGs are issues that not only Japan but also developing countries should actively address. Unfortunately, the current situation is that the achievement of the SDGs has yet to progress, especially in developing countries. For example, Vietnam ranks 55th out of 165 countries (Sachs et al., 2022) and needs further improvement (MONRE, 2020).

1.1.1 Oil contamination problem

One of the things that the SDGs must especially solve is the solution of water environment problems. Among them, oil and grease in water are major pollutants of the water environment. The improper discharge and treatment of oily wastewater cause significant environmental pollution of surface and groundwater, rivers and ponds, and seawater. Especially, developing countries with rapid urbanization, industrialization, and population growth face serious water pollution by oily wastewater due to the insufficient development of wastewater treatment systems, resulting in severe impacts on human health and natural ecosystems (e.g., Walker, 2017; Huynh et al., 2021; Murawski et al., 2020).

Recently, the frequency of oil spill accidents during exploration, transportation, storage, and processing has been rising (Yu et al., 2013). These massive volumes of untreated oily wastewater have become a widespread pollutant worldwide and are now a serious global environmental concern. For example, a typical mining operation produces 140,000 L of oil-contaminated water daily. The frequent oil leakages/spillages during marine transportation or oil production are a potential catastrophe to marine environments /ecology and a significant waste of valuable natural resources (Gupta et al., 2017). Therefore, developing efficient, sustainable, and cost-effective technology for treating this oily wastewater water is essential.

Figure 1 shows the typical (a) discharge of untreated oily wastewater (EPA, 2010), and Figure 2 shows the Mauritius oil spill (25th July 2020). The spilled oil in Mauritius was spread over a vast area of endangered corals, affecting fish and other marine life. Some scientists have called this oil spillage Indian Ocean island's worst ecological disaster. Moreover, Figure 3 shows that in Norilsk, Russia's Arctic Circle, an oil spill accident occurred from an attached facility of a thermal power plant, and it appears to have polluted a wide area of rivers (19th May 2020). The spilled oil was light and lubricating, totaling approximately 21,000 tons. Of this, approximately 15,000 tons flowed into the Dardikan River, a tributary of the Ambarnaya River, and approximately 6,000 tons flowed into the ground. The spill caused an environmental disaster. The area contaminated by the oil spill covers approximately 350 square kilometers (AFPBB News, 2020).

Figure 1. Typical discharge of untreated oily wastewater (EPA, 2010).

Figure 2. Mauritius oil spill ((Photo sources are CNN.com, 25th July 2020).

Figure 3. In Norilsk, Russia's Arctic Circle, an oil spill accident.
(Photo sources are AFP BB NEWS, 4 June, 2020)

1.1.2 National technical regulations of oil and grease content in Vietnam

Treatment of oily wastewater is necessary all over the world, and permissible levels of oil and grease must be regulated before discharging the treated effluents into the environment. For example, the Water Pollution Prevention Act (1970) of Japan limits the maximum permissible levels of treated water discharge to 5 mg/L for mineral oil and 30 mg/L for animal and vegetable oils.

On the other hand, Table 1 shows in Vietnam, the permissible levels of surface water, groundwater, seawater, and others range between 0.05-1.0 mg/L in QCVN 08-MT:2015/BTNMT, QCVN 10: 2015/BTNMT and QCVN 38: 2011/BTNMT. And the permissible levels of animal and vegetable oils and grease in domestic wastewater and specific wastewater from industries and service sectors range between 5–30 mg/L in QCVN 14:2008/BTNMT, QCVN 40: 2011/BTNMT , QCVN 28:2010/BTNMT, QCVN 29:2010/BTNMT, QCVN 52:2013/BTNMT and QCVN 11-MT:2015/BTNMT depending on the destination of the discharge. Therefore, the oil and wastewater standards in Vietnam are the same as those in Japan.

1.1.3 Reported values of oil and grease content in water and wastewater in Vietnam.

Table 2 shows the Reported values of oil and grease content in water and wastewater in Vietnam. Among surface waters, Ha Thanh River has a very high measured value of 250 mg/L. We do not know the source of pollution in this area, but we can say that it needs to be improved. For coastal water, the maximum was 1.3 mg/L, and all values were below 1.0 mg/L. Regarding domestic wastewater, some showed high values of up to 140 mg/L. Regarding industrial wastewater, the landfill leachate shows a very high value of 3.79×10^4 mg/L, causing environmental problems.

1.1.4 Reported values of oil pollution loads and oil spills in Vietnam.

Oil leaks from crude oil exploitation. A total of 9.2×10^4 tons is estimated to flow into the coastal and marine environment. This is the high environmental impact of the oil spill, with oil pollution loads approaching 7.72×10^5 tons/year, which significantly impacts the environment and the economy. That is why total financial losses caused by a significant oil spill in 2001 were estimated at 250 billion VND (17 million USD), while costs for cleaning up polluted waters and beaches reached 60 billion VND (4 million USD). The oil pollution load of the river shows a value of 3.45×10^4 kg/day in the southern Ho Chi Minh City area. The northern Cau River basin and Cau bay basin had values of 66 tons/day and 6.34 kg/day. This is smaller than in the southern part of the country. The source of these contaminants appears to be from domestic wastewater.

Table 1. National technical regulations of oil and grease content in Vietnam.

Act name	Parameter	Environmental standards (mg/L)				Analysis method
Environmental standards: Surface water, groundwater, seawater, and others						
QCVN 08-MT:2015/BTNMT National technical regulation on surface water quality	Total oil and grease	Domestic use		Irrigation		TCVN 7875: 2008$^{5)}$ SMEWW 5520B: 2012
		A1$^{1)}$	A2$^{1)}$	B1$^{1)}$	B2$^{1)}$	
		0.3	0.5	1.0	1.0	
QCVN 10: 2015/BTNMT National technical regulation on marine water quality	Total mineral oil and grease	Area of aquaculture and conservation	Beach and water sport area		Other areas	TCVN 7875:2008$^{5)}$ SMEWW 5520B:2012 SMEWW 5520C:2012
		0.5	0.5		0.5	
QCVN 38: 2011/BTNMT National technical regulation on surface water quality for protection of aquatic lifes	Total mineral oil and grease	0.05				
Emission limits: Domestic and industrial wastewater						
QCVN 14:2008/BTNMT National technical regulation on domestic wastewater	Animal and vegetable oil and grease	A$^{2)}$		B$^{2)}$		EPA Method 1664: 2010
		10		20		

Table 1. Continued.

QCVN 40: 2011/BTNMT National technical regulation on industrial wastewater	Total mineral oil and grease	$A^{2)}$	$B^{2)}$			TCVN 7875: $2008^{5)}$
		5	10			
Emission limits: Specific wastewater from industries and service sectors						
QCVN 14:2008/BTNMT National technical regulation on domestic wastewater	Animal and vegetable oil and grease	$A^{3)}$	$B^{3)}$			EPA Method 1664: $2010^{5)}$
		10	20			
QCVN 29:2010/BTNMT National technical regulation on the effluent of petroleum terminal and stations	Mineral oil (Total hydrocarbon)	$A^{4)}$	$B^{4)}$			TCVN 7875: $2008^{5)}$
			Warehouse	Car wash	Stations	
		5	15	18	30	
QCVN 52:2013/BTNMT National technical regulation on wastewater of steel industry	Total mineral oil	$A^{3)}$	$B^{3)}$			TCVN 7875: $2008^{5)}$ SMEWW 5520C: 2012
		5	10			
QCVN 11-MT:2015/BTNMT National technical regulation on the effluent of aquatic products processing industry	Total animal and vegetable oil	$A^{3)}$	$B^{3)}$			TCVN 7875: $2008^{5)}$ SMEWW 5520C: 2012
		10	20			

1) A1: Good for domestic need and other purposes (A2, B1, and B2); A2: Good for domestic need with prior suitable treatment, protection of aquatic habitats, and other purposes (B1 and B2); B1: Good for irrigation and agricultural uses; B2: Others (water transport and low priority of water treatment)

2) A: Effluents reach water sources used for domestic purposes; B: Effluents reach water sources used for other purposes

3) A: Effluents reach water sources used for drinking purposes; B: Effluents reach water sources used for other purposes

4) A: Effluents reach water sources used for aquaculture and aquatic conservation; B: Effluents reach water sources used for other purposes

5) Analysis methods with equivalent or higher accuracy than those of the listed standards can be accepted. N/D: Not detected

Table 2. Reported values of oil and grease content in water and wastewater in Vietnam.

Location	Province/ Prefecture or City	Year	Oil and grease (mg/L)	Remarks	Reference
Surface water					
Cau River	Thai Nguyen / Thai Nguyen	2004 2005	0.02－0.12 0.02－0.16	6 monitoring points	MONRE, WB and DANIDA (2006)
Dong Nai River	Hoa An / Cao Bang Cat Lai / HCMC	2000－2006	0.025－0.029	Monitoring points from Hoa An water pumping station to Cat Lai station	
Saigon River	Binh Phuoc / Binh Phuoc Phu Cuong / Binh Duong Phu An / Binh Duong	2000－2006	0.025－0.12 0.025－0.056 0.025－0.094		
Saigon-Nha Be River	Thu Dau Mot / Binh Duong Nha Be / HCMC		0.0－0.3	5 monitoring points from upstream (Thu Dau Mot) to downstream (Binh Khan ferry, Nha Be)	IGES (2007)
Ha Thanh River	Quy Nhon / Binh Dinh	2016	250	Doi bridge at Ha Thanh Bridge	Binh Dinh PPC (2016)
Canal			27, 120	A canal at Phu Hoa	
Channel (1)			40, 85	A channel at bridge construction area	
Channel (2)	Tuy Phuoc / Binh Dinh		123	An irrigation channel behind Long My waste landfill	
Ditch	Quy Nhon / Binh Dinh	2019	15	An upstream ditch of Bau Sen Lake	Nguyen et al., (2020)
Coastal water					
Red River Delta , South central coastal, Mekong River Delta		1996-2001	> 0.05－2.4, 0.13－1.12 0.18－1.29		MONRE, WB and DANIDA (2003)
Coastal zone (1)	Rach Gia / Kien Giang: Dry season Wet season	1997－2015	0.12－0.79 0.19－0.68	Rach Gia monitoring station	Le and Pham (2017)

Table 2. Continued.

Coastal zone (2)	Nha Trang / Khanh Hoa	2013−2017	0.35−0.55	Nha Trang monitoring station	Pham (2018)
Coastal zone (3)	Khanh Hoa:, Trung binh Cuc tieu, Cuc dai, So mau	2010−2018	0.35−0.50, 0.27−0.40 0.43−0.65, 0.006−0.007	4 monitoring stations	Pham (2019)
Coastal zones	Hue / Thua Thien Hue Tho Quang / Da Nang Dung Quat / Quang Ngai Ha Long / Quang Ninh	2011−2015	0.15−0.28 1.2−1.3 0.3−0.4 0.012−0.826	Total of 16 monitoring stations data are given. Ha Long: Bai Chay Bridge	MONRE (2015)
Domestic wastewater					
Wastewater (1)	Quy Nhon / Binh Dinh	2016	86	Nearby Dam market area	Binh Dinh PPC (2016)
Influent of WWTP (1)			140, 160	Nhon Binh WWTP	
Effluent of WWTP (1)			0.8, 10.5		
Influent of WWTP (2)			4.2	Bau Luc WWTP	
Effluent of WWTP (2)			0.8		
Influent of WTF	Hai Ba Trung / Hanoi	2016	14.6	WTF for condominium in Hanoi	JICA (2019)
Effluent of WTF			2.0		
Industrial wastewater					
Landfill leachate Land fill leachate (after treatment)	Tuy Phuoc / Binh Dinh	2016	3.79×10^4	Long My waste landfill	Binh Dinh PPC (2016)
Wastewater from construction site	Quy Nhon / Binh Dinh	2016	200	Cleaning and washing of equipment and materials at a bridge construction site	

Table 3. Reported values of oil pollution loads and oil spills in Vietnam.

Location	Year	Type and sources	Oil pollution loads / Oil spills	Descriptions and other remarks	Reference
East sea	1995−2002	Oil spills	Approx. 7.72×10^5 tons / year	Oil leaks from crude oil exploitation. A total of 9.2×10^4 tons is estimated to flow into the coastal and marine environment. Total financial losses caused by a major oil spill in 2001 were estimated at 250 billion VND (17 million USD) while costs for cleaning up polluted waters and beaches reached 60 billion VND (4 million USD).	ADB (2006); MONRE, WB and DANIDA (2006)
Dong Nai River basin	2004	Domestic wastewater: HCMC 5 provinces	 3.45×10^4 kg/day $90-4.1\times10^3$ kg/day		MONRE, WB and DANIDA (2003)
Cau River basin	2005	Domestic wastewater from 6 provinces	66 tons/day		
Cau Bay River basin	2013	48 enterprises at Long Bien District, Hanoi	6.34 kg/day		JICA (2013)
HCMC	2000	Industrial wastewater		Major industrial contributors are oil refining, chemical and food processing industries (20-30% of the total industrial wastewater discharges into river systems in Vietnam from HCMC)	ADB (2000)

Table 4. Some information on other pollution loads in Vietnam.

Location	Year	Type and sources	Oil pollution loads / Oil spills	Descriptions and other remarks	Reference
Craft village	2002	Tra Co cassava processing village Bao Loc silk village	BOD_5 kg/day, COD kg/day 218, 544 379, 145	Pollution loads of SS, TN, TP, CN, and NH^{4+} are also given.	MONRE, WB and DANIDA (2006)
Whole country	2003	Volume of wastewater Chemical industry Milk production Pulp production Aquatic product processing Leather production Sugar production Textile production Alcohol, wine, and soft-drink production Total	m^3/year 300×10^6 250×10^6 110×10^6 92×10^6 70×10^6 30×10^6 25×10^6 19×10^6 896×10^6		ADB, GEF, UNEP (2006); WWF (2018)
Whole country: Industrial zones	2005	Load of pollutants HCMC Dong Nai Binh Duong BR-VT	BOD_5 kg/day, COD kg/day 1.28×10^4, 2.84×10^4 6.26×10^3, 4.68×10^4 2.24×10^2, 6.51×10^2 3.66×10^2, 1.06×10^3	Pollution loads of TSS, TN, TP, and wastewater volume are also given.	MONRE, WB and DANIDA (2006)
Hanoi	2005	Wastewater discharge from industrial sectors Chemical factories Textile and dyeing Foodstuff companies Mechanical factories	m^3/day 2.45×10^4—2.65×10^4 1.45×10^4—1.72×10^4 3.87×10^3—1.6×10^4 3.73×10^3—4.50×10^3		MONRE, WB and DANIDA (2006)
Food processing villages	2005	Wastewater discharge Phu Do rice noodle Vu Hai rice noodle Ninh Hong rice noodle Tan Do wine Duong Lieu starch production	BOD_5 tons/year, COD tons/year 53, 77 15, 23 10, 15 13, 2.3×10^3 (9.3×10^2, 1.3×10^4)		MONRE (2008)

Table 4. Continued.

Red River Delta	2006	Wastewater discharge Food processing, husbandry, slaughtering Weaving, dyeing, leatherprocessing, Waste recycling, Construction material, rick mining	COD tons/year ~ 1.5×10^4 ~ 1.5×10^3 ~ 1.5×10^3 ~ 0		MONRE (2008)
Nhue-Day River	2006	Proportion of wastewater discharge Domestic Industrial Farming and husbandry Craft village	56 % 24 % 16 % 4%		MONRE, WB and DANIDA (2006)
Hanoi Hai Phong HCMC	2009	Left: Domestic wastewater Middle: Industrial wastewater Right: Hospital wastewater	BOD_5 tons/day 161, 60.8, 0.9 55.1 — 0.3 214 — 3		Hoang (2020)
Hanoi Hai Phong Da Nang HCMC	2010	Share of pollution load on the sum of domestic and industrial wastewater. Left: Domestic wastewater Right: Industrial wastewater	70 %, 30 % 75 %, 25 % 85 %, 15 % 84 %, 26 %	90 % of domestic wastewater not treated. The capacities of wastewater treatment plants in big cities only meet about 30% of the demand.	Do and Nguyen (2014)
HCMC Binh Duong Dong Nai	2010 2019	Wastewater discharge into canals from agricultural activities Domestic wastewater discharge rate and amount.	BOD_5 tons/day, COD tons/day 193, 305 56, 102 17, 26	Pollution loads of SS, TSS are also given.	VEA (2012) JICA (2019)
Whole country	2019	Domestic wastewater discharge rate and amount. Upper: Urban area Lower: Rural area	150 L/capita/day (4.66×10^6 m^3/day) 80 L/capital/day (4.85×10^6 m^3/day)	Treated wastewater by septictank.HaNoi: Blackwater=94%, Blackwater+Gray-water=6%,HaiPhong: Blackwater93%,Blackwater+Graywater=7%	JICA (2019)

1.1.5 Some information on other pollution loads in Vietnam.

Table 4 shows various information on wastewater in Vietnam, such as BOD and COD. Since there were no concentration and river flow data available for BOD and COD, it is difficult to say for sure, but it can be said that they are causing significant pollution loads. Concentrations of BOD and COD after sewage treatment were also measured at the sewage treatment plant in Hanoi in this study, and BOD = 4.0 mg/L and COD = 8.0 mg/L. When n-hexane extract (mineral oils) and the content of n-hexane extract (animal and vegetable oils) were also measured, no oil concentration was detected. Also, according to Do and Nguyen (2014), the percentage of wastewater is higher in domestic wastewater than in industrial wastewater, and it can be said that there are issues with their treatment.

1.2 Construction-Demolition Waste and Industrial by-Products in Vietnam

The construction industry plays a vibrant part in developing the country's economy and the prosperity of the people. Every infrastructure requires activities like maintenance, renovation, new construction, and demolition of structures. These activities produce massive amounts of solid waste, called construction-demolition waste (CDW), especially in urban areas of the developed and developing world. Similarly, industrial by-products (IBPs) are the substantial amounts of industrial residues generated from industrial processes that can be technically suitable and environmentally acceptable for use in different applications, particularly within the construction industry (Fernando et al., 2020). CDW accounts for a large amount of total waste generated all over the world, and the quantity and the composition of CDW vary between regions and depend on region- specific factors such as population, construction activities and materials, and traditions (Fernando et al., 2020).

Southeast Asia countries have been experiencing remarkable growth in the construction industry, and the numbers of construction and demolition projects have been increasing rapidly due to urbanization and population growth. It was reported that the construction industry contributed approximately 5% of the total value added in Southeast Asia countries; however, construction is one of the main sources of energy and natural resource consumption (Giang et al., 2021; UNSD, 2019). It was also reported that approximately 40% of input materials of the global economy are used for construction activities, and unrestrained disposal of CDW becomes a serious waste of finite natural resources (California Environmental Protection Agency, 2000; Agamuthu, 2008).

With rapid urbanization and economic growth, the generation of CDW has increased rapidly in Vietnam. Especially in large cities in Vietnam such as Hanoi, Hai Phong, Da Nang, and Ho Chi Minh City, the daily waste generation in Vietnam has reached approximately 6000 tons, in which the CDW accounts for 10–12% of total solid waste according to the Ministry of Natural Resources and Environment (MONRE, 2011). In Hanoi, it was reported that the daily CDW generation was projected to increase from 1500 in 2011 to 4000 tons in 2020 (Lockrey et al., 2016), and the annual increment in the generation of building demolition waste was estimated to be 4–5% from 2016 to 2020 (Nghiem et al., 2020). The construction industry, on the other hand, is one of major sectors of hazardous waste production in Vietnam. Nguyen (Thai, 2009) reported that the industrial hazardous waste from construction industry accounted for 23.5% of total hazardous waste, including corrosive, toxic, and combustible materials.

1.2.1 Current CDW condition in Vietnam

Currently, the generated CDW is not fully recycled in Vietnam, and a major disposal method of generated CDW is dumping at designated sites. The collected CDW is landfilled without any treatment or recycling (hereafter, the CDW dumping sites are called 'CDW landfills'). For example, approximately 40–50% of CDW generated daily is estimated to be brought to CDW landfills in Hanoi (Decision No.609/2014/QD-TTg). In addition, illegal dumping of CDW is found frequently at roadsides and drainage canals in both urban and rural areas of the city (Cham et al., 2021), creating risks to human health and the environment, including soil and groundwater contamination, air pollution, transportation obstacles (traffic accidents), degradation of the urban landscape, and economic loss (Chanakya et al., 2017; da Paz et al., 2017).

To implement better and sound CDW management, various policies and regulations that promote reuse and recycling of CDW were implemented in Vietnam (Tuan et al., 2018; Giang et al., 2020). The amended 'National Strategy for Integrated Solid Waste Management to 2025' with a vision towards 2050 (Decision No. 1216/2012/QD-TTg; Decision No.491/2018/QD-TTg) set a target of 90% for CDW collection and 60% for reuse or recycling of CDW. Circular No. 8/2017/TT-BX-D on Construction Solid Waste Management formulated legal procedures such as separation, storage, transportation, reuse, recycling, and disposal of CDW, responsibilities of stakeholders, reporting forms, and a database of CDW management of responsible agencies. To develop proper CDW management and promote reuse and recycling of CDW in Vietnam, further challenges and opportunities are highly expected (Tuan et al., 2018).

1.2.2 CDW landfill condition in Hanoi

The survey results (Giang et al., 2021) of CDW in Hanoi has been shown in Figure 4 which includes materials like "brick (7.3% and 28.9%)", "concrete (21.8% and 53.8%)", "soil, soil-like (19.6% and 21.8%)" and "metal, plastic, others (10% and 13.1%)". The most common method of CDW management is indiscriminate dumping at landfill sites which leads towards the challenges like illegal dumping, open burning, untreated disposal of hazardous waste and depletion of natural resources. This is a serious threat to natural environment and ecosystem (Giang et al., 2021). Figure 5 shows that with the rapid development of the construction industry, autoclaved aerated concrete (AAC), one of the prominent construction wastes, poses many potential disasters to the environment and society because of the leading disposal way of landfill/open dumping.

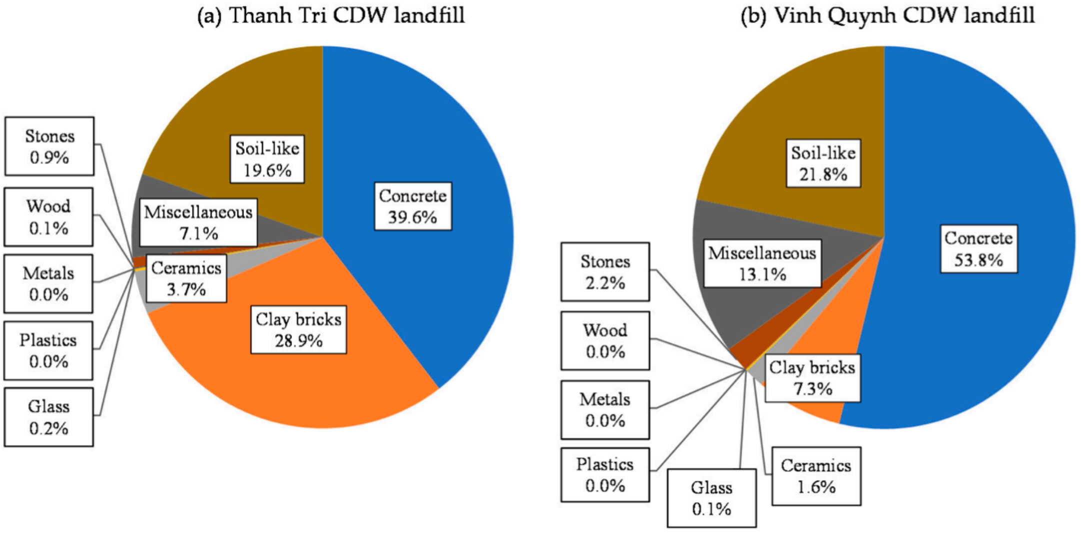

Figure 4. Waste composition of dumped CDW on dry mass basis: (a) Thanh Tri CDW landfill, (b) Vinh Quynh CDW landfill (Giang et al. 2021).

Figure 5. Pile of scrap autoclaved aerated concrete (AAC) in Vietnam.

1.3 Research motivation and applicability of Autoclaved Aerated Concrete from Vietnam (VN-AAC)

As given in Section 1.1, it was found that there are places where the oil concentration exceeds the environmental standard value in places such as rivers in Vietnam, and it is a situation that must be treated. Moreover, it turned out that those pollution sources were mainly domestic wastewater. Data from sewage treatment plants do not suggest that sewage treatment is not working but that there is too much untreated oily wastewater from households, restaurants, etc. Therefore, there is a need for a filter material for oil treatment or oil/water separation that can be used in small and medium-sized facilities.

Nowadays, many technologies such as flotation, coagulation, chemical treatment, gravity separation, biological treatment, and oil/water separation have been developed and applied to treat oily wastewater (Wang et al., 2015; Yong et al., 2018). Among of them oil/water separation technologies using hydrophobic and oleophilic membranes/meshes/grains as filtration and adsorbent materials have been intensively developed due to their high treatment performance and cost effectiveness (e.g., Pintor et al., 2016). Because the oil/water separation technologies do not need a centralized wastewater collection system and a large volume of water treatment tanks/ponds, they can be incorporated into small-scale decentralized wastewater treatment systems such as fixed-bed filtration tanks targeting domestic wastewater in rural areas (with a small number of households) and wastewater from food processing factories and craft villages (MONRE, 2008). From the viewpoint of durability and feasibility, furthermore, the filtration and/or adsorbent materials used in the oil/water separation made from easily available and environmentally sound recycled materials are desirable, particularly in Vietnam (MONRE, 2008). In addition to these, in general, oil (as well as grease) in wastewater exists as various forms such as free and floating oil, dispersed oil (emulsified by a surfactant and/or mechanically), and dissolved oil. Among them, mainly contained in sewage is dispersed oil, and these have characteristics that cannot be easily separated due to the difference in density. Therefore, these treatment is a challenge, and that's what we were aiming for this study. Besides, as given in Section 1.2, there is a problem with the disposal of construction waste in Vietnam, which must be reused. In particular, there is a need to utilize construction wastes and apply them to the treatment like oil/water separation. It is imperative to reutilize the waste scrap of AAC from Vietnam (VN-AAC) effectively and economically as a resource.

1.4 Objectives of Research

Therefore, the objects of the research are to development of an oil-water separation material that uses recycled materials such as construction waste like VN-AAC.

Among them,

- Understand oil/water separation research using grain materials from previous research.
- Use eco-friendly agents and check their effectiveness.
- Verify the physical properties of materials to understand their oil/water separation capabilities.
- Evaluation and quantification of hydrophobicity and hydrophilicity when coating is applied.
- Evaluation of the dispersed oil sorption amount of the material.

Figure 6 shows the flow of research based on these.

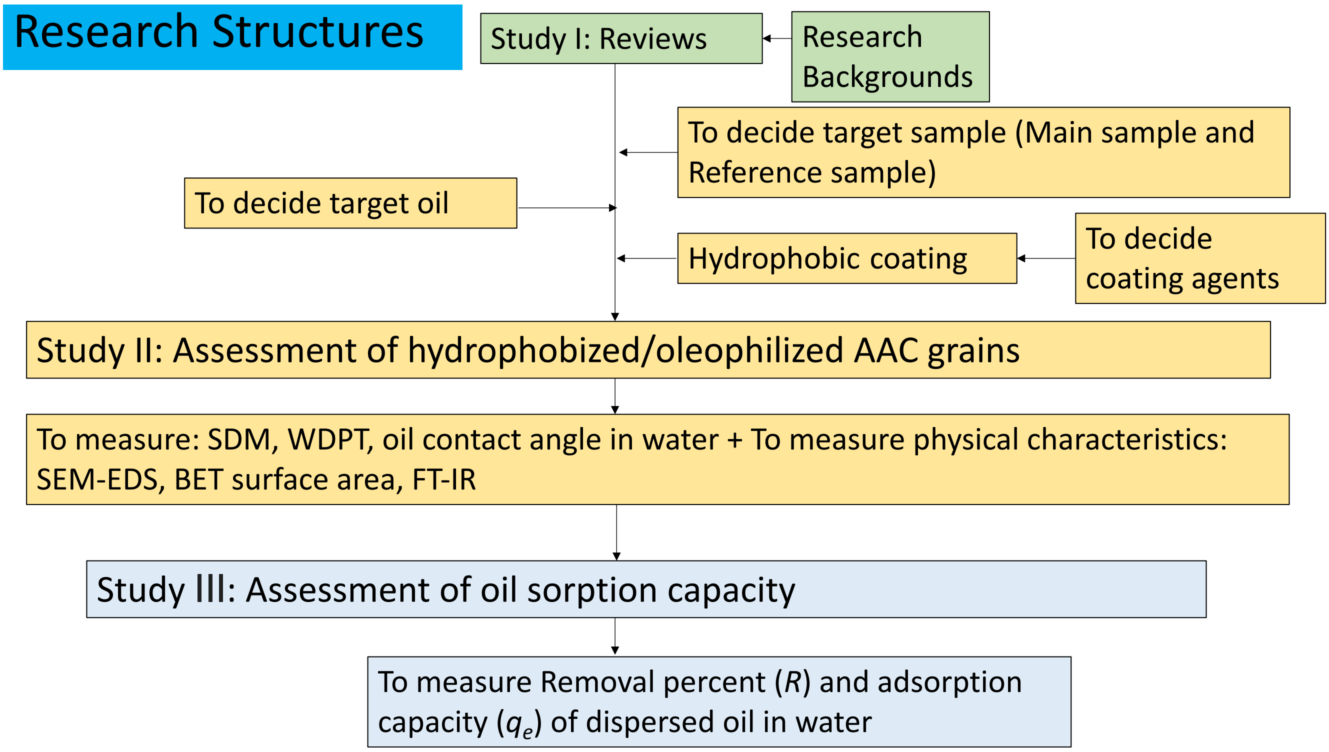

Figure 6. The flow of this research.

Chapter 2 Reviews on previous studies (Study I)

In this chapter, previous research on oil/water separation of grains is investigated to proceed with this study.

2.1 Introduction

In recent years, many techniques for treatment of oily wastewater such as flotation, coagulation, chemical treatment, gravity separation, biological treatment, filtration and membrane separation, and adsorption have been developed (Chakrabarty et al., 2008; Xue et al., 2014). Figure 7 shows the overall summary of special wettable materials. Among them, the oil/water separation techniques based on adsorption and filtration have been advanced by using various types of materials such as membrane, mesh, film, porous media, grains (powders), and so on. Not only natural hydrophilic/oleophobic (or natural hydrophobic/oleophilic) materials but also synthetic materials with hydrophobic/oleophilic substances for oil/water separation can be used to improve the surface hydrophobicity/oleophilicity (Xue et al., 2014; Wang et al., 2015; Zhang et al., 2020; Zhao et al., 2020). Although various types of oil/water separation techniques have been reported, the further development of cost-effective and environmentally friendly (e.g., use of recyclable/reusable materials) methods is required, especially to treat large volumes of oily wastewater with high efficiency (Gupta et al., 2017).

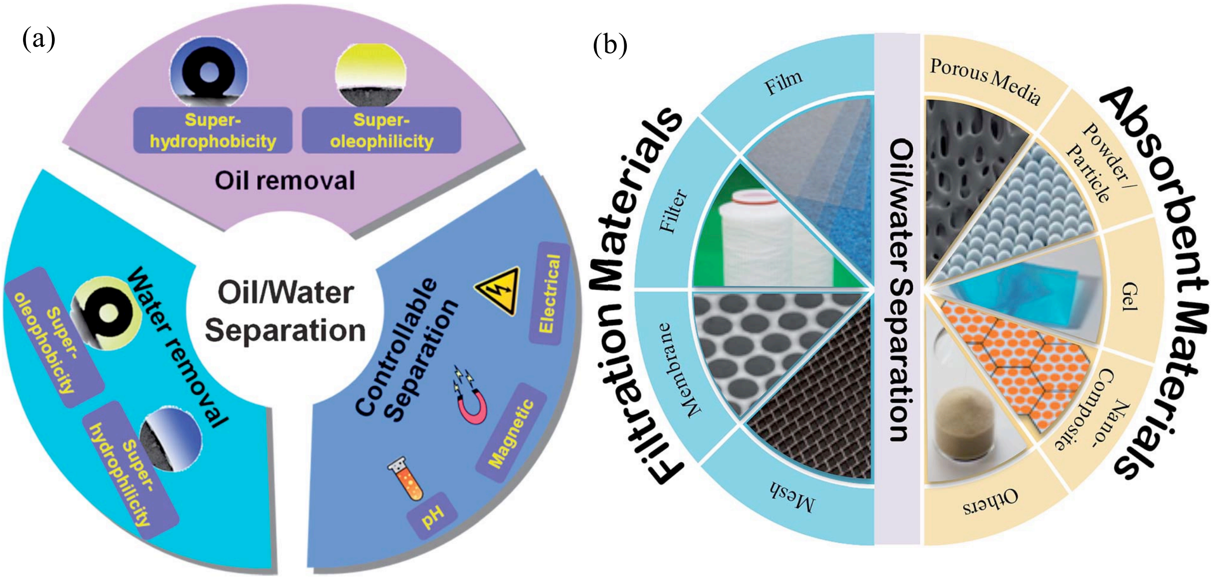

Figure 7 . Illustration of (a) Special wettable materials and (b) typical materials used for oil/water separation (Xue et al., 2014).

Among the oil/water separation techniques based on adsorption and filtration, the utilization of naturally hydrophilic sands and hydrophobized/oleophilized grains are of the most interest due to the ease of application and their cost effectiveness. In this study, we especially reviewed the recent progress in the utilization of naturally hydrophilic sands and hydrophobized/oleophilized grains for oil/water separation and compared the treatment performance, categorizing types of grains, coating substances, oil used, and testing methods.

2.2 Methodology

The data review was based on keywords such as oil/water separation, oily wastewater, hydrophobicity (oleophilicity), hydrophilicity (oleophobicity), hydrophobized/oleophilized grains, adsorption, and filtration. Figure 8 shows that the numbers and corresponding citations of the published articles on oil/water separation has been attaining bigger interest among researcher from all over the world (Yong et al., 2018). Tens of journal papers, books, and reports published in English after the year 2000 were searched in this study [e.g., Web of Science^{TM} (Clarivate Analytics)]. After checking the searched literature from the viewpoint of utilizations of hydrophobized/oleophilized grains for the oil/water separation, 16 papers were selected to summarize and compare the data.

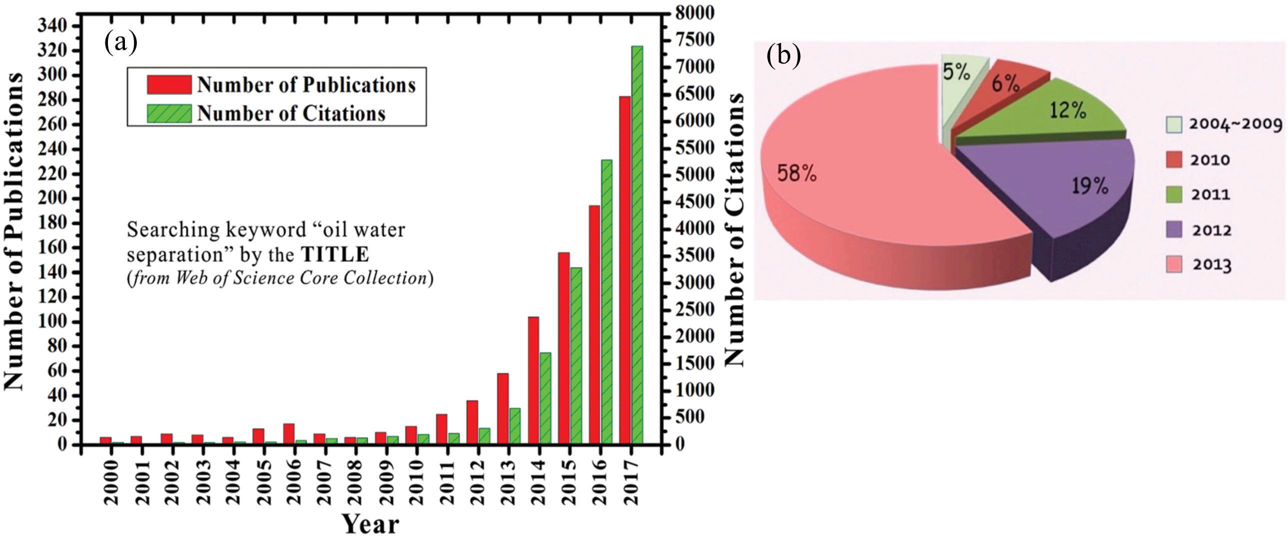

Figure 8. (a) Numbers and corresponding citations of the published articles related to oil/water separation indexed in ISI Web of Science by the title of "oil water separation" and (b) The percentages of published papers on special wettability stimulated oil/water separation materials retrieved from the RSC, ACS, Wiley, Elsevier and Springer.

2.3 Results and Discussion

Table 1 summarizes the oil/water separation techniques utilizing naturally hydrophilic sands and hydrophobized/oleophilized grains, categorizing types of grains, coating substances, measuring the contact angle of water in air (CA_{wa}) and the contact angle of oil in water (CA_{ow}), oil used and concentration (or oil/water ratio), testing methods, and separation efficiency and/or separation capacity. The oil/water separation techniques are classified into two types: one is the adsorption-based technique, and the other is the filtration-based technique.

2.3.1 Types of Grains and Measured Contact Angles

For both adsorption-based and filtration-based oil/water separation techniques, sand materials were generally used for the oil/water separation techniques except for (Li et al., 2020a; Li et al., 2020b; Li et al., 2020c; Liu et al., 2020). This is because sand materials are easily available, inexpensive, and nontoxic to environment (Men et al., 2016). Among the sand materials, quartz sand was commonly used for fabricating hydrophobicity/oleophilicity on the grain surface (Liu et al., 2018; Wei et al., 2019, Wei et al., 2018; Liu et al., 2018), and natural desert sand was used for the filtration-based oil/water separation due to its surface hydrophilicity/oleophobicity (Yong et al., 2016; Li et al., 2017; Chen et al., 2017). The tested grain sizes ranged <1 mm and were mostly around 0.2 mm, which is a typical boundary between fine and medium sand in the fields of geotechnical engineering and soil science.

CA_{wa} is used to characterize the hydrophobicity/oleophilicity of a grain surface, and CA_{ow} is used to characterize the hydrophilicity/oleophobicity of a grain surface. The relationship between measured CA_{wa}/CA_{ow} and the grain size is plotted in Figure 9. The contact angles >150° are identified as materials with a "superhydrophobic/superoleophilic" surface or a "superhydrophilic/ superoleophobic" surface (Wang et al., 2016). The measured CA_{wa} and CA_{ow} were dependent on the tested oils, but most of the tested grain surfaces were >150° , indicating that the tested grains were categorized as "superhydrophobic/superoleophilic" or "superhydrophilic/superoleophobic".

2.3.2 Used Oils for Oil/Water Separation Studies

As shown in Table 5, various types of oils such as gasoline, diesel, crude oil, vegetable oils (soybean cotton seed, rapeseed, and so on) including so-called volatile organic compounds (VOCs) such as petroleum ether, hexane, and chloroform were used depending on the purposes of the studies. In addition, both "oil in water" and "water in oil" were used, and both concentration (given in mg/L or mL/L in Table 1) and oil/water ratio (given in O/W in Table 5) were used in the oil/water separation studies.

2.3.3 Testing Methods and Separation Efficiency for Oil/Water Separation Studies

Basically, all reported studies on both adsorption- and filtration-based methods gave a good oil/water separation performance. The relationship between measured CA_{wa} or CA_{ow} and the separation performance. The relationship between measured CA_{wa} or CA_{ow} and the separation efficiency and capacity are plotted in Figure 10. For adsorption-based techniques using batch and mixing methods, the adsorption/adhesion capacities ranged between 110 and 500 mg/g. Atta et al. (2019) reported that the adsorption capacity of the crude oil was increased from 160 mg/g (uncoated silica particles) to 500 mg/g after coating the grain surface. Wei et al. (2019) reported that the adsorption capacities of hydrophobized quartz sands increased 54% for the engine oil and 45% for the rapeseed oil compared to those of uncoated quartz sands. For filtration-based techniques, the gravity-driven method was commonly used to assess the separation efficiency and capacity. The separation capacity was validated based on the performance under repeated separation tests (i.e., cycles).

2.3.4 Concluding Remarks

In this chapter, recent studies and progress on oil/water separation techniques based on adsorption and filtration utilizing natural hydrophilic sands and hydrophobized/oleophilized grains were reviewed. All reviewed methods performed well and gave high oil/water separation efficiency and capacity in the laboratory tests. Most of the studies used sands as tested grains. It is worth to note that Li et al. (2020a) used grains from waste clay brick (originating from construction waste). In addition, Shi et al. (2020) utilized waste brick powders to coat a membrane for the oil/water separation. Use of these harmless waste materials and industrial by-products should be encouraged to utilize for the oil/water separation techniques from the viewpoints of reuse and recycle of waste, sustainability, and green development.

Regarding the practical applications of tested materials to the actual treatment of oily wastewater, not only assessment of the grain size and coating substances but also examination of suitable packing density (porosity) and flowing conditions of oily wastewater, such as line velocity, hydraulic retention time, and mass transport analysis under continuous flowing conditions, are important. Further studies and challenges are necessary to evaluate the performance of oil/water separation techniques utilizing naturally hydrophilic sands and hydrophobized/oleophilized grains, fully considering the packing density and flow conditions

Table 5. Oil/water separation techniques utilizing natural hydrophilic sands and hydrophobized/oleophilized grains (Matsuno et al., 2021).

Grains/sands (size in mm)	Coating substances	CA_{wa} / CA_{ow} (°)	Used oil*	Oil concentration or O/W	Method	Separation efficiency (in %) and/or separation capacity**	Ref.
Adsorption-based							
Silica particles (~0.4)	1,7-octadiene monomer	$\mathrm{CA}_{wa} = 129\text{-}144$	Motor oil, crude oil, kerosene	20 g/L (in water)	Batch (4 g solid to 80 mL oil)	> 99% 330-500 mg/g	Akhavan et al. (2017)
Quartz sand (0.55-0.83)	ODTS, ZnO nanoparticles	$\mathrm{CA}_{wa} = 150\text{-}154$	Engine oil, rapeseed oil, and so on	N.C.	Mixing (10 g solid to 5 mL oil)	96.5-99.7% 180-380 mg/g	Liu et al. (2018)
Sand (0.1-0.25)	TEOS, VTS	$\mathrm{CA}_{wa} = 140\text{-}170$	Crude oil	20 mL/L (in seawater)	Mixing (Sand : oil = 1:1, 1:2, 1:10)	80-92% (Coating substances: sand = 1:2)	Atta et al. (2019)
Quartz sand (0.6-0.9)	Chitosan, SiO_2 nanoparticles	$\mathrm{CA}_{ow} = 152$	Engine oil, rapeseed oil	N.C.	Mixing (20 g solid to 100 mL oil)	99.9% ~ 280 mg/g (Engine oil) ~ 110 mg/g (Rapeseed oil)	Wei et al. (2019)
Filtration-based							
Quartz sand (0.6-0.9)	Chitosan, SiO_2 nano-particles	$\mathrm{CA}_{ow} = 152$	Engine oil	O/W = 1:19 (in weight)	Gravity-driven (Porosity: 45 %)	~ 100%	Wei et al. (2019)
Sand (0.1-0.5)	ODTS	$\mathrm{CA}_{wa} = 155$	Hexadecane, chloroform	O/W = 5:3 (in volume)	Gravity-driven with vacuum (Oil: chloroform)	High separation capacity remained even after 5 cycles of separation	Men et al. (2016)

Table 5. Continued.

Desert sand (0.13-0.27)	(Non-coating)	CA_{ow} = 146-152	Decane, sesame oil, crude oil, diesel oil, etc.	N.C.	Gravity-driven (Oil: petroleumether)	High separation capacity depending on the thickness sand layer	Yong et al. (2016)
Desert sand (> 0.05)	(Non-coating)	CA_{ow} = 112^{***} (CA_{wa} = 0)	Diesel, petroleumether, etc.	O/W = 50:1 (in volume)	Gravity-driven (Porosity: 79.6 %)	> 99.8% (Separation capacity was maintained even after 10 cycles of separation)	Li et al. (2017)
Desert sand (0.1-0.2)	Cu $(OH)_2$ nano-needles	CA_{wa} = 158	1,2-dichloro-ethane	O/W = 2:1 (in volume)	Gravity-driven	Up to 99.5%	Chen et al. (2017)
Quartz sand (0.55-0.83)	IDT, 3-MPS	N.D.	Gasoline engine oil	17.3 mg/L (in water)	Steady effluent flow rate	74-87% (in the first 9 hours)	Wei et al. (2018)
Quartz sand (0.1-0.3)	HMDS (nano silica)	CA_{ow} = 154	Xylene, chloroform, diesel oil	O/W = 1:1 (in weight)	Gravity-driven	97-98% (96% even after 50 cycles of separation)	Liu et al. (2018)
Waste brick grains (0.1-0.4)	(Non-coating)	CA_{ow} = 145.7 ± 2.8 (CA_{wa} = 138.3 ± 3.4)	Soybean oil, hexane, etc.	N.C. (water-in-oil and oil-in-water emulsions)	Gravity-driven (Porosity: 47 %)	~ 98% (Separation capacity remained even after 10 cycles of separation)	Li et al. (2020a)

Table 5. Continued.

Waste brick grains (0.05-0.4)	ZnO nanopillars	CA_{ow} = 152-153 (CA_{wa} = 145-147)	Gasoline, Chlorobenzene, etc.	N.C. (water-in-oil and oil-in-water emulsions)	Gravity-driven (Porosity: 47 %)	95.5-98.5% (Separation capacity remained even after 10 cycles of separation)	Li et al. (2020b)
Waste brick grains (0.05-0.4)	TiO_2	CA_{ow} = 148.6 ± 2.5 (CA_{wa} = 143.8 ± 3.1)	Heavy oil	N.C.	Gravity-driven (Porosity: 47 %)	99.2%	Li et al. (2020c)
Macroporous ceramic materials (Al_2O_3)	PDMS	CA_{wa} = 153.04 to 133.12	1,2-dichlorobenzene, Hexane, Isooctane, Dichloromethane, Petroleumether	O/W = 1:1 =10 ml:10 ml	Gravity-driven (Porosity: 65 %)	99.7 ± 0.92% (Separation capacity remained even after 10 times of separation)	Liu et al. (2020)
Sand grains (<0.075)	PDMS	CA_{wa} = 143 ± 3 to 152 ± 1)	Chloroform, Kerosene, etc.	O/W = 1:1=10 ml (Kerosene):10 ml (Water) O/W = 1:3=10 ml (Chloroform):30 ml (Water)	Gravity-driven	94-98% (Separation capacity remained even after 25 cycles of separation)	Mosayebi et al. (2020)

Note: *Used oil including volatile organic compounds (VOCs).**Capacity: Adsorbed amount of oil / grains (g/g) is given for the adsorption-based technique. Applicable range and observed performance of oil/water separation are given for the filtration-based technique. ***CA_{ow} was read by the figure in the literature.

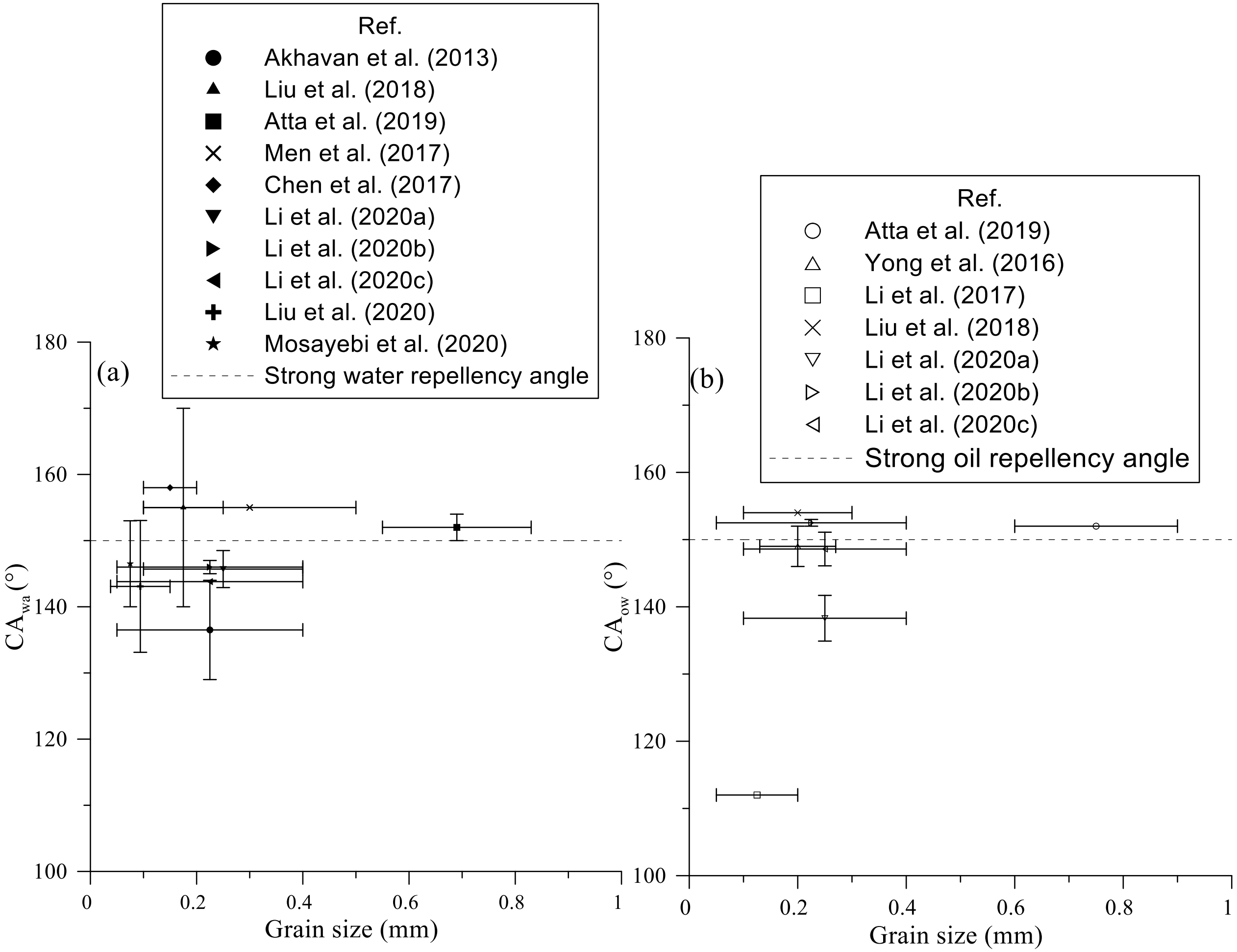

Figure 9. Relationship between grain size and (a) Contact angle of water in air (CA$_{wa}$), (b) Contact angle of oil in water (CA$_{ow}$) (Matsuno et al., 2021).

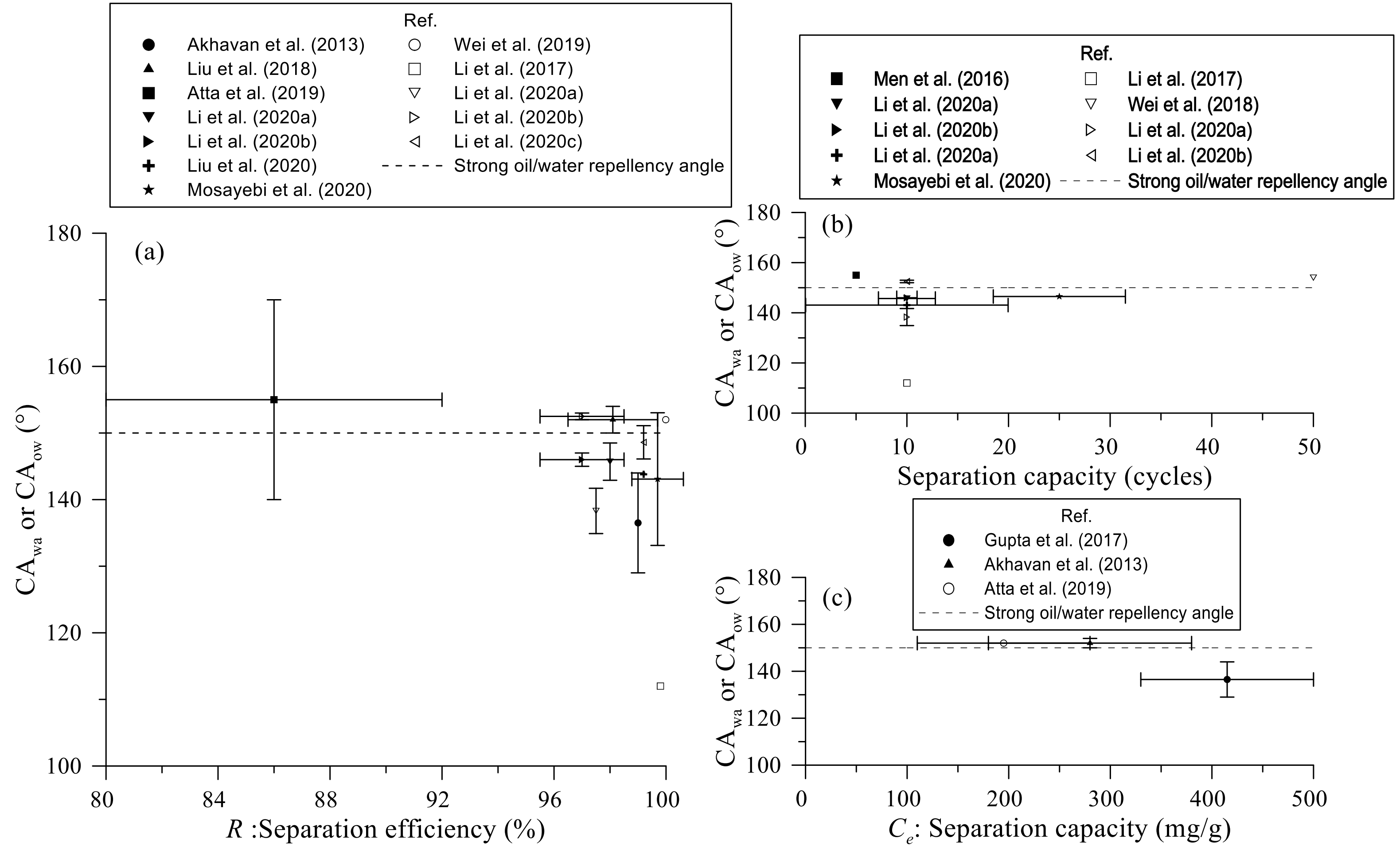

Figure 10. Relationship between CA_{wa} or CA_{ow} and (a) Separation efficiency R (%), (b) Separation capacity (cycles), (c) Separation capacity C_e (mg/g) (Matsuno et al., 2021).

Chapter 3 Assessment of Hydrophobic/Lipophilic of recycled construction materials in Vietnam (Study II)

3.1 Introduction

As described above, many studies to assess the surface hydrophobicity/oleophilicity of filtration and/or adsorbent materials in the oil/water separation were based on the CA measurements. However, the CA measurements of hydrophobized/oleophilized surfaces in both oily water–air and oil–water systems (i.e., oil contact angles in air and water) have not been fully investigated, even though the oil contact angles in both air and water are needed to characterize the degree of hydrophobicity/oleophilicity of filtration and ad-sorbent materials and to assess the oil/water separation performance under both continuous (oil-in-water) and discontinuous (oily water in air) water flow conditions. Moreover, most previous studies that use hydrophobized grains for the oil/water separating materials used non-porous gains with a small specific surface area, such as quartz sands, and a limited number of studies have examined the applicability of porous grains (rich in fine pores inside and with a large specific surface area) as oil/water separating materials.

The specific objectives were 1) to measure the CA of water droplets in air (CA_{wa}) and the CA of oil droplets in water (CA_{ow}) of hydrophobized AAC grains in three grain sizes (0.106–0.250, 0.250–0.850, and 0.850–2.00 mm) and assess the hydrophobicity (oleophilicity) by examining the measured CA_{wa} and CA_{ow} values as a function of the amount of coated hydrophobic agents, and 2) to examine the correlations of measured CA_{wa} and CA_{ow} with physicochemical parameters such as specific surface area and organic carbon content. For comparing the tested results from AAC grains to those from non-porous grains, commercially available sands (grain sizes of 0.18–2.00 and 0.30–2.00 mm) used for sand filtration systems were also used in this chapter.

3.2 Materials and Methods

3.2.1 AAC and Sands

AAC has a unique pore structure that consists of inner-pores (μm to nm scale) and inter-pores (mm to μm scale) (Alexanderson, 1979; Tada, 1983; Wittmann, 1983; Aroni, 2014; Lam et al., 2018). Thus, this study is needed to promote development utilizing the unique porous characteristics of AAC. Therefore, to promote low cost and high-performance oil/water separating filtration and adsorbent materials utilizing porous grains made from AAC scrap in Vietnam (VN-AAC), this research assessed the hydrophobicity (oleophilicity) of AAC grains coated with hydrophobic agents harmless to humans and the environment, such as oleic and stearic acids (Subedi et al. 2012).

Figure 11 shows Block-like AAC scrap (approximately 500 kg) was taken from Viglacera Joint Stock Company in Bac Ninh Province, Vietnam (21°11′50.8″ N, 106°00′42.8″ E) (Thai et al., 2022).

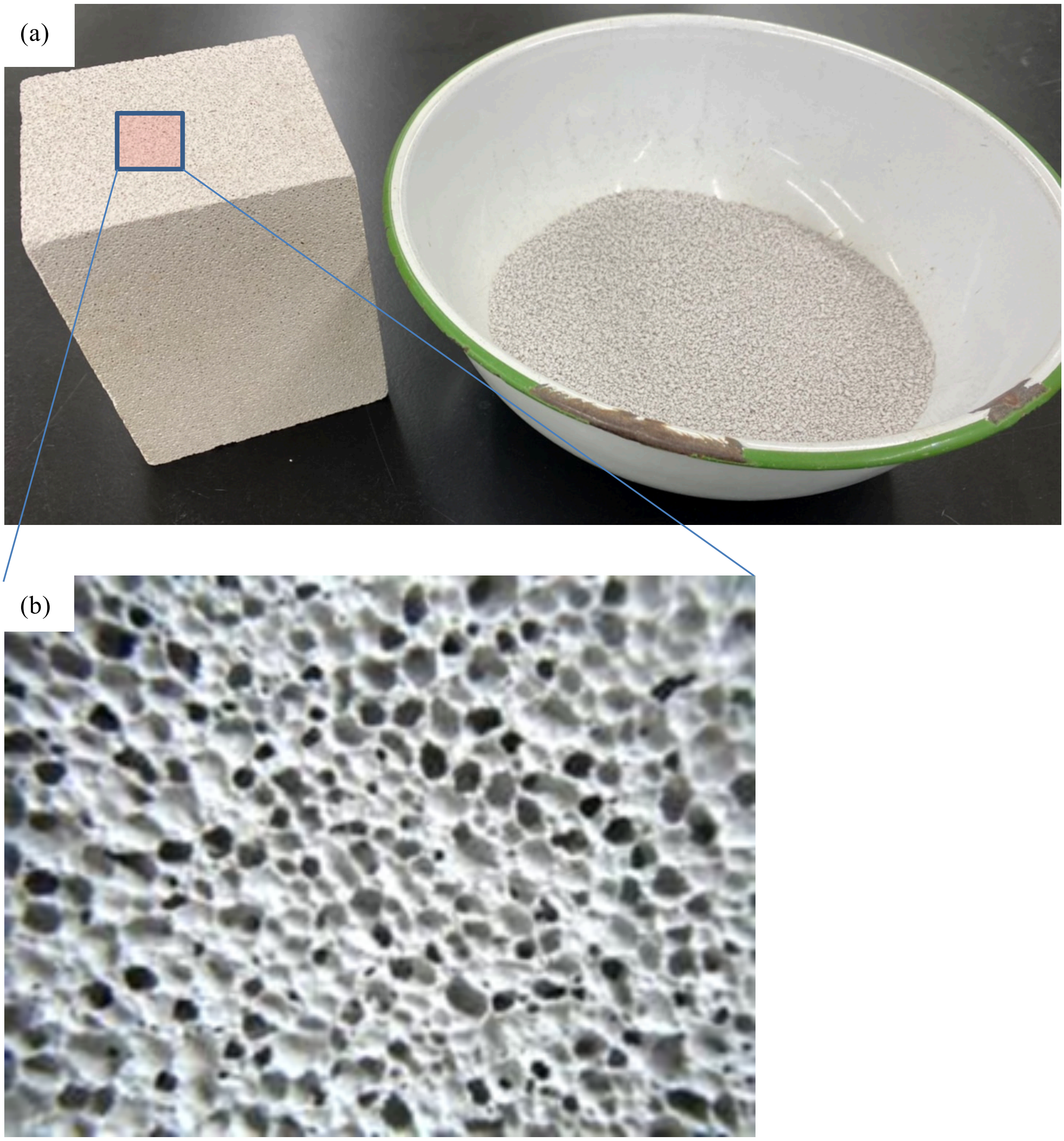

Figure 11. The photos of VN-AAC (a) Block and granular sample (b)Surface (SEM image).

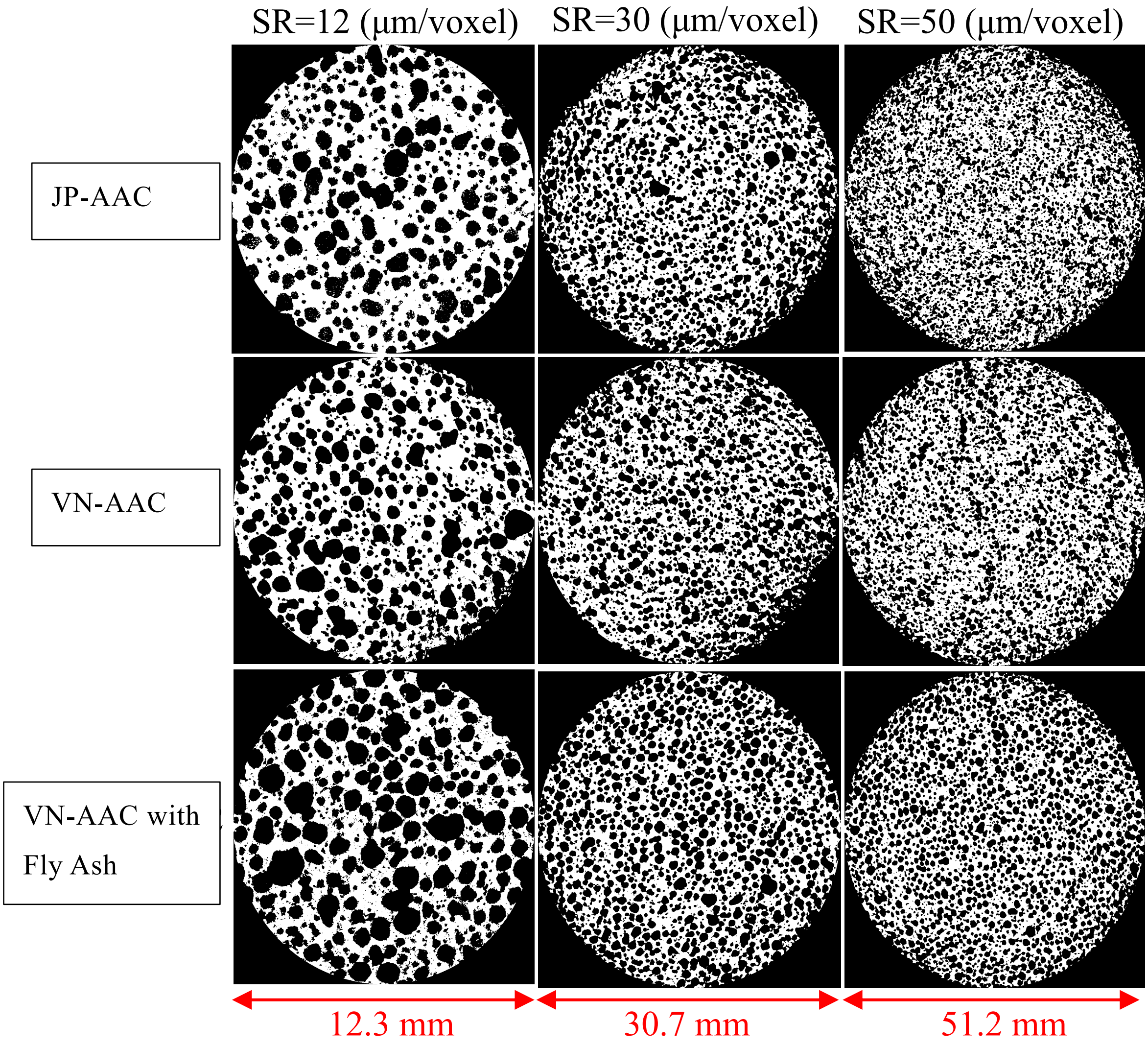

Figure 12. Binalized images for tested AAC samples with three scanning resolutions (SR) (Matsuno et al., 2020).

AAC is a typical lightweight cementitious material with a robust skeleton and pore structure (porous medium) and is widely used in many architectural applications worldwide due to its low density, thermal conductivity, and high heat resistance (van Boggelen et al., 2018, Matsuno et al., 2020). Figure 12 shows binarized MPR images of AAC from Japan and AAC from Vietnam taken by MFXCT. Figure 13 exemplifies three-dimensional reconstructed images, medial axis skeleton for macropores, and shortest paths in the ZZ direction for tested AAC samples (Matsuno et al., 2020).

AAC is known to form a calcium silicate hydrate, tobermorite [$Ca_5Si_6(O, OH, F)_{18}5H_2O$], during the manufacturing process (Matsuno et al., 2020, Kikuma et al., 2010). Figure 14 shows the tobermorite crystal of VN-AAC taken by SEM-EDS. The block-like AAC scrap was first crushed to less than 10 mm and sieved in the laboratory to make AAC grains. Then, the AAC grains were washed gently with a low-foaming neutral detergent and rinsed thoroughly with distilled water. After being rinsed, the AAC grains were air dried and sieved again into three grain fractions, 0.106–0.250 mm (fine), 0.250–0.850 mm (middle), and 0.850–2.00 mm (coarse) (JIS Z 8801-1: 2019). For comparison of tested data from AAC grains, two commercially available sands (Nihon Genryo Materials Co., Ltd., Kanagawa, Japan) that meet the Japanese standards of filtration (JWWA A 103-1:2006-2) were also used in this research. Sand with the size of 0.18–2.00 mm was used for slow filtration, and sand with the size of 0.30–2.00 mm was used for rapid filtration. The AAC grains and sands tested in this research are shown in Figure 15. And additional crystal and individual ions information and international water filter media standards are available in the Appendix.

3.2.2 Oil

In this study, soybean oil with a high percentage of linoleic acid (53.5%) and linolenic acid (6.9%) (Wako 1st grade; Fujifilm Wako Pure Chemical Corp., Tokyo, Japan) was used. Soybean oil is a commonly consumed domestic oil in Vietnam (The chemical daily, 2010) and is liquid at room temperature. The appearance is colorless to pale yellow, and the basic composition of soybean oil and different vegetable oils are shown in Table 6 (Gerde et al., 2020; JOPA web page). Linoleic acid and linolenic acid are the main component. The molecular formula of linoleic acid is $CH_3(CH_2)_3(CH_2CH{:}CH)_2(CH_2)_7COOH$ (molecular weight: 280.45) while the molecular formula of linolenic acid is $CH_3(CH_2CH{:}CH)_3(CH_2)_7COOH$ (Molar: 278.43). Soybean oil is one of the common domestically consumed oil with high %age of linoleic and linolenic acid, high flash point. It is easy to handle during our experimental work.

Table 6. Basic composition of different vegetable oils.

Material	Flash point (°C)	Density (25 °C) (g/ml)	Linoleic acid (%)	Linolenic acid (%)	Oleic acid (%)	Other saturated and unsaturated fatty acids (%)
Soybean oil	331	0.917~0.920	53.5	6.9	23.7	15.9
Corn oil	321	0.912~0.920	54.6	1.2	29.9	14.3
Cottonseed oil	220-230	0.917~0.923	55.8	0.7	18.3	25.2
Grape seed oil	216	0.915~0.923	72.2	0.4	16.6	10.8

3.2.3 Hydrophobic Agents and Coating

Two types of hydrophobic agents (HA), stearic and oleic acids (SA and OA), were chosen to hydrophobically (oleophilically) coat the grains tested in this research (Subedi et al., 2012; 47–49). Figure 16 shows a graph of CA_{wa} (Subedi et al., 2016) effect of increasing hydrophobic agent (HA) on the initial contact angle, α_i, in hydrophobized Toyoura sand before and after the wetting and drying cycle for OA and SA coatings.

	3D Model	MA (Medial Axis)	Shortest Paths	Isolated pore (%)
JP-AAC	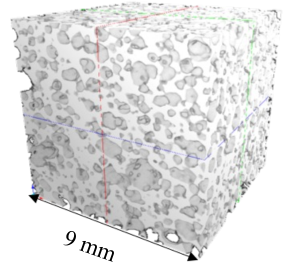	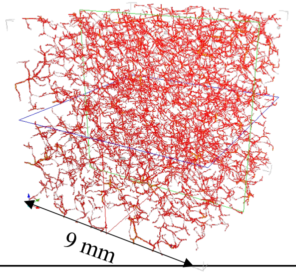	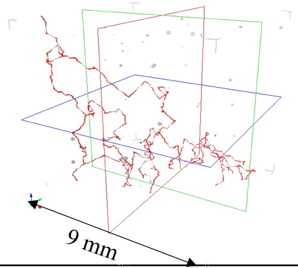	39
VN-AAC	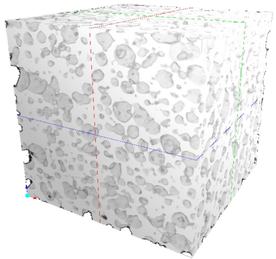	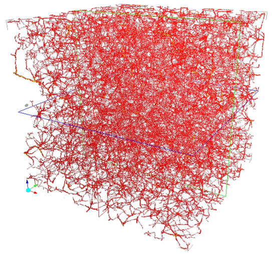	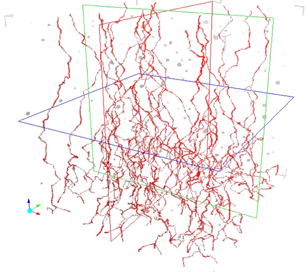	1.2
VN-AAC with Fly Ash	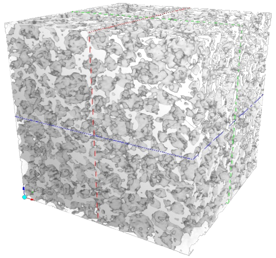	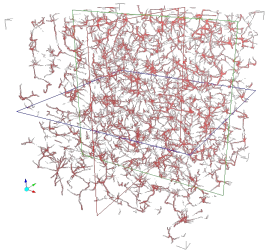	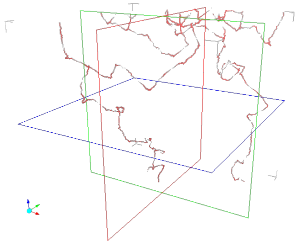	13

Figure 13. Three-dimensional reconstructred images, medial axis skelton for macropores, shortest paths in ZZ direction, and isolated pores (%) for tested AAC samples (SR = 30 μm/voxel, ROI = 300×300×300).

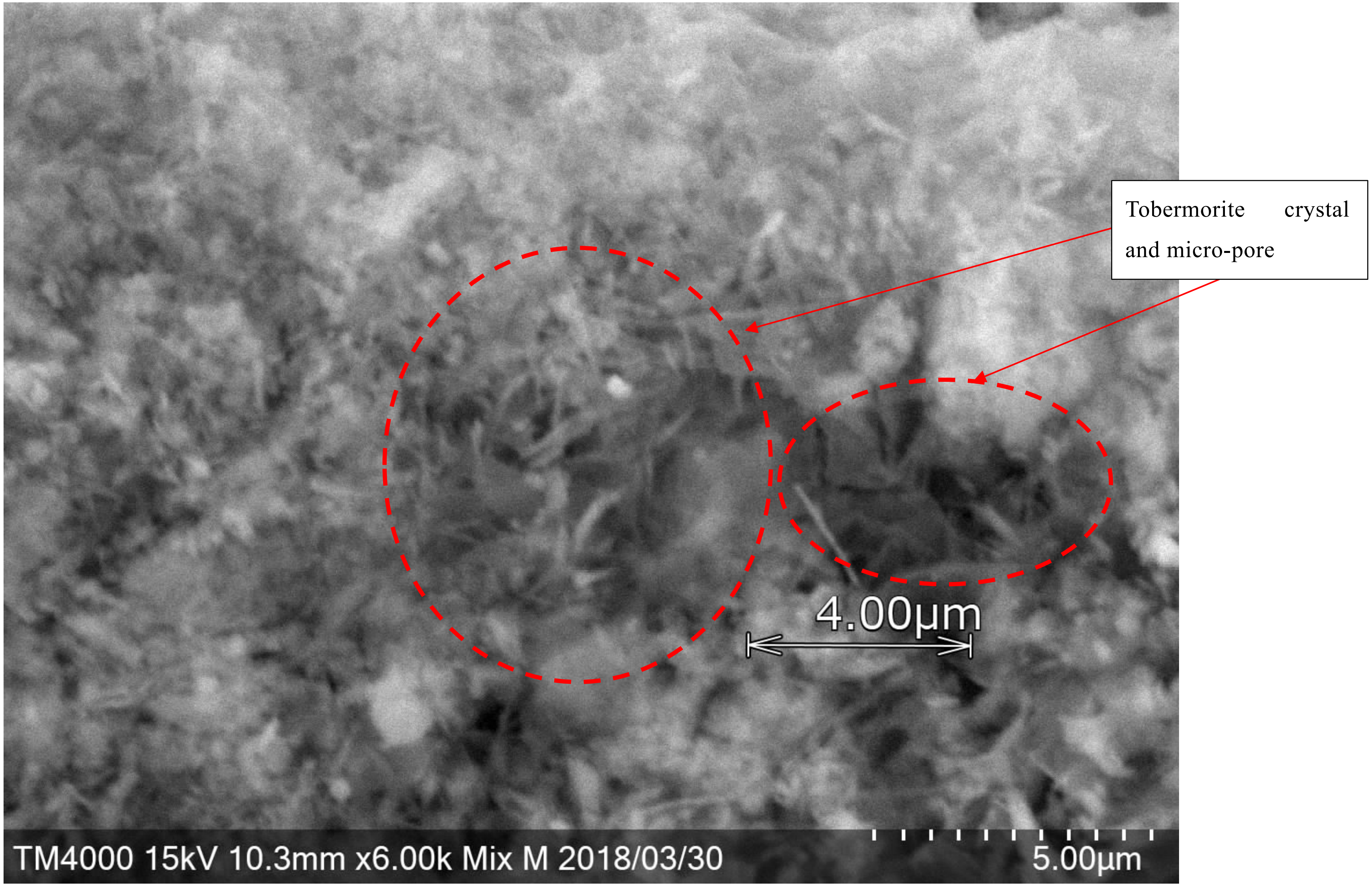

Figure 14. SEM image of VN-AAC.

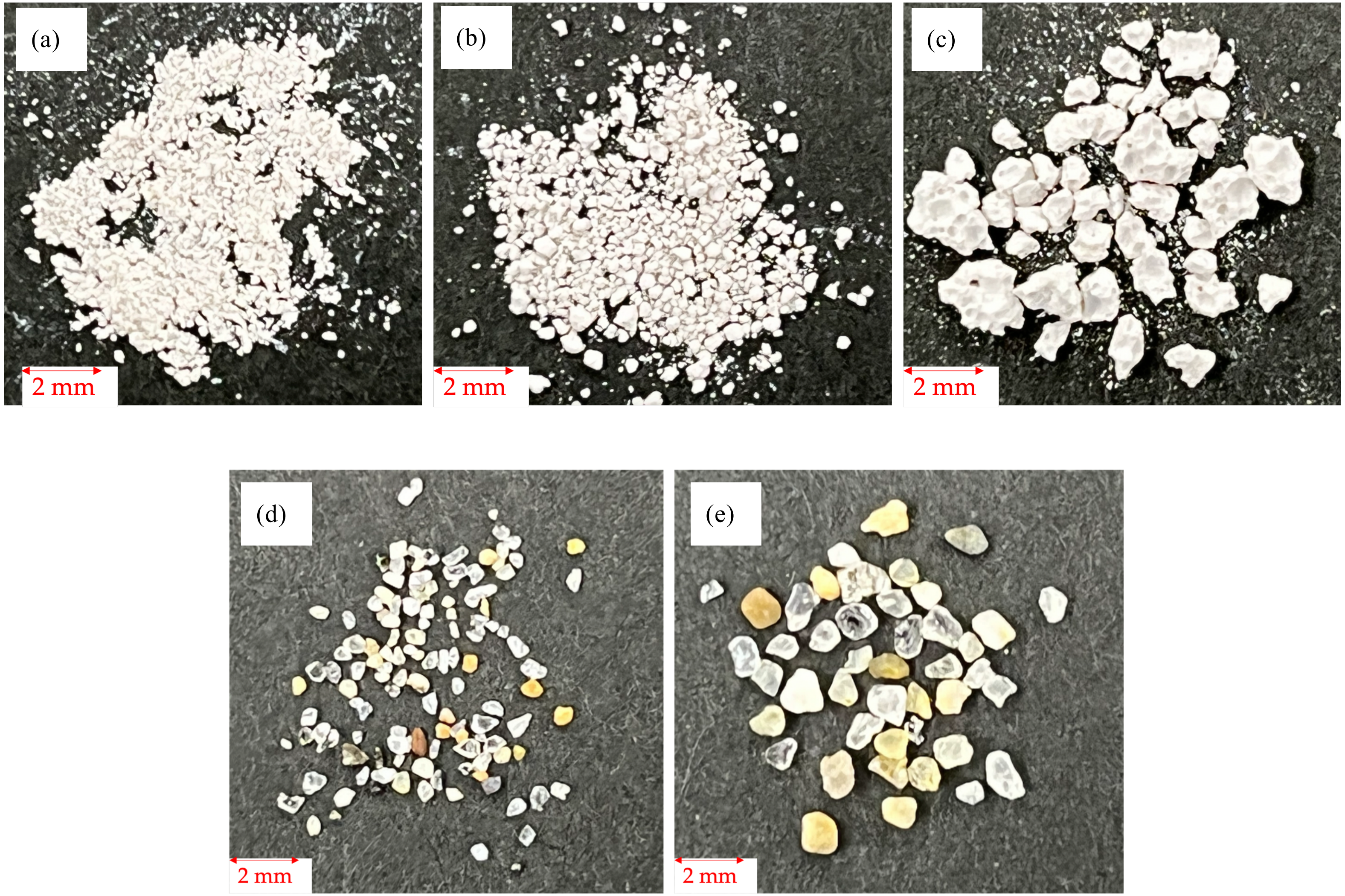

Figure 15. Samples: (a) VN-AAC (Grain size: 0.106–0.25 mm); (b) VN-AAC (Grain size: 0.25–0.85 mm); (c) VN-AAC (Grain size: 0.85–2.00 mm) (d) Sand (Grain size: 0.18–2.00 mm); (e) Sand (Grain size: 0.30–2.00 mm).

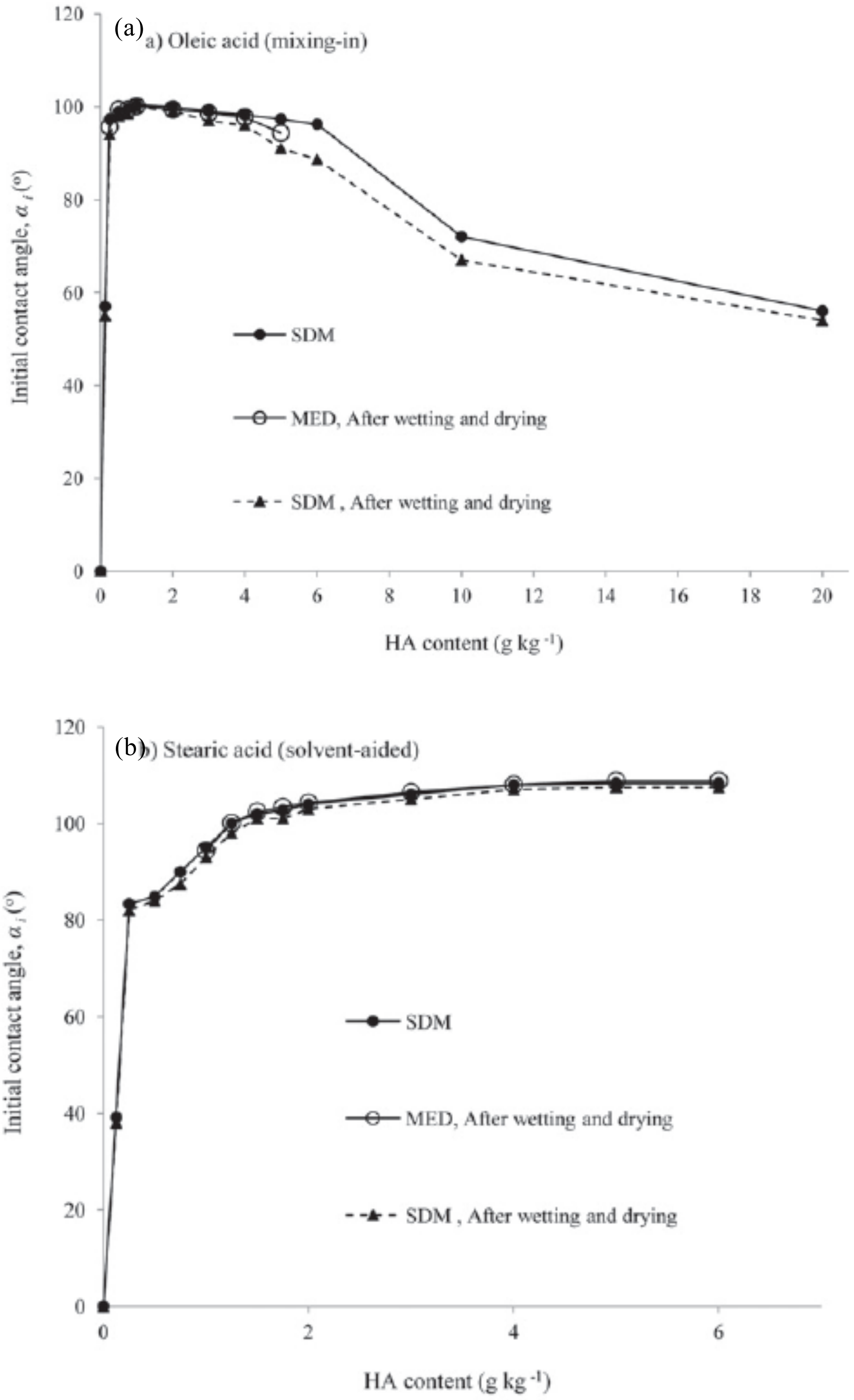

Figure 16. Effect of increasing hydrophobic agent (HA) on the initial contact angle, α_i, in hydrophobized Toyoura sand before and after the wetting and drying cycle for (a) oleic acid (OA) (mixing-in) and (b) stearic acid (SA) (solvent-aided) samples.

Both OA and SA are harmless to humans and the environment. Olive oil is known to be rich in OA, and SA is plentiful in beef tallow and other animal and vegetable fats, materials readily available at low cost in Vietnam. In the laboratory, commercially available OA (molar mass: 282.46 g/mol, density: 0.895 g/cm^3) (Kanto Chemical Corp., Tokyo, Japan) and SA (molar mass: 284.47 g/mol, density: 0.940 g/cm^3) (Fujifilm Wako Pure Chemical Corp., Tokyo, Japan) were used. OA is a mono-unsaturated omega-9 fatty acid with the chemical formula $CH_3(CH_2)_7CH{:}CH(CH_2)_7COOH$, and SA is a saturated fatty acid with the chemical formula $CH_3(CH_2)_{16}COOH$.

The hydrophobic coating was done as follows: air-dried AAC grains and sands were soaked in a beaker along with the solvent to reach target HA concentrations (g/kg) [= M_s/M_d, where M_s is the dry mass of HA (g) and M_d is the dry mass of tested grains (kg)]. It is noted that at average room temperature, SA is a solid (powder) (melting point: 69 °C), and OA is a liquid (melting point 13–16 °C). Therefore, considering the polarities of SA and OA, diethyl ether and ethanol were used as solvents for SA and OA, respectively. The SA and diethyl ether were thoroughly mixed using an electronic mixer before adding the sample. After volatilization of the solvent, the coated samples were stored for at least 48 h in a climate-controlled lab at 20 °C and 60% humidity to equilibrate and stored in a plastic bag after air-drying.

3.2.4 Measurement of Contact Angles

Contact angles of water droplets in air (CA_{wa}) for tested grains were measured by the sessile droplet method (SDM) (Wijewardana et al., 2015; Bardet et al., 2014) using a digital microscope (VHX-900 series, KEYENCE Japan, Tokyo, Japan). The grains were put on a smooth glass slide to which double-sided tape was attached. The glass slide was then lightly tapped to remove the excess sample, the glass slide was placed on the microscope camera stage, and a small drop of distilled water (50 ± 5 μL) was dropped onto the grains using a syringe. Horizontal microscope images were recorded to determine CA_{wa} with time, as shown in Figure 17 (a).

The contact angles of an oil droplet in water (CA_{ow}) were measured following the previous literature (Zhang et al., 2013; Lu et al., 2014; Fan et al., 2016): the test grains were placed on a smooth glass slide using a piece of double-sided tape. Then the glass slide was attached to a glass rod, and the glass rod was placed in a 2 L beaker filled with distilled water. A small drop (0.1 mL) of soybean oil was dripped from a microsyringe with the needle bent and pointing upward toward the sample attached to the underside of the slide glass. The CA_{ow} between the oil droplet and the grains is exemplified in Figure 17 (b).

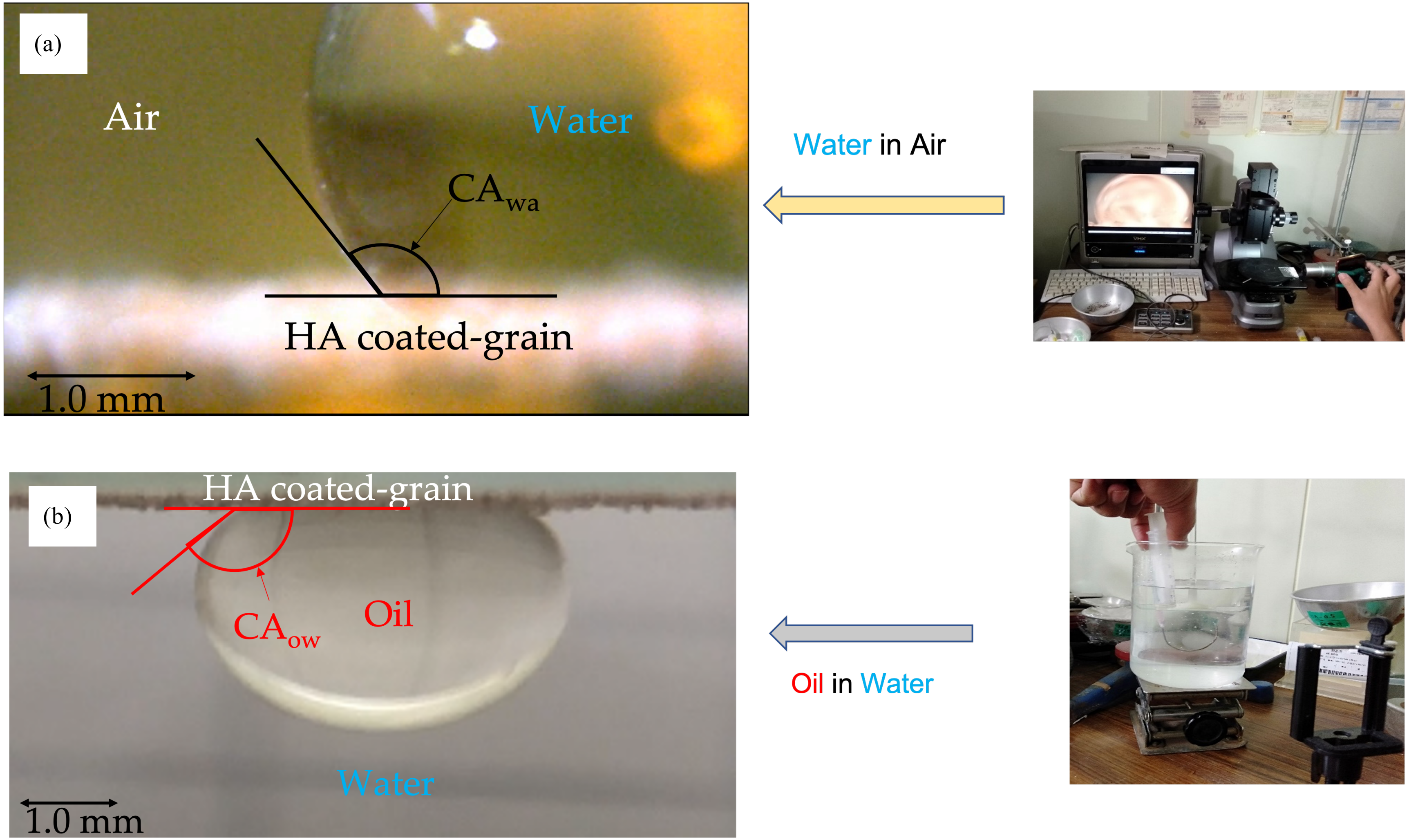

Figure 17. Sessile droplet method to measure contact angles: (a) Water in air (CA_{wa}); (b) Oil in water (CA_{ow}).

3.2.5 Physical and Chemical Properties of Tested Grains and Characterization of Hydrophobicity of HA-Coated Grains

Basic physical and chemical properties such as specific gravity (G_s), loss on ignition (LOI), moisture content in the air-dried condition (w_{AD}), pH, and electrical conductivity (EC) were measured (Miyazaki et al., 2011; JGS, 2011). The organic carbon (OC) content of HA-coated grains was measured by an elemental analyzer (FLASH 2000, Thermo Fisher Scientific, Inc., Waltham, MA, USA). To characterize the surface hydrophobicity (oleophilicity) of tested grains, the A/B ratio was calculated based on the spectra measured by a Fourier transform infrared (FT-IR) spectrometer (Tensor II, Bruker Ltd., Banner Lane, UK). The FT-IR spectra focused on two absorption bands that primarily represent hydrophobic (C-H group) and hydrophilic (C = O group) functional groups. For hydrophobic methyl and methylene groups, the C-H bands occur at 2920 cm^{-1} (asymmetric stretch) and 2860 cm^{-1} (symmetric stretch) (Capriel et al., 1995). Here, both bands are combined into one band (3020–2800 cm^{-1}), which we designated as absorption band A. Hydrophilic C = O groups occur at 1640–1615 and 1740–1720 cm^{-1} (Celi et al., 1997; Tasumi, 2012). Here, we used slightly different bands, 1640 to 1620 and 1740 to 1710 cm^{-1}, to exclude a possible overlap with C = C and amide bands and denoted both as absorption band B. The OH bands were not considered because they could reflect differences in water content. From this, the ratio of hydrophobicity to hydrophilicity (A/B ratio) was determined (Ellerbrock et al., 2015).

The surface properties of the coated/non-coated grains were characterized by measuring the Brunauer–Emmett–Teller (BET) specific surface area (SSA in m^2/g) using a porosity analyzer (TriStar II, Micromeritics Instruments Corp., Norcross, GA, USA) (Brunauer et al., 1938). The total pore volume (V_T) of non-coated grains was also measured using a porosity analyzer based on the Barrett–Joyner–Halenda method (Barret et al., 1951). In addition, a scanning electron microscope (SEM) (TM4000plus, Hitachi High-Technologies Corp., Tokyo, Japan) and an energy dispersive X–ray spectroscope (EDS) (AZtecOne, Oxford Instruments, Abingdon, Oxon, UK) were used to investigate the morphological features and chemical compositions of HA-coated grains.

3.3 Results and Discussion

3.3.1 Physical and Chemical Characterization

Table 7 shows the physical and chemical properties of tested samples. The values of the uniformity coefficient ($U_c = D_{50}/D_{10}$) of tested samples ranged from 0.83 to 1.64, indicating that the samples were “uniform” (González-Peñaloza et al., 2013). For VN-AAC samples, the measured specific surface area (SSA) decreased with increasing grain size. The total pore volume (V_T), loss on ignition (LOI), and air-dried water content (w_{AD}) of VN-AAC, on the other hand, did not vary with grain size, and those values were one order of magnitude greater than those of sand. In particular, the high values of SSA and V_T of VN-AAC indicated that these samples were porous. VN-AAC samples were alkaline in water (pH = 8.6~9.0) and neutral in KCl solution (pH = 7.2–7.3). Figure 18 and Figure 19 show the particle size distribution measured by sieve test. SEM-EDS images of OA- and SA-coated VN-AAC grains are exemplified in Figure 20. It can be seen the carbon (C) originating from coated HA materials (OA and SA) covered the tested grain surfaces well. Figure 21 and Figure 22 show the nitrogen adsorption isotherm and pore particle size distribution data of VN-AAC and Sand, which are the basis for obtaining V_T. The measured OC was also used to examine the relationships between added (mixed) HA and calculated HA based on OC (Figure 23). A coefficient of this relationship was used to correct for HA.

3.3.2 Contact Angles of Water in Air (CA_{wa})

Measured contact angles of water droplets in air (CA_{wa}) of tested samples as a function of the HA coating concentration are shown in Figure 4. For both OA- and SA-coated VN-AAC samples, the CA_{wa} values increased linearly with increasing HA concentration and reached 98–140°, and then became almost constant (Figure 24a,b,f) and/or gently increased (Figure 24c,g,h) after a specific point (i.e., point of intersection, hereafter labeled "PoI" and the contact angle at PoI labeled "$CA_{wa,PoI}$"). The slopes in the linear increment section (ΔS_1) and those in the gentle increment section (ΔS_2) were calculated and are given in the figure. As well, the HA concentrations corresponding to the PoI ($HA_{wa,PoI}$) and the maximum contact angles of a water droplet in air in the measured range ($CA_{wa,max}$) were read and are summarized in Table 8 For VN-AAC coated with both OA and SA, both $CA_{wa,max}$ and $CA_{wa,PoI}$ decreased with increasing grain size, indicating that a finer grain gave a higher hydrophobicity.

For both OA- and SA-coated sands, on the other hand, the CA_{wa} values increased rapidly, reached a peak, and decreased linearly with increasing HA concentration (Figure 24d,e,i,j; Table 2). The $CA_{wa,max}$ values of sands were smaller than those of VN-AAC (73–82° for OA-coated and 130–131° for SA-coated). In particular, $CA_{wa,max}$ = 73–82° of OA-coated slow sand means that the tested sand does not show hydrophobicity in air (non-water repellency). The measured $CA_{wa,max}$, $CA_{wa,PoI}$, $HA_{wa,PoI}$, ΔS_1, and ΔS_2 in this study were compared to values of sands and glass beads reported by previous studies (Subedi et al., 2012; Wijewardana et al., 2015; Gon-za´lez-Pen˜aloza et al., 2013) (Table 8). Basically, the values of OA- and SA-coated sands in this study were similar to those in the previous studies and the difference in $CA_{wa,max}$ was within 10° (Subedi et al., 2012; Wijewardana et al., 2015; Gon-za´lez-Pen˜aloza et al., 2013). Again, it can be found that the OA- and SA-coated AAC grains in this study gave high hydrophobicity with high values of $CA_{wa,max}$ and $CA_{wa,Po}$

Table 7. Basic physical and chemical properties of tested samples in this study (Matsuno et al., 2022).

Sample	Grain Size (mm)	D_{10} (mm)	D_{50} (mm)	D_{60} (mm)	U_c (D_{50}/D_{10})	SSA (m^2/g)	V_T (cm^3/g)	LOI (%)	w_{AD} (%)	G_s (g/cm^3)	EC (mS/cm)	pH (H_2O)	pH (1 mol KCl)
VN-AAC	0.106–0.25	0.15	0.20	0.21	1.44	15.3	4.5×10^{-2}	9.2	1.44	2.57	1.04	8.90	7.27
VN-AAC	0.25–0.85	0.34	0.51	0.56	1.64	16.9	4.9×10^{-2}	9.5	2.03	2.55	0.94	8.57	7.20
VN-AAC	0.85–2.00	0.90	1.20	1.30	0.83	17.1	4.8×10^{-2}	9.4	2.01	2.46	0.83	8.97	7.33
Slow sand	0.18–2.00	0.31	0.48	0.55	1.54	3.0	6.0×10^{-3}	0.6	0.44	2.66	0.01	7.83	6.13
Rapid sand	0.30–2.00	0.62	0.79	0.83	1.28	3.5	7.0×10^{-3}	0.5	0.40	2.63	0.02	7.27	6.00

D_{10}: Grain size at 10% passing, D_{50}: Grain size at 50% passing (Median diameter), D_{60}: Grain size at 60% passing, U_c: Uniformity coefficient, SSA: Specific surface area, G_s: Specific gravity, w_{AD}: Air-dried water content, EC: Electrical conductivity, pH: Potential hydrogen was measured by using distilled water and 1 mol KCl solution (S:L = 1:2.5).

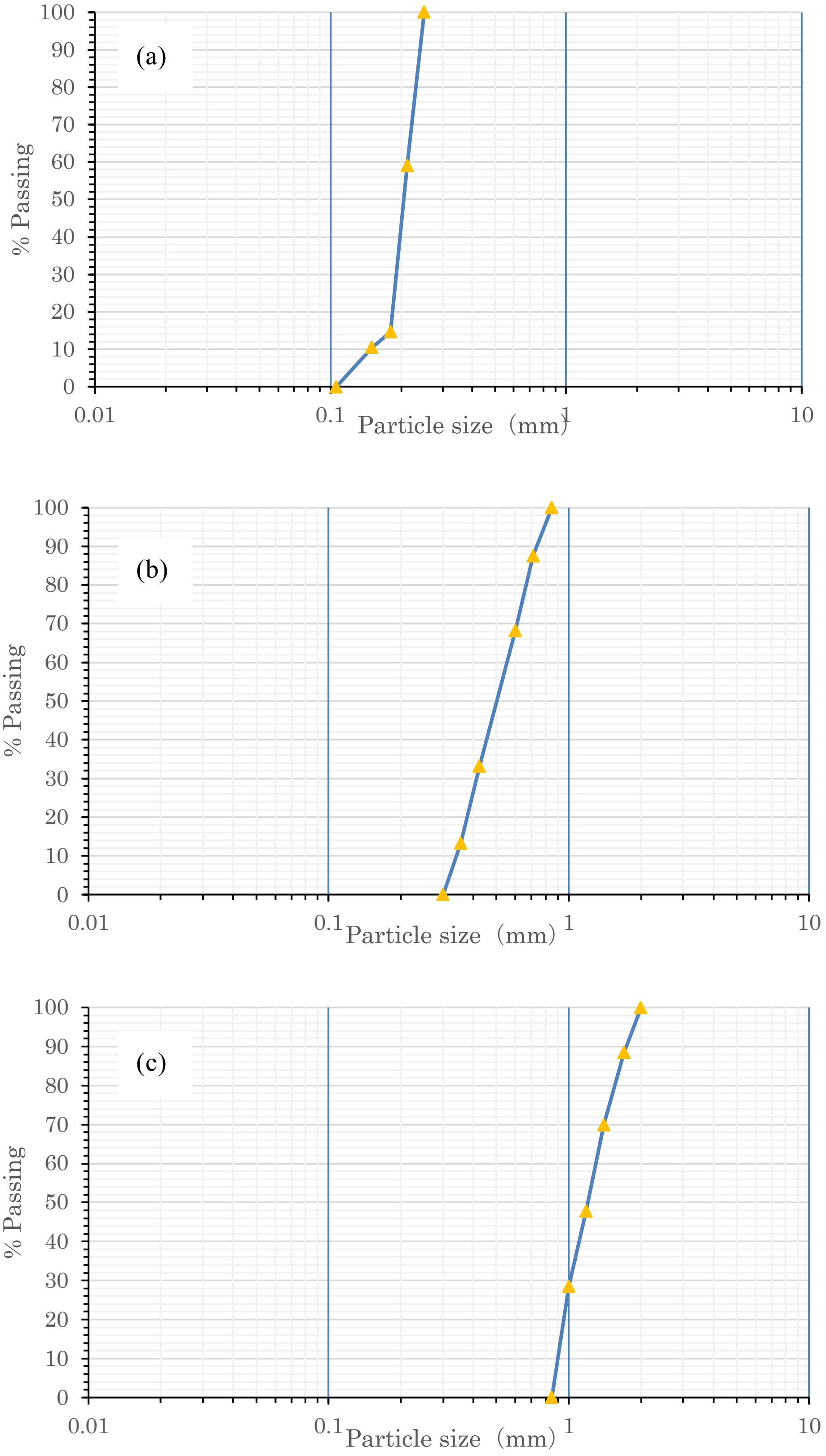

Figure 18. Particle size distribution of VN-AAC (a) 0.106-0.25 mm (b) 0.25-0.85 mm (c) 0.85-2.00 mm.

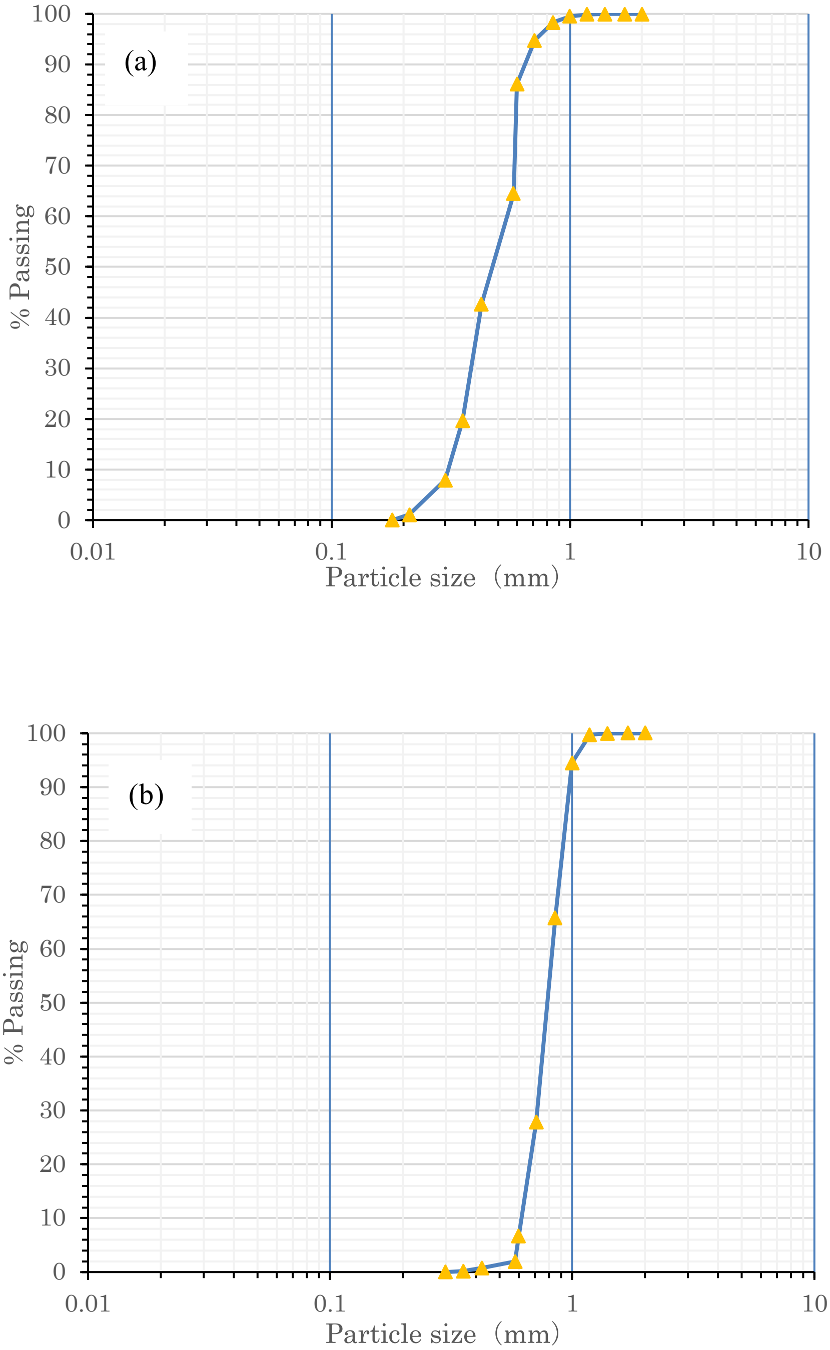

Figure 19. Particle size distribution of VN-AAC (a) 0.18-2.00 mm (b) 0.30-2.00 mm.

(a) OA-coated VN-AAC

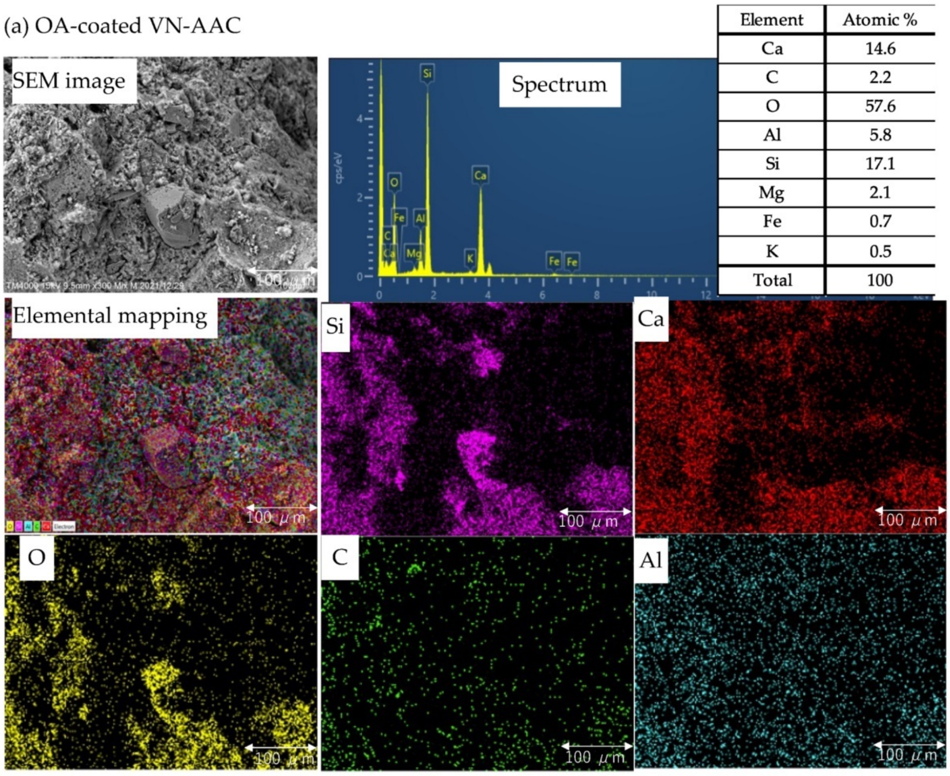

Element	Atomic %
Ca	14.6
C	2.2
O	57.6
Al	5.8
Si	17.1
Mg	2.1
Fe	0.7
K	0.5
Total	100

(b) SA-coated VN AAC

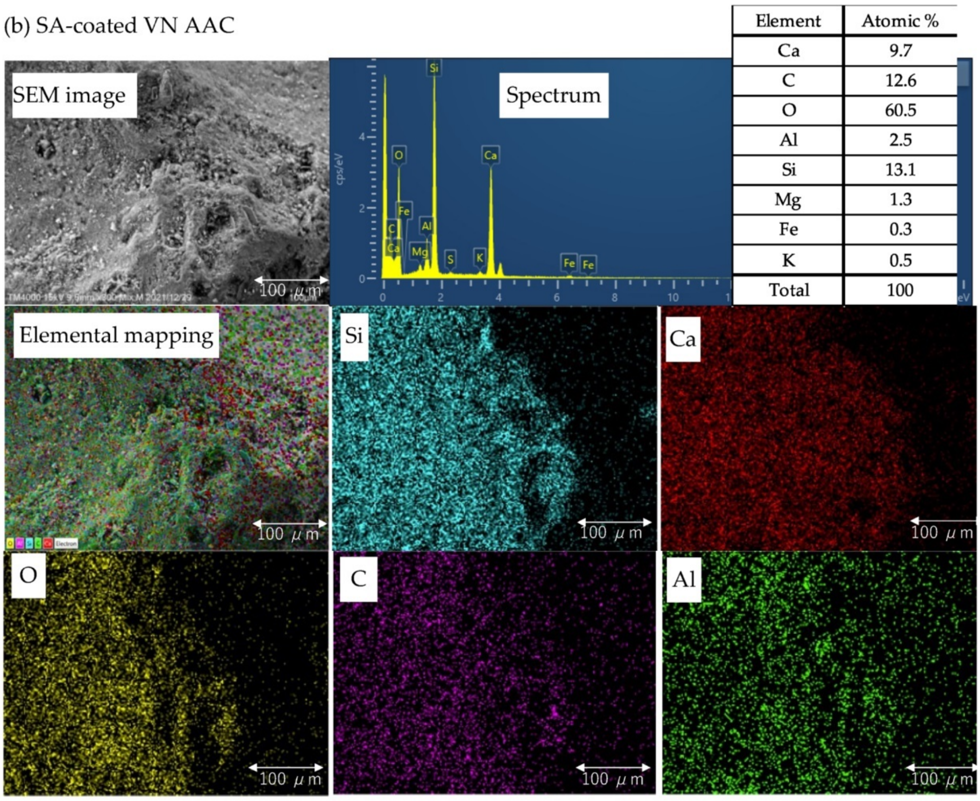

Element	Atomic %
Ca	9.7
C	12.6
O	60.5
Al	2.5
Si	13.1
Mg	1.3
Fe	0.3
K	0.5
Total	100

Figure 20. SEM-EDS images of (a) OA-coated VN-AAC grain (0.85–2.00 mm) at HA concentration = 14 g/kg and (b) SA-coated VN-AAC grain (0.85–2.00 mm) at HA concentration = 42 g/kg (Matsuno et al., 2022).

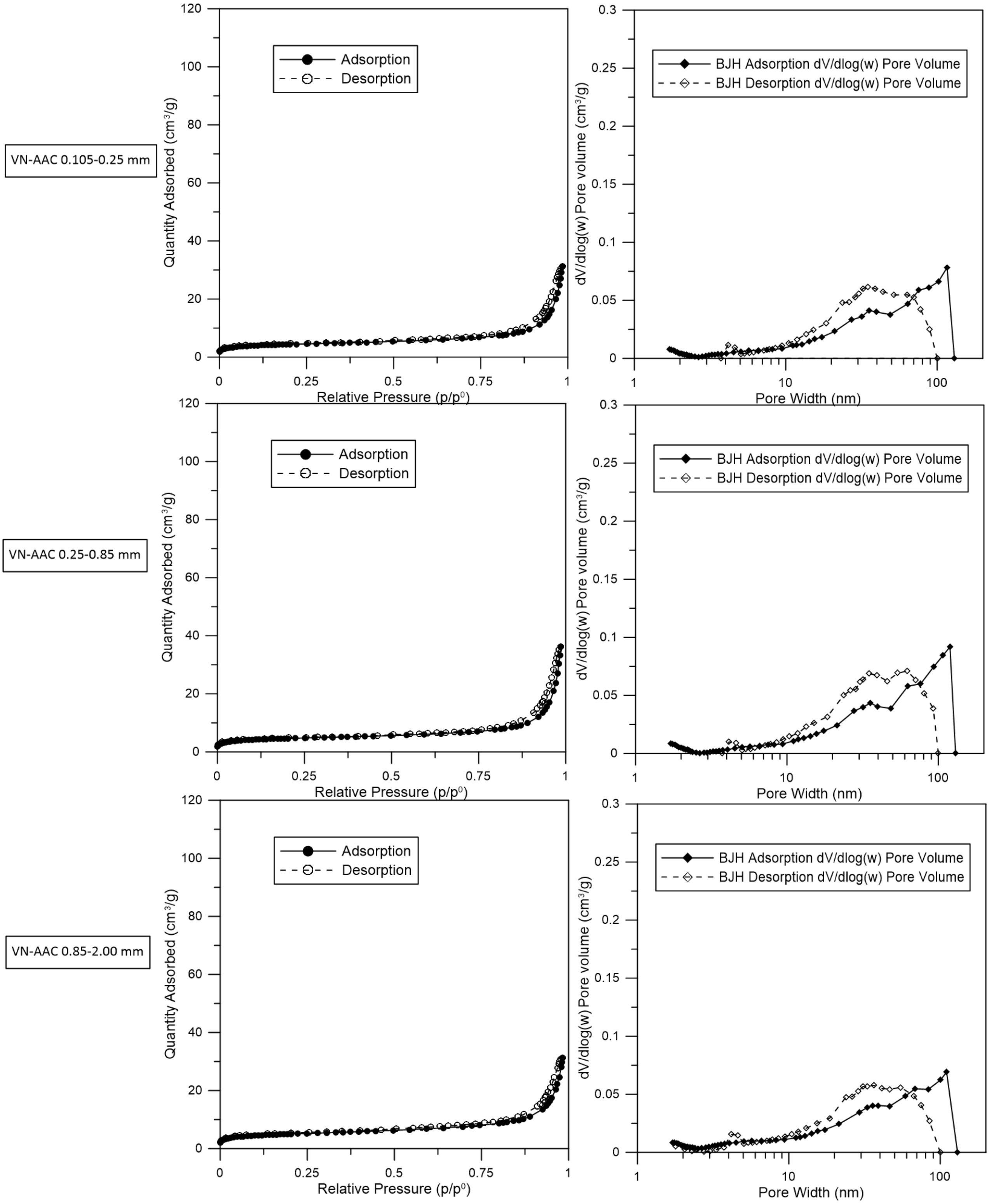

Figure 21. The nitrogen adsorption isotherm and pore particle size distribution data of VN-AAC.

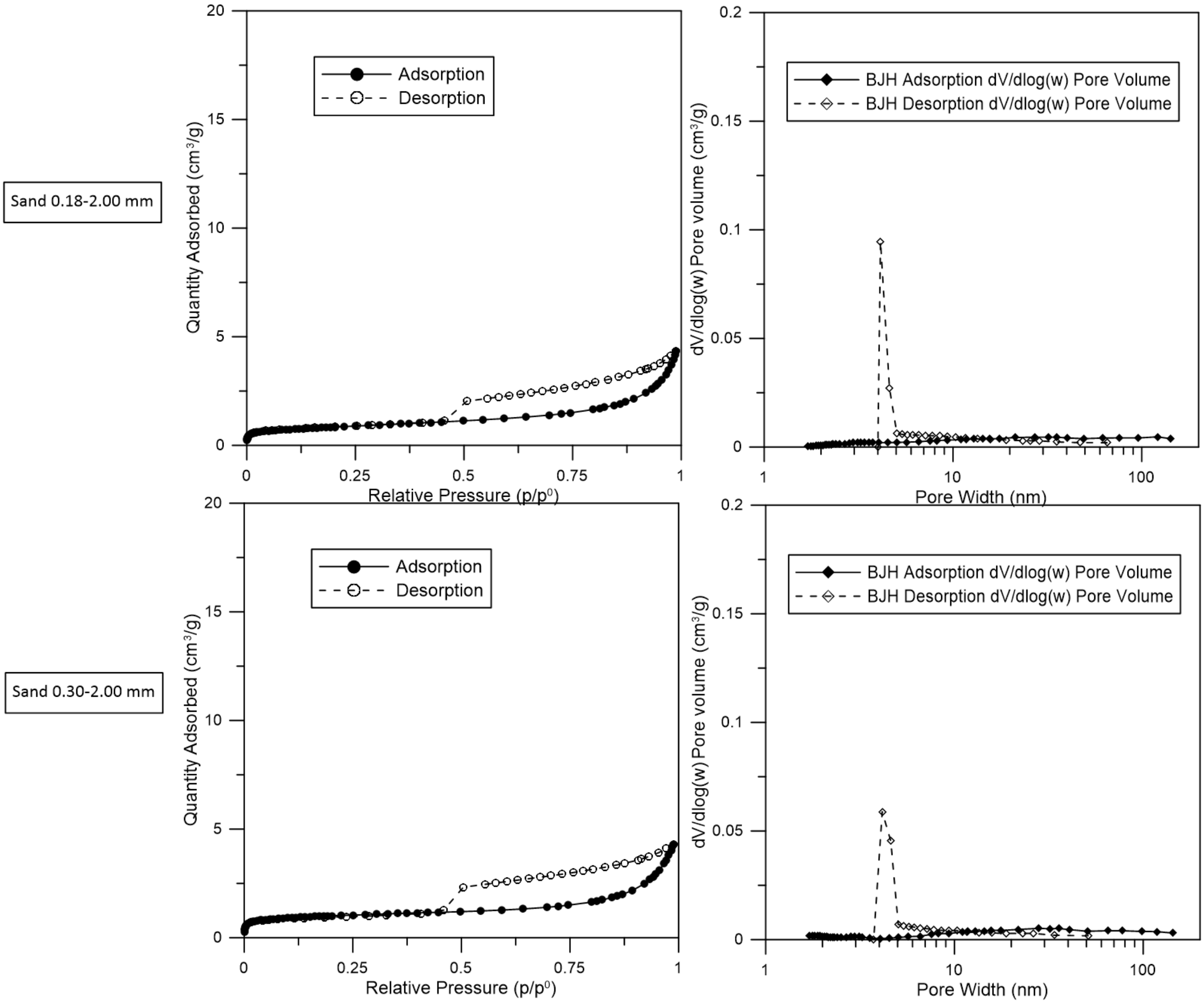

Figure 22. The nitrogen adsorption isotherm and pore particle size distribution data of Sand.

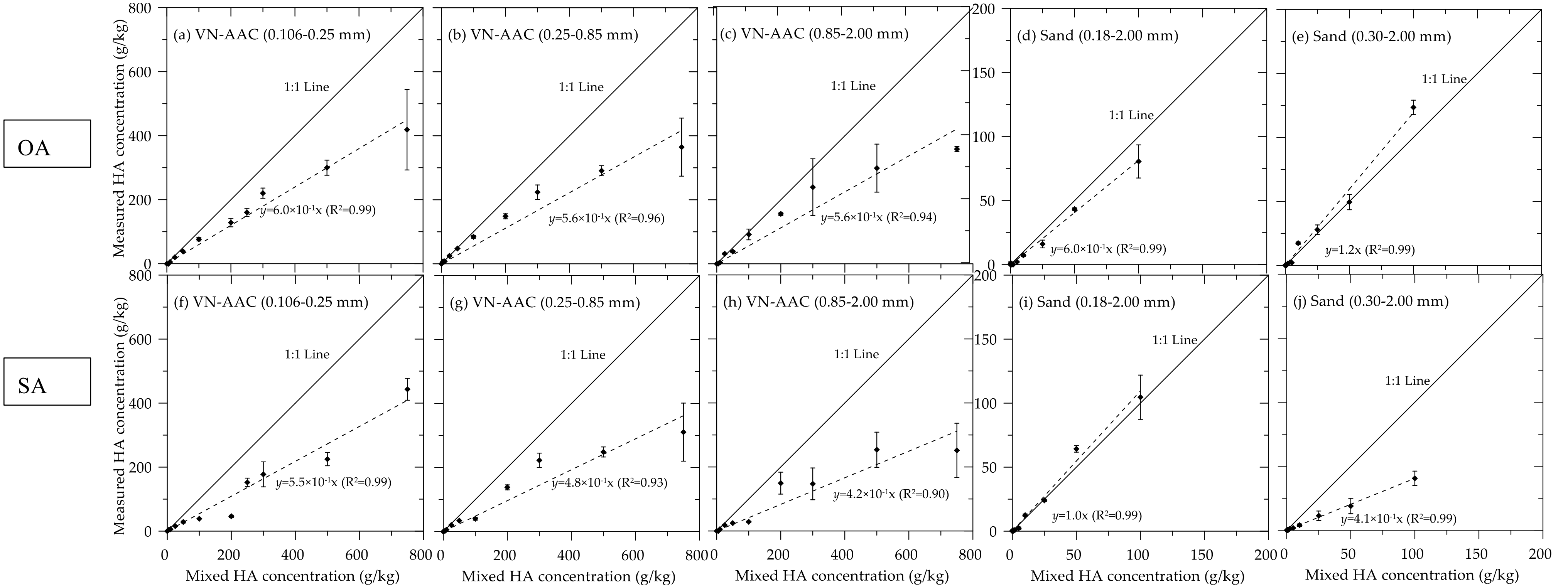

Figure 23. Relationships between measured and mixed HA concentrations for OA- and SA-coated VN AAC grains and sands. OA-coated VN-AAC grains: (a) Grain size = 0.106–0.25 mm, (b) Grain size = 0.25–0.85 mm, and (c) Grain size = 0.85–2.00 mm. OA-coated sands: (d) Grain size = 0.18–2.00 mm and (e) Grain size = 0.30–2.00 mm. SA-coated VN-AAC grains: (f) Grain size = 0.106–0.25 mm, (g) Grain size = 0.25–0.85 mm, and (h) Grain size = 0.85–2.00 mm. SA-coated sands: (i) Grain size = 0.18–2.00 mm and (j) Grain size = 0.30–2.00 mm (Matsuno et al., 2022).

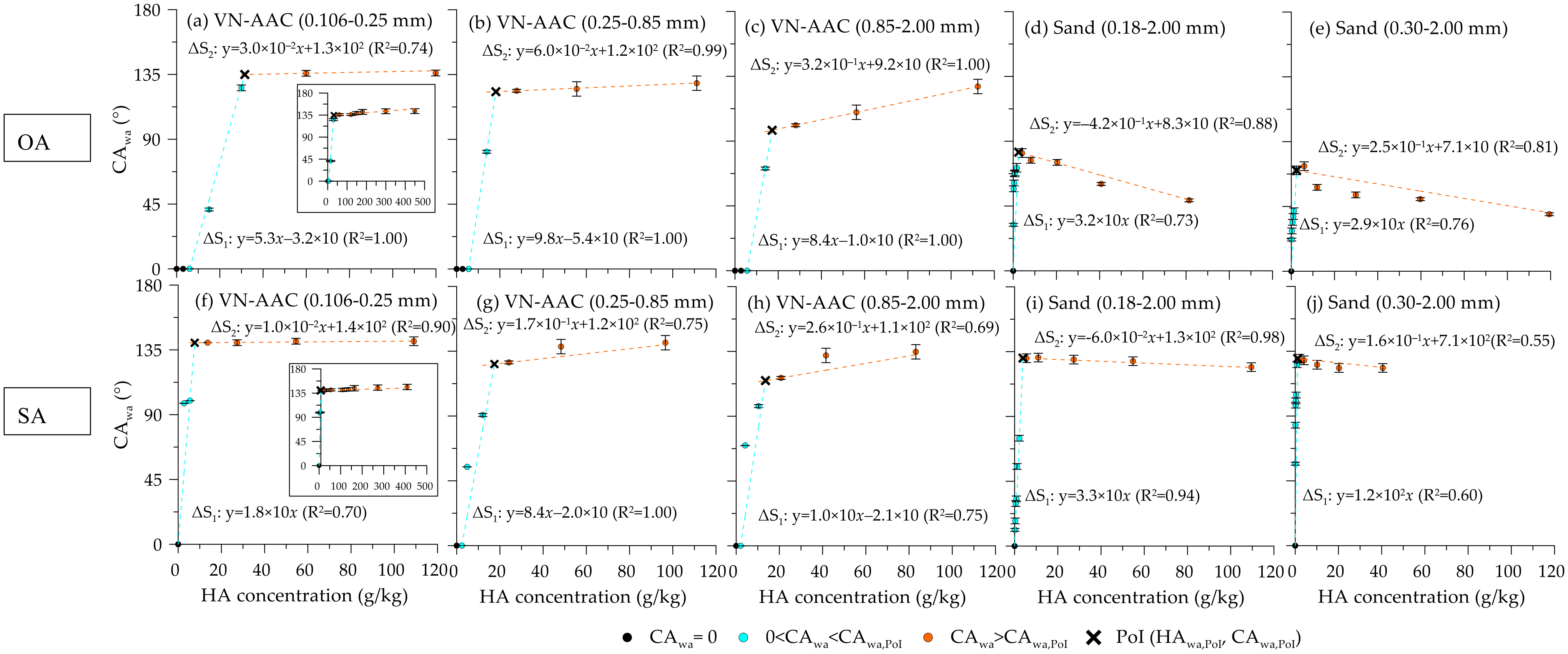

Figure 24. Relationships between $\mathrm{CA}_{\mathrm{ow}}$ and HA concentration of OA- and SA-coated VN-AAC grains and sands. OA-coated VN-AAC grains. (a) Grain size = 0.106–0.25 mm, (b) Grain size = 0.25–0.85 mm, and (c) Grain size = 0.85–2.00 mm. OA-coated sands: (d) Grain size = 0.18–2.00 mm and (e) Grain size = 0.30–2.00 mm. SA-coated VN-AAC grains: (f) Grain size = 0.106–0.25 mm, (g) Grain size = 0.25–0.85 mm, and (h) Grain size = 0.85–2.00 mm. SA-coated sands: (i) Grain size = 0.18–2.00 mm, and (j) Grain size = 0.30–2.00 mm (Matsuno et al., 2022).

Table 8. Summary of hydrophobicity/oleophilic parameters in this study and the literature (Matsuno et al., 2022).

Sample	Grain Size (mm)	Coating	CA_{wa}					CA_{ow}			Ref.
			$CA_{wa,max}$ (°)	$CA_{wa,PoI}$ (°)	$HA_{wa,PoI}$ (g/kg)	ΔS_1 (Slope)	ΔS_2 (Slope)	$CA_{ow,max}$ (°)	$CA_{ow,PoI}$ (°)	$HA_{ow,PoI}$ (g/kg)	
VN-AAC	0.106–0.25	OA	143	135	31.5	5.28	0.03	140	131	30.0	This Study
VN-AAC	0.25–0.85		129	123	18.2	9.77	0.06	130	124	13.9	
VN-AAC	0.85–2.00		128	98	17.2	8.42	0.32	124	119	28.1	
Slow sand	0.18–2.00		82	82	2.5	32.36	−0.42	138	0	20.3	
Rapid sand	0.30–2.00		73	70	2.4	28.77	−0.25	137	0	29.9	
VN-AAC	0.106–0.25	SA	146	140	7.7	18.29	0.01	138	80	54.5	
VN-AAC	0.25–0.85		141	126	17.5	8.37	0.17	130	121	12.2	
VN-AAC	0.85–2.00		135	115	13.6	9.99	0.26	124	106	20.8	
Slow sand	0.18–2.00		131	131	3.9	33.49	−0.06	138	0	27.4	
Rapid sand	0.30–2.00		130	130	1.1	115.14	−0.16	142	0	10.1	
Glass bead	0.075–0.25	OA	106	106	0.3	172.00	22.5	NA	NA	NA	Wijewardana et al., 2015
Accusand	0.105–0.25		76	76	1.0	58.00	15.1	NA	NA	NA	
Toyoura sand	0.105–0.25		97	97	0.3	388.00	0.25	NA	NA	NA	
Narita sand	0.105–0.25		94	94	1.3	86.00	0.25	NA	NA	NA	
Narita sand	0.25–0.425		93	93	1.0	93.00	0.1	NA	NA	NA	
Narita sand	0.425–0.84		79	79	1.3	89.00	0.11	NA	NA	NA	
Toyoura sand	0.105–0.25	OA	101	101	0.3	329.00	0.25	NA	NA	NA	Subedi et al., 2012
Quartz sand	0.05–0.25	SA	99	99	0.3	329.00	0.25	NA	NA	NA	Gonza´lez-Pen˜aloza et al., 2013
Quartz sand	0.25–0.5		100	100	1.0	36.00	0.06	NA	NA	NA	
Quartz sand	0.5–2.0		101	101	2.0	28.00	0.01	NA	NA	NA	

3.3.3 Contact Angles of Oil in Water (CA_{ow})

Measured contact angles of an oil droplet in water (CA_{ow}) of tested samples as a function of HA coating concentration are shown in Figure 25. For OA-coated VN-AAC samples (Figure 25a–c), the CA_{ow} values gradually decreased with increasing HA concentration (i.e., $CA_{ow,max}$ appeared at HA concentration = 0 g/kg). For SA-coated VN-AAC samples, on the other hand, the CA_{ow} decreased with increasing HA concentration in two steps, and a clear PoI (i.e., $HA_{ow,PoI}$) can be found. The measured values were fitted by an exponential equation in each step:

Step 1: $y = a \exp(-bx)$ (1)

Step 2: $y = a' \exp[-b'(x-c)]$ (2)

where a is the $CA_{ow,max}$ at HA concentration = 0 g/kg (°), b is the fitting parameter in Step 1, a' is the $CA_{ow,PoI}$ at $HA_{ow,PoI}$ (°), b' is the fitting parameter in Step 2, and c is the $HA_{ow,PoI}$ (g/kg). The measured $CA_{ow,max}$, $CA_{ow,PoI}$, and $HA_{ow,PoI}$ are also shown in Table 8.

As shown in Figure 25 and Table 8, the $CA_{ow,max}$ values of both OA- and SA-coated samples decreased with increasing grain size. The values of $CA_{ow,PoI}$ for SA-coated samples, however, were relatively constant (80–121°). The difference in the relationships between CA_{ow} and HA concentration for OA- and SA-coated VN-AAC might be attributed to characteristics of the HA coating. To understand this, the measured CA_{ow} were plotted against the measured specific surface area (SSA and A/B ratio measured by FT-IR) and are shown in Figure 26 and Figure 27. In the figure, the relationships between measured CA_{wa} and SSA are also shown as a reference. Compared to the relationship between CA_{wa} and SSA (Figure 26a,c,e), the relationships between CA_{ow} and SSA showed a big difference between SA- and OA-coated samples, especially in the region of Step 2 (Figure 26b,d,f). For each grain sample of VN-AAC, the SSA of SA-coated samples was higher than those of OA-coated samples. This indicates that SA coated porous grains (AAC) effectively without reducing SSA and reduced the CA_{ow} in Step 2 (oleophilicity) (Figure 25f–h) compared to OA-coated grains. In other words, the OA coating gave high CA_{ow} (oleophobicity) even when controlling the HA concentration. Considering the concept of affinity of dispersed oil and oil trap adsorbents (trapping of dispersed oil in wastewater), high oleophilic adsorbents (i.e., high hydrophobic adsorbents) are preferable for the fixed-bed grains in the oil/water separation system. Thus, an SA-coated AAC grain is likely to be more effective for oil/water separation compared to an OA-coated AAC grain.

The relationship between measured CA_{ow} as a function of HA concentration for sands, on the other hand, are shown in Figure 25d,e,j,i. The rapid linear decrease of CA_{ow} can be observed with increasing HA concentration and became CA_{ow} = 0° at HA= 9.4–28.9 g/Kg (corresponding to $HA_{ow,PoI}$; see also Table 8). The rapid decrease of CA_{ow} means that coated OA and SA easily formed the grain surface oleophilicity, indicating that HA-coated sands are more suitable for oil/water separation than HA-coated AAC grains. As shown in Table 7, however, the SSA of sands are much smaller than those of AAC grains, implying that the contact area between dispersed oil in wastewater and the oleophilized grain surface area is decreased. Thus, further studies are needed to examine the efficiency of oil/water separation and trapping capacity of dispersed oil in wastewater by carrying out oil adsorption tests (Akhavan et al., 2013; Qu et al., 2018; Atta et al., 2019; Wei et al., 2019) and fixed-bed column experiments (Wei et al., 2018, Mitra et al., 2021).

3.3.4 Relationships between Physicochemical Properties and Measured CA_{wa} and CA_{ow}

Finally, Pearson analysis was done to examine the correlations of measured CA_{wa} and CA_{ow} with physicochemical parameters in this study. The results are shown in Table 9. Note that data from the literature for sands (Lam et al., 2018; Kikuma et al., 2010; Ellerbrock et al., 2005) were also used in the analysis. The $|R^2|$values > 0.8 are given in bold in the Table.

It can be clearly seen that the SSA correlated well with both CA_{wa} and CA_{ow} for VN-AAC grains ($|R^2|$ > 0.80). The OC correlated well with CA_{wa} and CA_{ow} for OA-coated VN-AAC grains ($|R^2|$ = 0.72 and 0.92); however, it gave a low correlation with CA_{wa} for SA-coated VN-AAC grains (($|R^2|$ = 0.50). The A/B ratio calculated from FT-IR spectra, which are often used to characterize the hydrophobicity of soils (Tarchitzky et al., 2007; Bachmann et al., 2008; Voelkner et al., 2015; Parolo et al., 2017), gave low correlations with CA_{wa} for both VN-AAC grains and sands, suggesting the A/B ratio does not characterize the hydrophobicity (i.e., contact angle of water droplet in air) for tested cementitious AAC grains and sands.

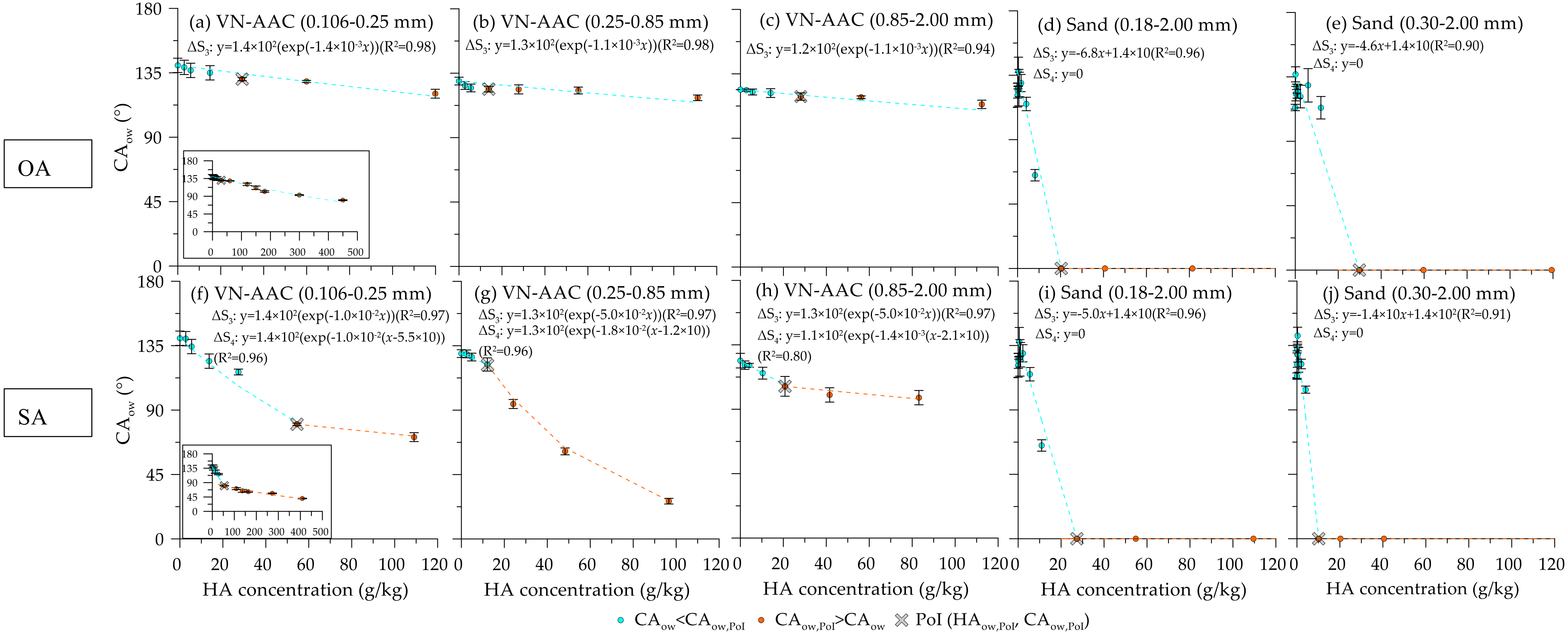

Figure 25. Relationships between CA_{ow} and HA concentration of OA- and SA-coated VN-AAC grains and sands. OA-coated VN-AAC grains. (a) Grain size = 0.106–0.25 mm, (b) Grain size = 0.25–0.85 mm, and (c) Grain size = 0.85–2.00 mm. OA-coated sands: (d) Grain size = 0.18–2.00 mm and (e) Grain size = 0.30–2.00 mm. SA-coated VN-AAC grains: (f) Grain size = 0.106–0.25 mm, (g) Grain size = 0.25–0.85 mm, and (h) Grain size = 0.85–2.00 mm. SA-coated sands: (i) Grain size = 0.18–2.00 mm, and (j) Grain size = 0.30–2.00 mm (Matsuno et al., 2022).

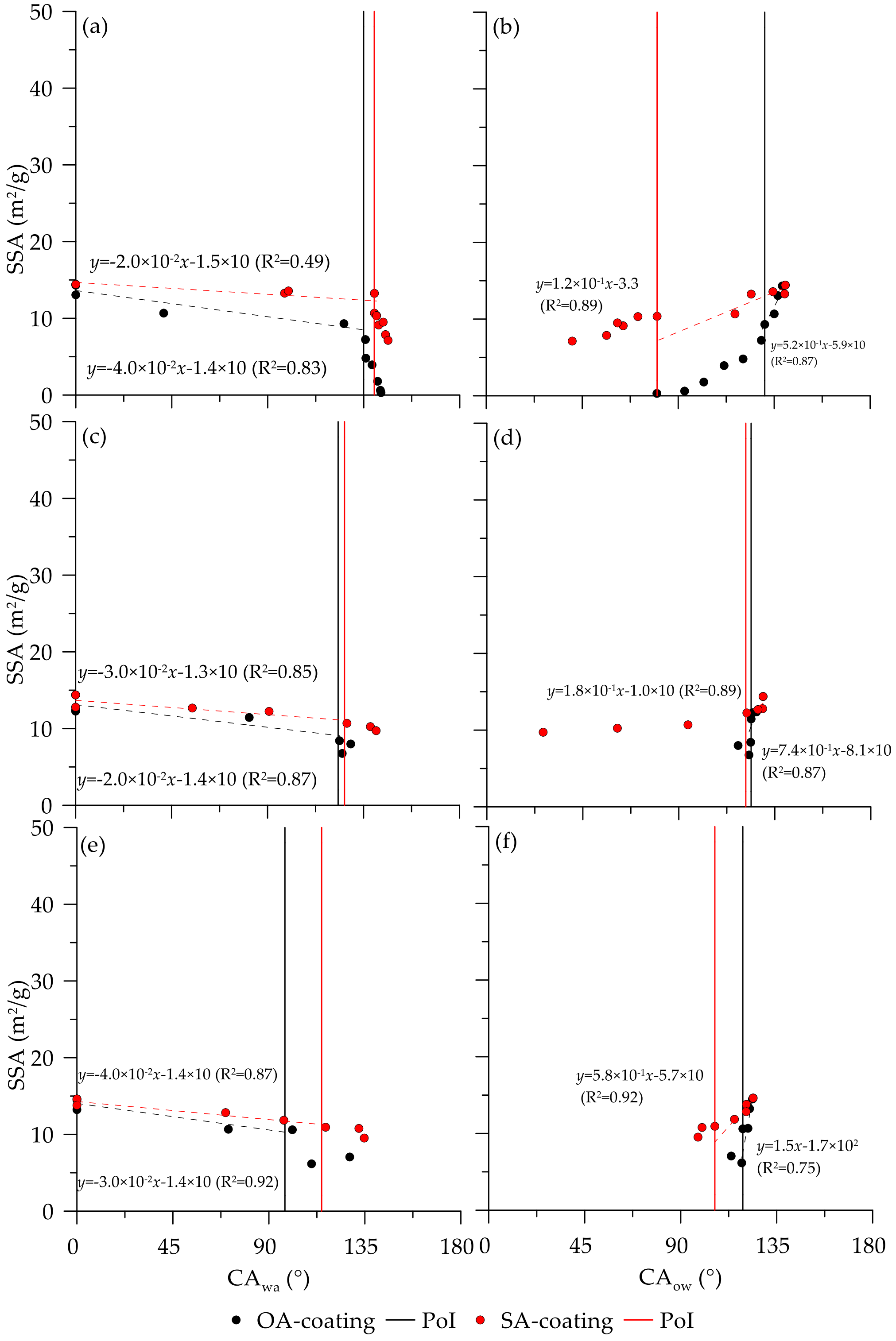

Figure 26. Relationships between SSA and CA_{wa}/CA_{ow} for OA- and SA-coated VN-AAC grains. OA-coated VN-AAC grain: (a,b) Grain size = 0.106–0.25 mm, (c,d) Grain size = 0.25–0.85 mm, and (e,f) Grain size = 0.85–2.00 mm (Matsuno et al., 2022).

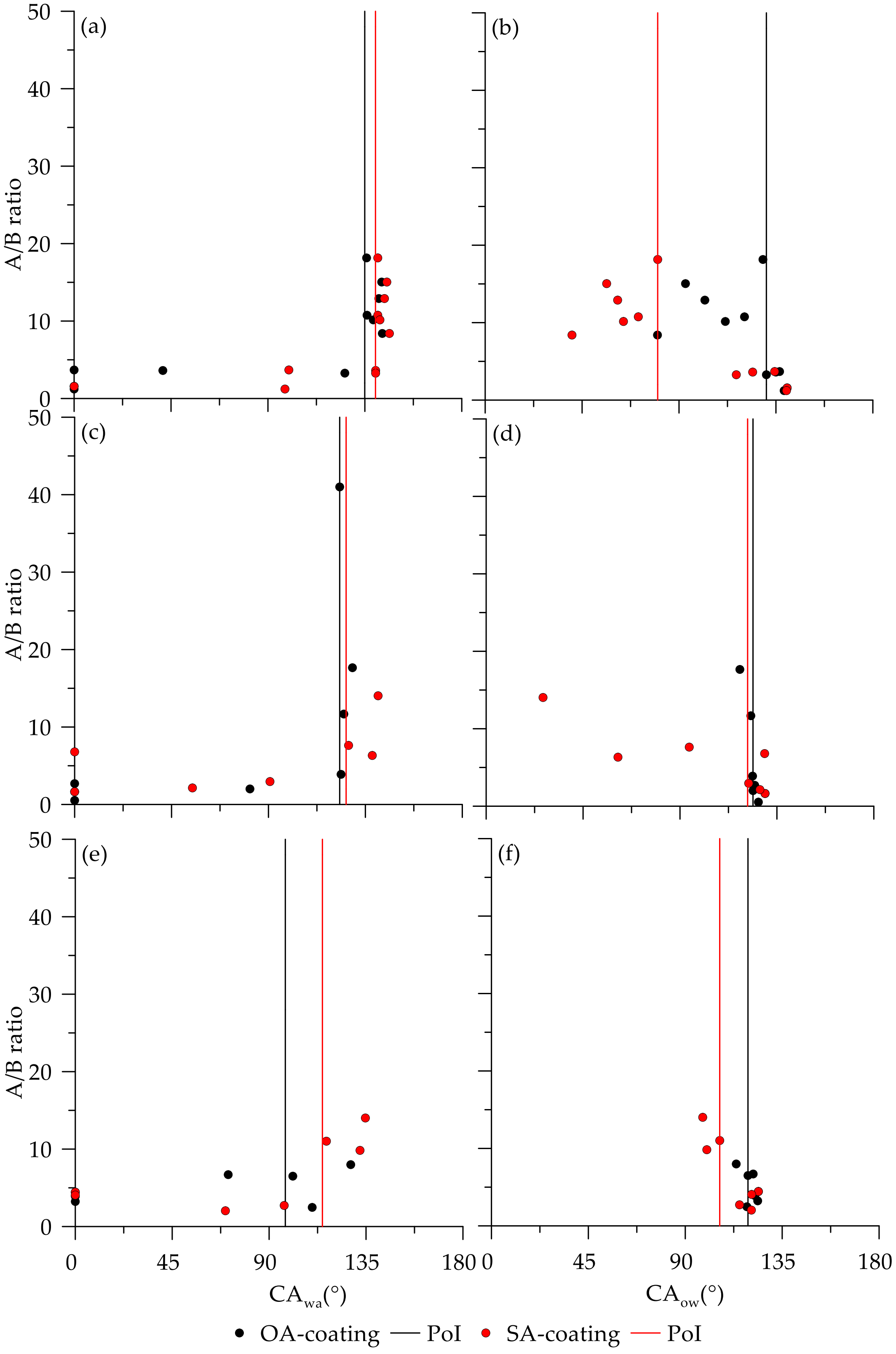

Figure 27. Relationships between A/B ratio and CA_{wa}/CA_{ow} for OA- and SA-coated VN-AAC grains. OA-coated VN-AAC grain: (a,b) Grain size = 0.106–0.25 mm, (c,d) Grain size = 0.25–0.85 mm, and (e,f) Grain size = 0.85–2.00 mm.

Table 9. Pearson correlation matrix of measured parameters for VN-AAC grains and sands tested in this study. Values >|0.80| are given in bold (Matsuno et al., 2022).

Sample	Coating		CA_{wa} (°)	CA_{ow} (°)	SSA (m^2/g)	OC (%)	A/B	No. of Samples
VN-AAC	OA	CA_{wa} (°)	1.00	−0.61	−0.88	0.72	0.72	25
		CA_{ow} (°)		1.00	0.82	−0.92	−0.49	
		SSA (m^2/g)			1.00	−0.91	−0.69	
		OC (%)				1.00	0.61	
		A/B					1.00	
	SA	CA_{wa} (°)	1.00	−0.66	−0.80	0.50	0.59	25
		CA_{ow} (°)		1.00	0.86	−0.75	−0.75	
		SSA (m^2/g)			1.00	−0.81	−0.74	
		OC (%)				1.00	0.50	
		A/B					1.00	
Sand	OA	CA_{wa} (°)	1.00	−0.15	−0.70	−0.01	0.59	23
		CA_{ow} (°)		1.00	0.75	−0.78	−0.61	
		SSA (m^2/g)			1.00	−0.54	−0.82	
		OC (%)				1.00	0.69	
		A/B					1.00	
	SA	CA_{wa} (°)	1.00	−0.55	−0.91	0.41	0.58	24
		CA_{ow} (°)		1.00	0.66	−0.75	−0.31	
		SSA (m^2/g)			1.00	−0.43	−0.85	
		OC (%)				1.00	0.29	
		A/B					1.00	

3.4 Concluding Remarks

In order to develop low-cost and high-performance oil/water separating filtration media, this study assessed the hydrophobicity/oleophilicity of porous grains made from AAC scrap coated with harmless hydrophobic agents (HA) such as oleic and stearic acids (OA and SA). For both OA- and SA-coated AAC grains, it was newly found the contact angles of water droplets in air (CA_{wa}) increased linearly with increasing HA concentration and then became almost constant and/or gently increased after a specific point (point of intersection, PoI). The HA concentration corresponding to PoI ($CA_{wa,PoI}$) can be applied to determine the minimum coating amount that gives the approximately maximum hydrophobicity of HA-coated porous grans as well as sands. The measured contact angles of an oil droplet in water (CA_{ow}) for AAC grains gave a gradual decrease exponentially with increasing HA concentration for both OA- and SA-coated AAC grains. Especially, the relationship between CA_{ow} and HA concentration for SA-coated AAC became a unique one, and the CA_{ow} decreased with increasing HA concentration in two steps. Based on Pearson correlation analysis, both CA_{wa} and CA_{ow} for HA-coated AAC grains were well correlated with the specific surface area (SSA) of tested materials, indicating that the SSA is a good indicator to quickly assessment hydrophobicity/oleophilicity (i.e., CA_{wa} and CA_{ow}) of HA-coated porous grains. Further studies are planned to quantitatively characterize oil/water separation efficiency using the HA-coated AAC grains in this study using the oil adsorption and fixed-bed column experiments (as given in Chapter 4).

Chapter 4 Oil sorption capacity of AAC

4.1 Introduction

There are various oil forms in oily wastewater, and it is challenging to treat emulsified dispersed oil and dissolved oil (Stuwart et al., 2009). However, these treatments are currently difficult to remove using simple oil/water separation techniques. Moreover, in this study, we will use AAC scrap and try to use it for oil/water separation techniques. Therefore, it is essential first to understand the sorption capacity of AAC. Although oil can be efficiently removed using physical or chemical methods, treatment is usually expensive and difficult to maintain—even with advanced technologies (Hassanshahian et al., 2014; Cheng et al., 2017). Adsorption is an attractive treatment process for oily wastewater because it is environmentally benign and offers excellent removal efficiencies. However, an effective and economical bio-sorbent is required (Yao et al., 2017).

Sorption is an attractive treatment process for oily wastewater because it is environmentally benign and offers excellent removal efficiencies. Sorption is a general term referring to two specific processes that occur simultaneously, i.e., adsorption, a process referring to the surface adhesion of molecules that acts according to their chemical and electrostatic interactions, and absorption, a phenomenon related to the assimilation of molecules through the sorbent mass (Medeiros et al., 2022; Oliveira et al., 2021). The intermolecular forces between a fluid and a sorbent material determine whether the liquid will tend to spread over the entire volume and surface of the sorbent (absorption) or minimize contact across the surface (adsorption). The occurrence of this mechanism depends on the molecular interactions of the fluid to be sorbed with the sorbent material. Polar chemical species in the fluid have a greater attractive force. In contrast, a nonpolar liquid tends to reach a state of conservation of energy, that is, when its molecules interact with each other and decrease contact with the surface (Medeiros et al., 2022; Torres et al., 2021).

In a previous study of oil sorption, Gong et al. (2007) showed the sorption effect of polycyclic aromatic hydrocarbons (PAHs) mixed with vegetable oil on activated carbon. Liu et al. (2018) showed adsorbed oily wastewater to raw and carbonized shells of fruit shell residue, respectively. Liu et al. (2018) found X. sorbifolia shell, without any modification, demonstrated highly efficient oil sorption compared to other biomaterials. Jain et al. (2020) showed that the adsorption performance of sesame (Sesamum indicum) oil cake (SOCP) and $ZnCl_2$ modified SOCP, a waste biomass from the oil extraction industry for remediation of Basic Blue 26 (BB 26) from aqueous media was examined. There are few previous studies on oil sorption, AAC, construction waste, and industrial by-products. Another feature is that few studies deal with oil in an emulsion and dispersed state and adsorb it. Therefore, the objective of this study is to use AAC to sorb oil in the dispersed state and to understand its characteristics, sorption capacity, and removal effect (*R*).

4.2 Material and Methods

4.2.1 Batch test

The AAC grains, Sands, Hydrophobic agents and coating used in this study are the same as in Chapter 3. In this study, dispersed oil was targeted, so the dispersed oil was created by dispersing soybean oil with an ultrasonic device (UP400st, Hielsher, Germany). Figure 28 shows the dispersing using this device. Batch test basically followed OECD (2000). However, the shaking speed was modified from 100 rpm/minute to 20 rpm/minute so that the coating does not peel off at high speed based on ASTM F726-99. The solid-liquid ratio was oil in water:sample=10:1 (L/S ratio=10) and horizontal shaking was applied. The horizontal shaking conditions were 20°C and 20 times/minutes for 1, 3, 6, 12, 24, and 48 hours. After that, it was allowed to stand still for 3 hours, and the oil in water and the solid sample in which the oil was adsorbed were separated (Figure 29).

4.2.2 Analysis

The oil concentration of the separated oil in water was measured by an oil content analyzer (OCMA–505–H, Horiba, Japan). Figure 30 compares the oil concentration of the n–hexane extract and the oil concentration measured by the oil content analyzer. A good linear relationship could be seen, so the actual value of the oil concentration was taken as the value obtained by multiplying the output value of the oil concentration meter by the linear regression equation in this study ($y=0.42x$; $R^2=0.99$).

Using this relationship, the equilibrium concentration C_e can be set for the measured oil concentration C from Eq. (3) in the case of OA, SA = 0 g/kg:

$$C_e = C/0.42 \tag{3}$$

In the case of OA, SA = 1, 2, 5, 10 g/kg:

$$C_e = (C - C_0)/0.42 \tag{4}$$

where C_0 is the oil concentration of $C_i = 0$ mg/L when OA and SA are 1, 2, 5, and 10 g/kg. Using the measured C_i and C_e, the removal percentage of dispersed oil in water (R, %) was calculated by Eq. (5):

$$R = 100 \times (C_i - C_e)/C_i \tag{5}$$

The oil sorption amount at equilibrium (mg/g) was obtained in Eq. (6):

$$q_e = (C_i - C_e)V/1000m_s \tag{6}$$

where V is the sorbate volume (= 100 mL of dispersed oil in water), and m_s is the sorbent amount (= 10 g of AAC grains or sand).

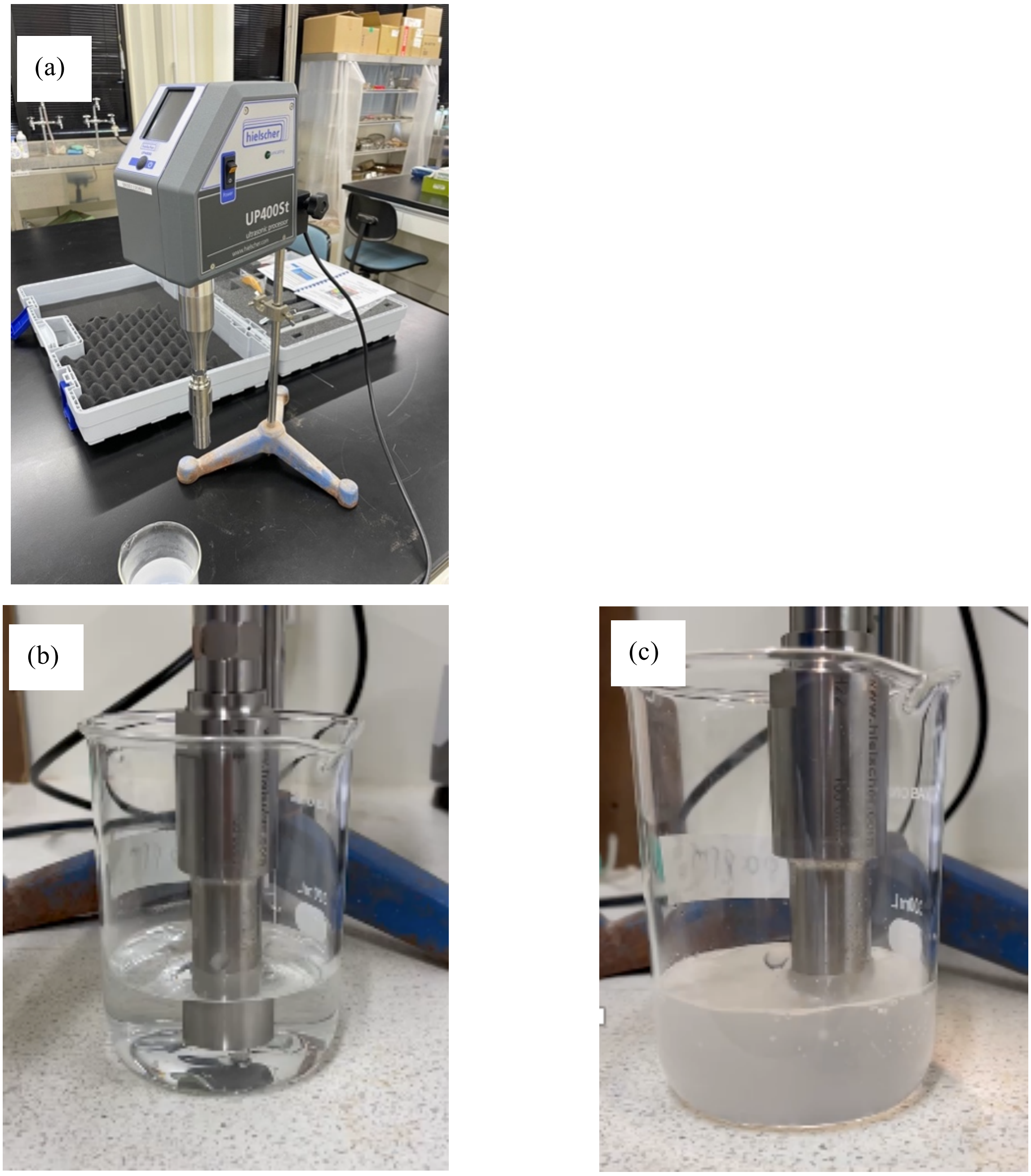

Figure 28. Dispersing soybean oil with an ultrasonic device. (a) UP400st (b)Before dispersing (c) After dispersing.

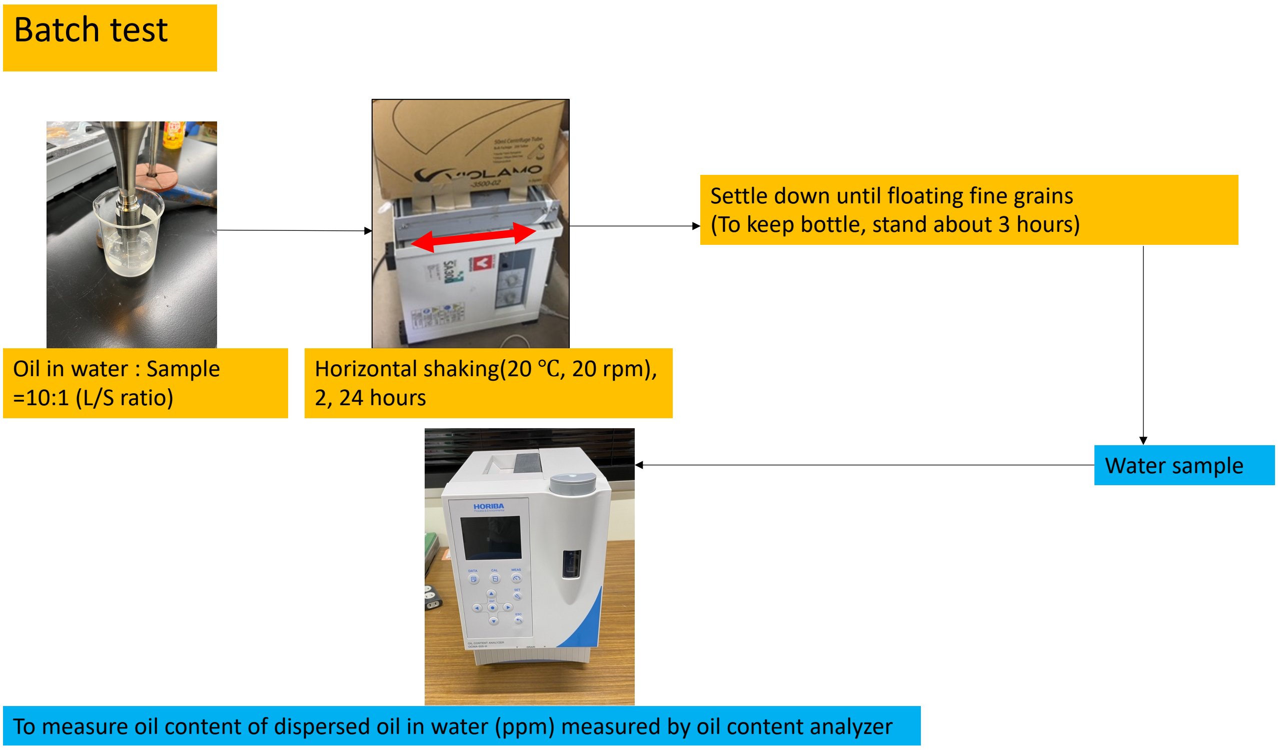

Figure 29. Flow of Batch test.

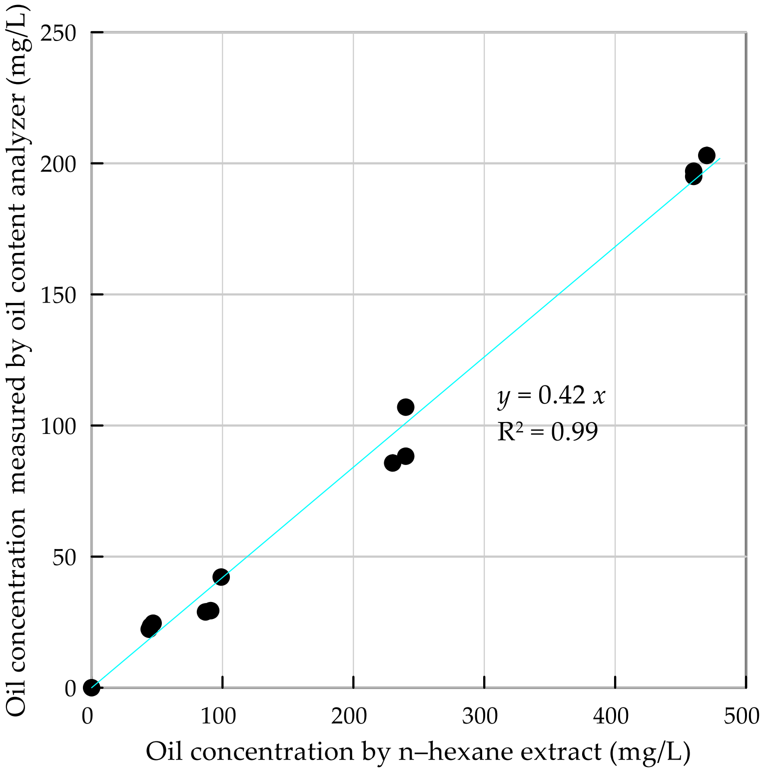

Figure 30. Relationship oil content measured by oil content analyzer to normal hexane measurement.

4.3 Results and Discussion

4.3.1 Particle size of dispersed oil

Figure 31 shows an image of each concentration that has been dispersed oil. Figure 32 shows the particle size of the dispersed oil measured by SALD. Looking at this, both C_i=1000 ppm and C_i=100 ppm dispersed oil have stable particle sizes for 24 hours. In addition, the most frequent particle size is about 0.1-1 µm.

4.3.2 Effects of shaking time on removal of dispersed oil in water

Figure 4 shows the effect of shaking time on the removal of dispersed oil, R (%), for tested AAC grains with different sizes at C_i = 1,000 mg/L. Although some variations in measured R values for all tested samples (non–coated, OA–, and SA–coated) were observed, the R values mostly increased with increased shaking time and became stable at 24 h of shaking. This suggests that the sorption process of dispersed oil onto AAC grains (especially, 0.250–0.850 and 0.850–2.00 mm in Figures. 4b and 4c) depends on the contact time to some extent, and that 24 h of shaking time would be suitable to examine the sorption capacity of tested AAC grains.

Figure 31. Dispersed oil each concentration (0, 10, 50, 100, 1000 ppm).

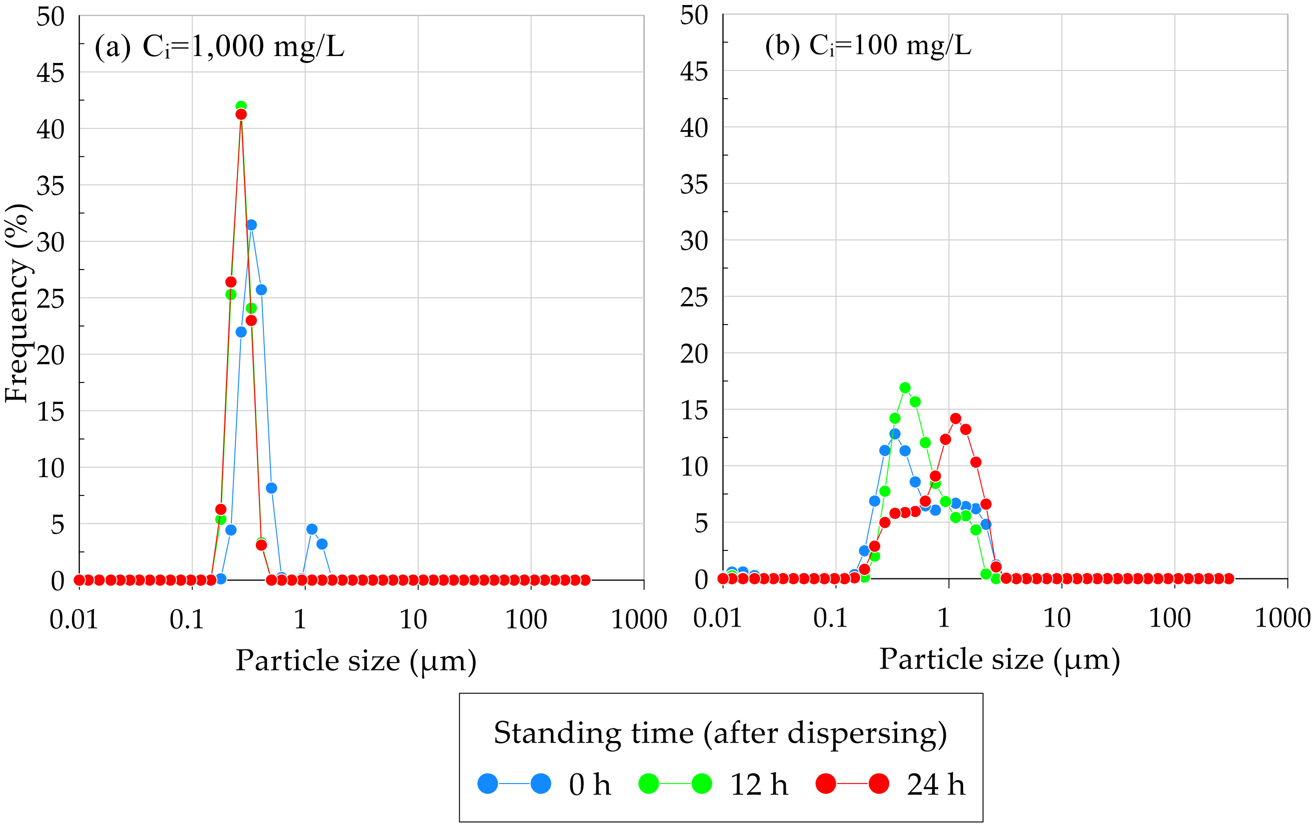

Figure 32. Particle size of the dispersed oil (a) C_i=1000 ppm (b) C_i=100 ppm.

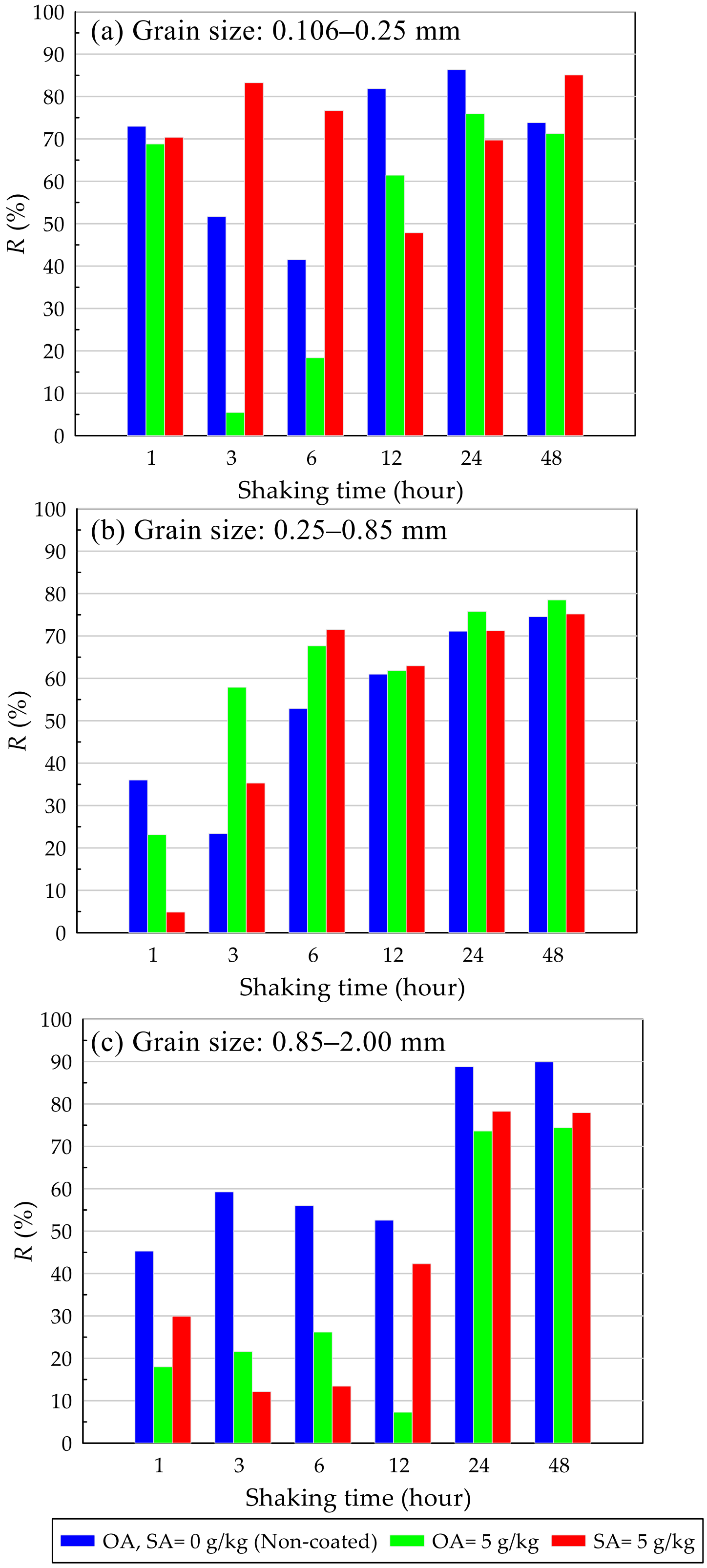

Figure 33. Measured *R* values for AAC grains with different shaking time at C_i = 1,000 mg/L: (a) 0.106–0.25 mm, (b) 0.25–0.85 mm, (c) 0.85–2.00 mm.

4.3.3. Effect of initial dispersed oil concentration on removal percent of dispersed oil

Measured R values for all tested AAC grains with different coating percent [OA/SA = 0 (non–coated), 1, 5, and 10%] at C_i = 10, 50, 100, and 1,000 mg/kg are shown in Figure 34. Overall, the grain size of AAC did not affect the measured R values for tested uncoated, OA–coated, and SA–coated samples in this study. For low C_i solutions such as 10 and 50 mg/L, AAC grains coated with OA = 1 g/kg (Figure 34b) and SA = 1 g/kg (Figure 34e) removed dispersed oil well, and measured R values became >80% irrespective of grain size. For high C_i solutions such as 100 and 1,000 mg/L, on the other hand, high SA–coated AAC grains (10 g/kg in Figure 34g) gave high R values of >80%. It is interesting that non–coated AAC grains also removed the high concentration dispersed oil solution (C_i = 1,000 mg/L) well, and the R values became > 80% (Figure 34a).

Figure 35, for reference, shows the measured R values of control sands with different sizes at C_i = 10, 50, 100, and 1,000 mg/L. The measured R values were lower than those from AAC grains (Figure 5) in the whole range of C_i. Especially, the coating of hydrophobic/oleophilic agents for sands did not contribute to the removal of dispersed oil at the low concentration of C_i = 10 mg/L (i.e., R values became < 5%).

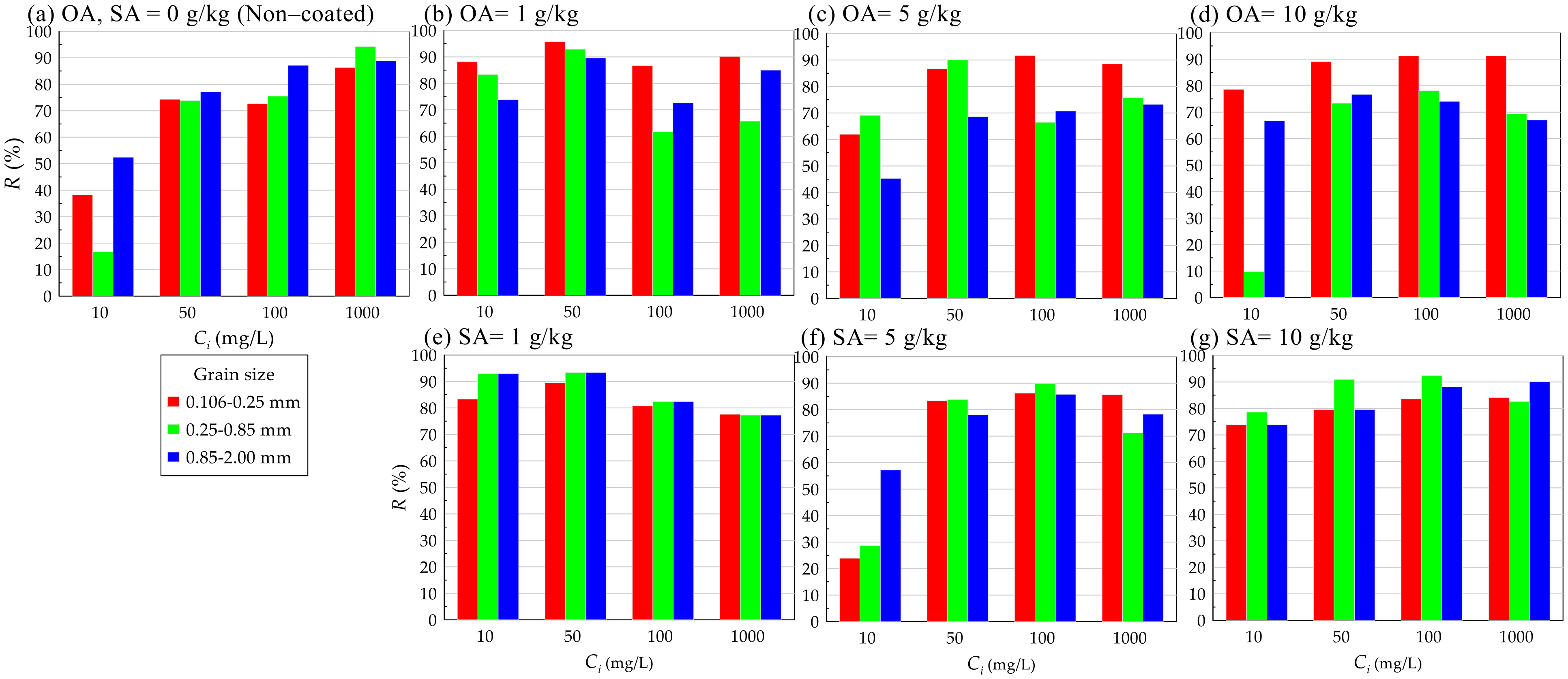

Figure 34. Measured *R* values for AAC grains with different size and different coating conditions at C_i = 10, 50, 100, and 1,000 mg/kg.

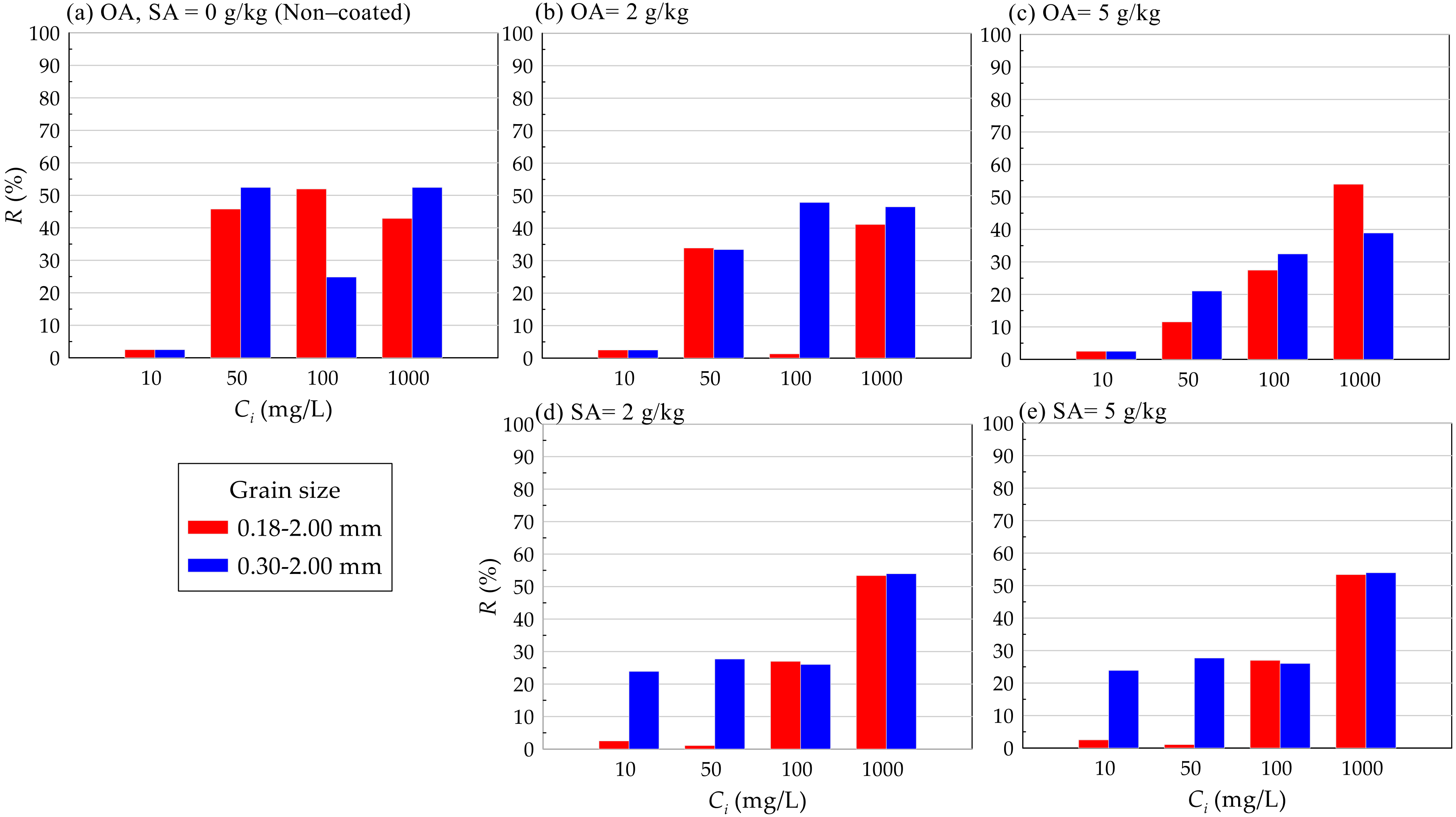

Figure 35. Measured *R* values for sands with different size and different coating conditions at C_i = 10, 50, 100, and 1,000 mg/kg.

4.3.4. Application of adsorption isotherm models to characterize the dispersed oil sorption onto AAC grains

In order to understand the sorption properties of dispersed oil in water onto AAC grains, adsorption isotherm models, Langmuir model (Langmuir, 1918), Freundlich model (Freundlich, 1922), and a simple linear model commonly used to characterize the adsorption process, and mechanism of dissolved ions and metals onto adsorbents were applied. The Langmuir model described the relationship between C_e and q_e :

$$1/q_e = 1/\mathrm{q}_{\mathrm{max}} + 1/(\mathrm{K}_{\mathrm{L}}\mathrm{q}_{\mathrm{max}}C_e) \qquad (7)$$

where $\mathrm{q}_{\mathrm{max}}$ (mg/g) is the maximum adsorption capacity, and K_{L} (L/mg) is the Langmuir adsorption equilibrium constant. The Freundlich model is described as:

$$q_e = \mathrm{K}_{\mathrm{F}}C_e^{1/n} \qquad (8)$$

where K_{F} (mg/g) is the Freundlich constant and 1/n is the adsorption intensity factor or surface heterogeneity. A simple linear adsorption model is described:

$$q_e = \mathrm{K}_{\mathrm{d}}C_e \qquad (9)$$

where K_{d} is the linear adsorption coefficient (L/mg).

The fitted parameters for adsorption isotherms models are summarized in Table 10, and the measured relationship between C_e and q_e for non–coated AAC grains and AAC grains coated at OA/SA = 5 g/kg are exemplified in Figure 36.

It can be seen that the Langmuir model did not capture the measured relationship between C_e and q_e, and unrealistic $\mathrm{q}_{\mathrm{max}}$ values (i.e., negative values) were given (not shown in Figure 36), indicating that the sorption mechanism of dispersed oil onto AAC grains did not follow the basic adsorption concept of dissolved ions (i.e., saturation of adsorption site) and surface chemical reactions (e.g., formation of surface complexation). Both the Freundlich and linear models, on the other hand, captured the C_e and q_e relationships well. However, the Freundlich model did not capture the measured relationships of SA–coated AAC grains with 5 g/kg in this study (e.g., Figure 36h). Thus, the simple linear model performed the best among the models (R^2 values became mostly 0.99), and the fitted K_{d} values became a good indicator to characterize the sorption ability of dispersed oil in water onto both non–coated and coated AAC grains with hydrophobic/oleophilic agents. In addition, it is interesting that non–coated AAC grains 0.25–0.85 mm gave the highest value of 0.136 among of fitted K_d values (Table 10). This may support choosing a suitable grain size for treating oily wastewater because we did not observe a clear difference in measured R values among three grain size samples (Figure 34). For reference, the measured relationship between q_e to C_e for sands was shown in Figure 37. It can be seen that only the linear model captured the relationships well.

Some previous studies examined the applicability of oil sorption onto adsorbents based on adsorption isotherm models (Langmuir and Freundlich) and reported the adsorption parameters (Huang et al., 2018; Gong et al., 2007; Jing et al., 2022) that are given in Table 10. Those studies showed a good applicability of Langmuir and Freundlich models and determined the parameters such as q_{max} and K_F. It is noted that these studies targeted the sorption of emulsified oil onto adsorbents. The existing form of oil in water is different from that in this study.

Table 10. Measured and reported parameters for adsorption isotherm models.

			Langmuir			Freundlich			Linear			
Sample	**Particle size (mm)**	**Coating (g/kg)**	**q_{max}**	**K_L**	**R^2**	**1/n**	**K_F**	**R^2**	**K_d**	**R^2**	**Target Oil**	**Ref.**
AAC	0.106–0.25	0	–0.21	–0.03	0.87	1.649	0.003	0.96	0.061	0.99	*Soybean oil	This Study
	0.25–0.85		–1.74	–0.01	0.99	2.979	0.0001	0.92	0.136	0.94		
	0.85–2.00		64.48	0.001	0.89	1.524	0.009	0.93	0.078	0.99		
	0.106–0.25	OA=1	–1.64	–0.05	0.84	0.921	0.117	0.92	0.091	0.99		
	0.25–0.85		–6.72	–0.01	0.87	0.697	0.089	0.88	0.019	0.99		
	0.85–2.00		–1.15	–0.03	0.87	1.036	0.040	0.92	0.056	0.99		
	0.106–0.25	OA=5	–0.27	–0.06	0.74	1.279	0.026	0.87	0.077	0.99		
	0.25–0.85		–1.02	–0.01	0.65	1.058	0.021	0.88	0.031	0.99		
	0.85–2.00		–0.25	–0.02	0.89	1.401	0.004	0.95	0.027	0.99		
	0.106–0.25	OA=10	–0.24	–0.01	0.38	2.951	0.00001	0.83	0.104	0.99		
	0.25–0.85		–0.05	–0.01	0.28	2.106	0.00001	0.60	0.023	0.99		
	0.85–2.00		–0.29	–0.01	0.58	1.573	0.001	0.87	0.020	0.99		
	0.106–0.25	SA=1	–3.05	–0.02	0.98	0.879	0.069	0.98	0.035	0.99		
	0.25–0.85		3.50	0.04	0.99	0.733	0.135	0.98	0.034	0.99		
	0.85–2.00		–6.86	–0.02	0.91	0.597	0.183	0.92	0.017	0.99		
	0.106–0.25	SA=5	–0.15	–0.03	0.35	1.562	0.004	0.71	0.060	0.99		
	0.25–0.85		–0.21	–0.03	0.33	1.037	0.023	0.65	0.025	0.99		
	0.85–2.00		–0.36	–0.03	0.92	1.158	0.020	0.92	0.036	0.99		

Table 10. Continued.

	0.106–0.25	SA=10	–1.42	–0.02	0.99	1.146	0.028	0.99	0.053	0.99		
	0.25–0.85		–0.54	–0.06	0.90	0.952	0.076	0.91	0.048	0.99		
	0.85–2.00		–0.92	–0.03	0.99	1.316	0.023	0.98	0.090	0.99		
Sands	0.18–2.00	0	–0.01	–0.02	0.90	1.470	0.020	0.76	0.005	0.99	*Soybean oil	This Study
	0.30–2.00		–0.02	–0.02	0.86	1.712	0.006	0.83	0.011	0.99		
	0.18–2.00	OA=2	–0.02	–0.01	0.78	1.843	0.00002	0.69	0.007	0.99		
	0.30–2.00	OA=5	–0.01	–0.01	0.82	1.991	0.00003	0.80	0.009	0.99		
	0.18–2.00	OA=2	–0.01	–0.01	0.82	2.746	0.0000004	0.93	0.011	0.99		
	0.30–2.00	OA=5	–0.01	–0.01	0.78	2.169	0.00001	0.84	0.006	0.99		
	0.18–2.00	OA=2	0.07	0.003	0.87	2.077	0.00001	0.85	0.011	0.99		
	0.30–2.00	OA=5	–0.40	–0.01	0.99	1.440	0.001	0.99	0.011	0.99		
	0.18–2.00	SA=2	–0.12	–0.01	0.79	1.413	0.0004	0.89	0.006	0.99		
	0.30–2.00	SA=5	–0.01	–0.02	0.62	1.328	0.001	0.61	0.007	0.99		
Graphite powders	<0.03	Activated carbons	25	0.004	0.9	0.82	0.16	0.77	–	–	*Diesel oil	Huang et al. (2018)
Activated carbons	0.5–2.0	0	16–86	0.007–0.01	0.94–0.99	0.18–0.5	0.4–5.0	0.93–0.99	–	–	Vegetable oil	Gong et al. (2007)
Wakame	–	Biochar/Ni	8.65–116.5	0.113–0.481	0.964–0.999	0.03–0.1	3.45–7.21	0.806–0.965	–	–	Diesel oil	Jing et al. (2022)

*Dispersed or Emulsified oil

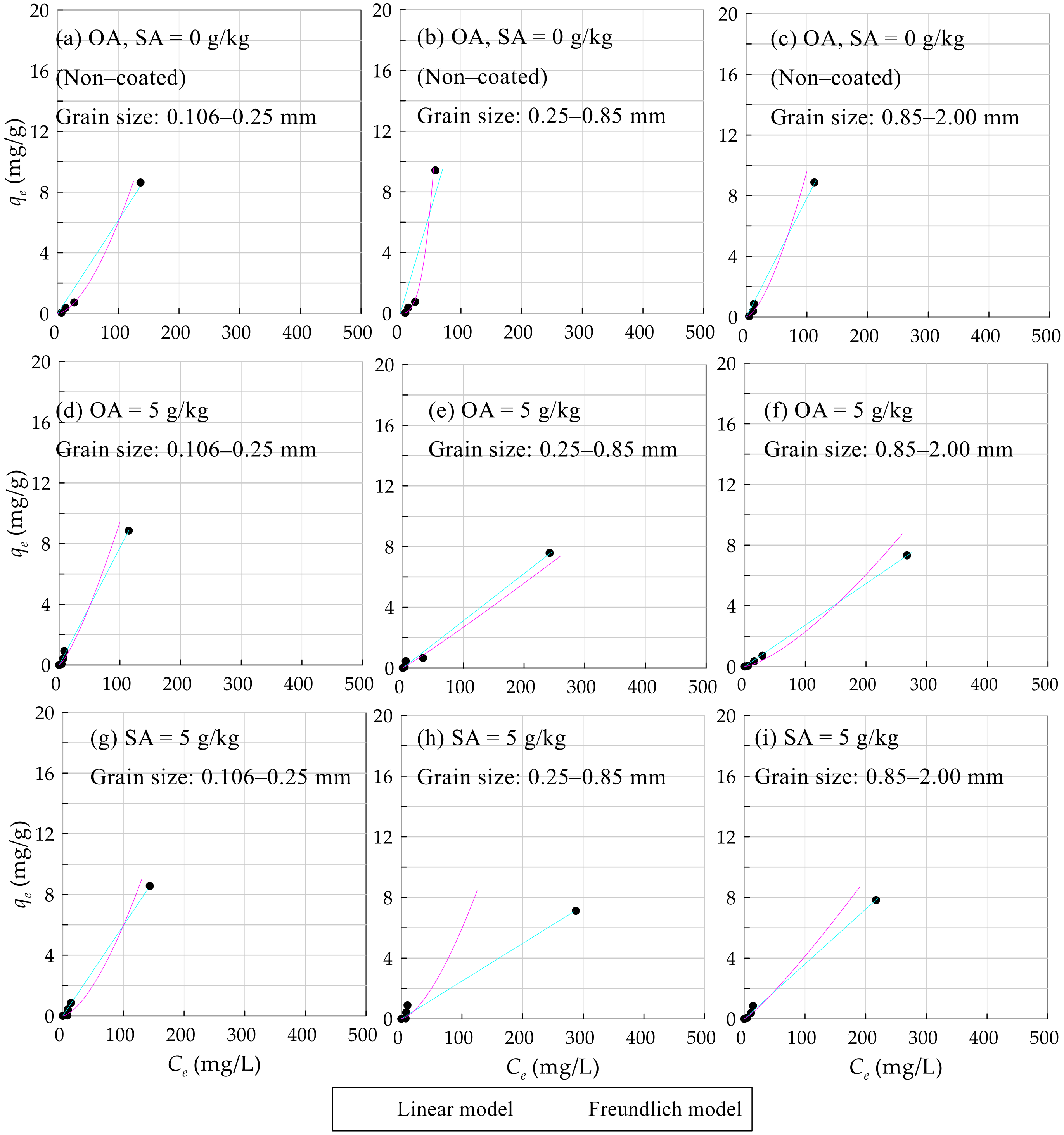

Figure 36. Relationship between q_e and C_e for AAC grains.

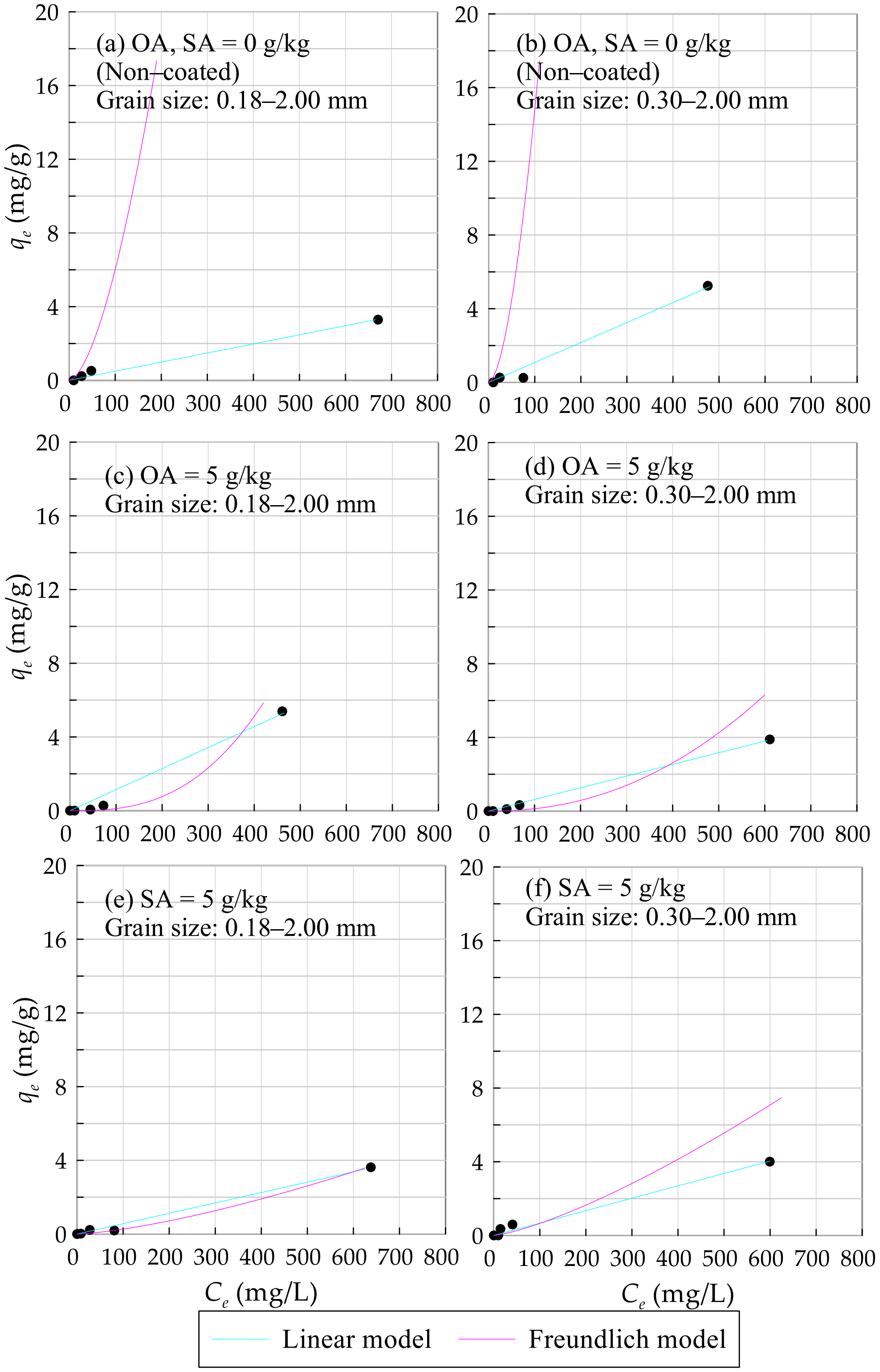

Figure 37. Relationship between q_e and C_e for sands.

4.4 Concluding Remarks

The study examined the applicability of hydrophobized/oleophilized AAC grains to treat dispersed oil in water. Based on the tested results from batch experiments, low-coated AAC grains with OA and SA (1 g/kg) removed dispersed oil well for low oil concentration solutions, and high SA-coated AAC grains (10 g/kg) gave high removal efficiency for high oil concentration solutions. Typical adsorption isotherm models for dissolved ions such as Langmuir, Freundlich, and a linear model were adapted to measured data. It was observed that the sorbed dispersed oil increased linearly with increasing equilibrium concentration for all tested samples, while the Langmuir model, on the other hand, did not capture the measured isotherms, indicating that the fitted K_d in the linear model became a good indicator to characterize the sorption ability of AAC grains. Further studies and more careful consideration are needed to understand the sorption mechanism and to determine the maximum sorption capacity of dispersed oil in water. Moreover, low-cost and reused AAC grains can be used for the treatment of oily wastewater. In the future, it is necessary to examine the removal characteristics of dispersed oil under solution flowing condition.

Chapter 5 Summary, Conclusions, and Perspectives

To develop low-cost and high-performance oil/water separating filtration media, this study assessed the hydrophobicity/oleophilicity of porous grains made from Vietnam AAC scrap coated with harmless hydrophobic agents (HA) such as oleic and stearic acids (OA and SA). According to a review of previous studies, the studies using granular materials were basically divided into studies using adsorption and filtration to examine the oil removal efficiency in water. Most of the tested samples in the previous studies gave high contact angles of water in air and oil in water (CA_{wa}, CA_{ow}) over 140°.

This study carefully examined the relationship between CA_{wa}, CA_{ow} and HA coating amount using three grains from VN-AAC and control sands with different grain sizes in the laboratory. As a result, Point of Intersection (PoI) was newly observed as the boundary between the saturated and unsaturated amounts of HA coating, suggesting that it can be understood that the coating conditions of the porous grain surface highly affect the measured CA_{wa} and CA_{ow}. These relationships between physical/chemical properties and measured CA_{wa} and CA_{ow} were also examined. It was found that the specific surface area (SSA) of tested samples were well correlated with observed PoI in CA_{wa} and CA_{ow}. Next, the oil sorption tests were carried out using a batch test in the laboratory for OA- and SA-coated VN-AAC grains. The results showed that the removal rate (removal % of dispersed oil) depended on the grain size of VN-AAC, OA-coated samples with 1 g/kg gave the high oil removal efficiency, and SA-coated samples with 10 g/kg gave the maximum oil removal percent in the full range of initial dispersed oil concentration from 10 to 1000 ppm.

Based on the above tested results in this study, it can be understood that the surface condition of HA coated samples, i.e., (a) Non-coated (b) unsaturated and (c) saturated with HA coating materials, highly affects the assessment of CA_{wa} and CA_{ow}, and the removal efficiency of dispersed oil in water (Figure 38). At the Non-coated surface condition hydrophilic functions would contribute to oil adsorption (Figure 38a), only unsaturated surface condition (Figure 38b), a well-balanced oleophobic, lipophilic, hydrophobic and hydrophilic functions would contribute to oil adsorption. At the saturation surface condition (Figure 38c), on the other hand, it could be understood that the coating materials fully covered the surface pores of AAC (i.e., adsorption sites) resulting only hydrophobic and lipophilic functions contributed to the adsorption of dispersed oil (means low adsorption site with low removal rate).

Finally, the relationship between CA_{wa} or CA_{ow} and *R* is shown. Figure 39 shows that there is a correlation between CA_{ow} and *R*, especially in the case of *R*. This indicates the contribution of the contact angle to oil removal in this study. This is also consistent with previous studies, although there are differences in the use of emulsified or dispersed oil and differences in solid-liquid ratios that preclude simple comparisons.

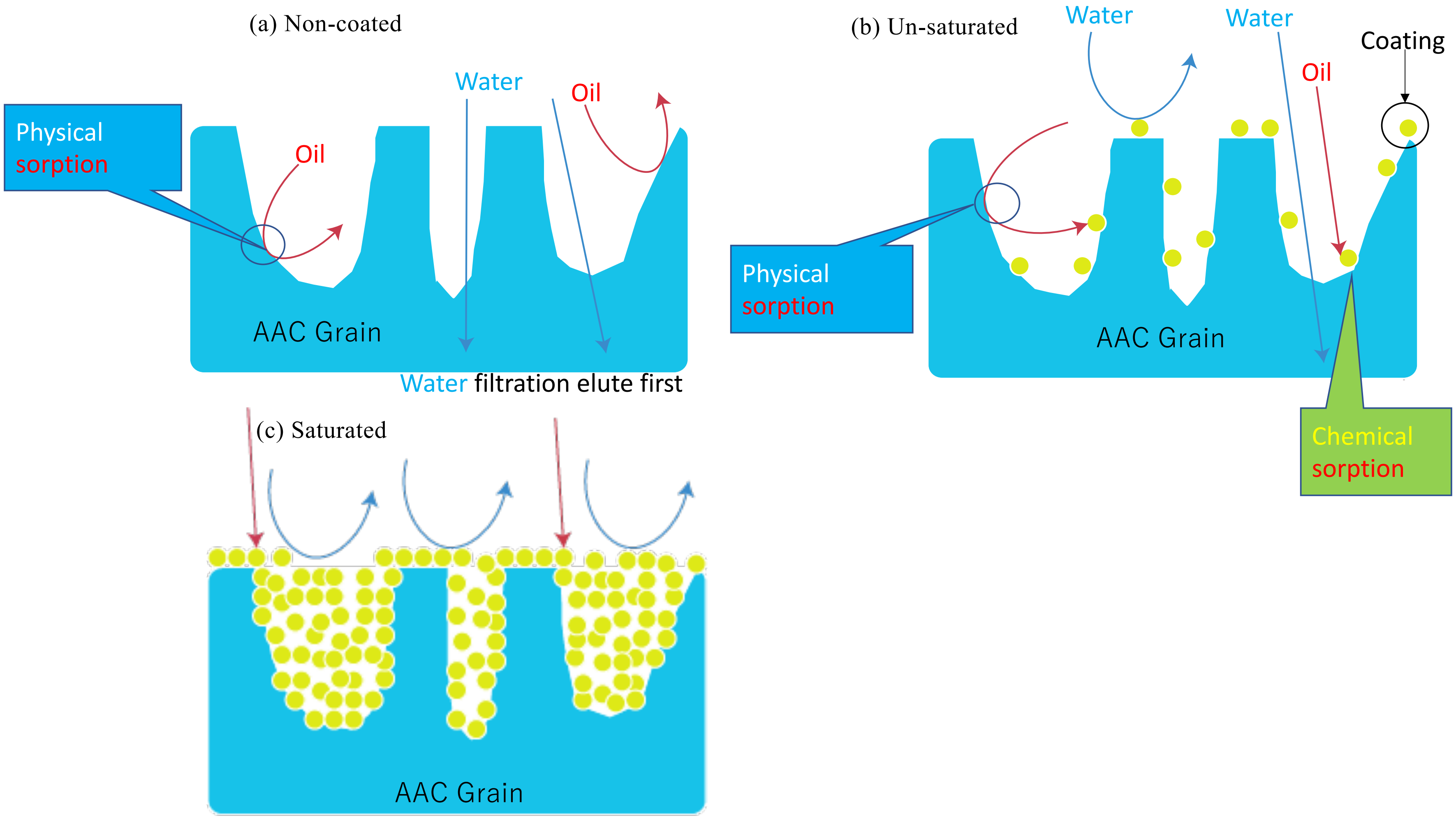

Figure 38. Image of porous material after coating.

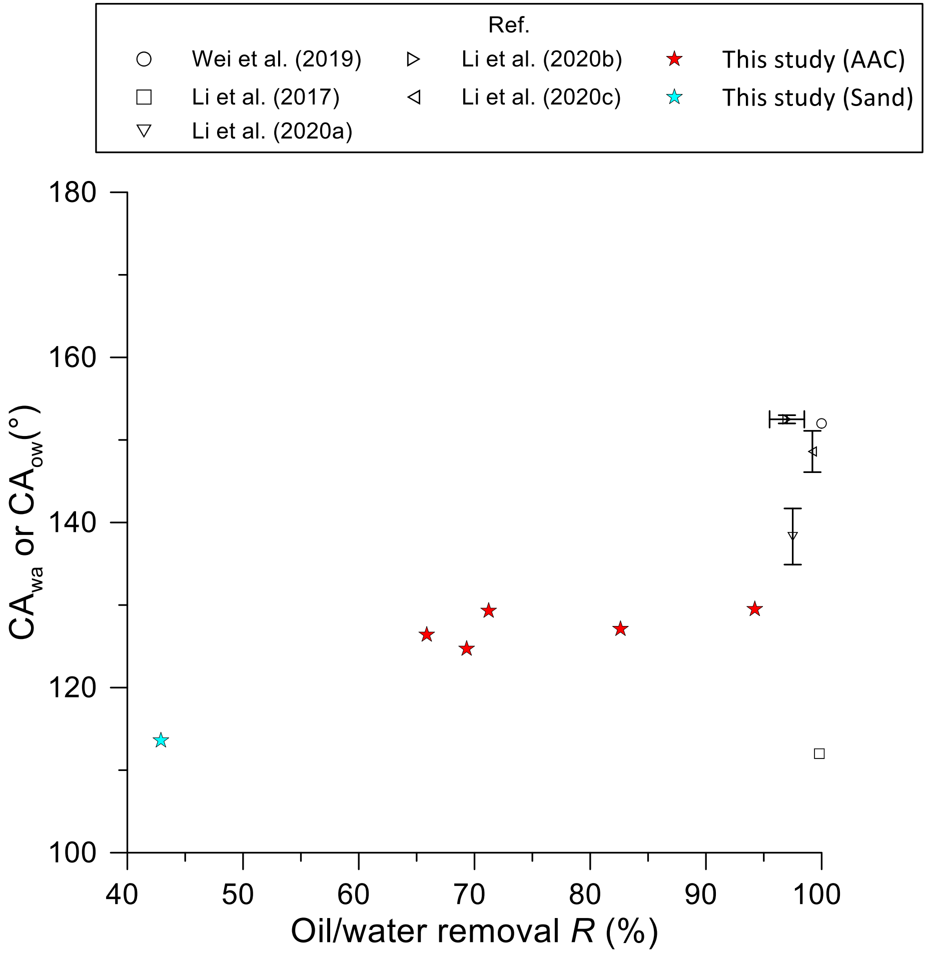

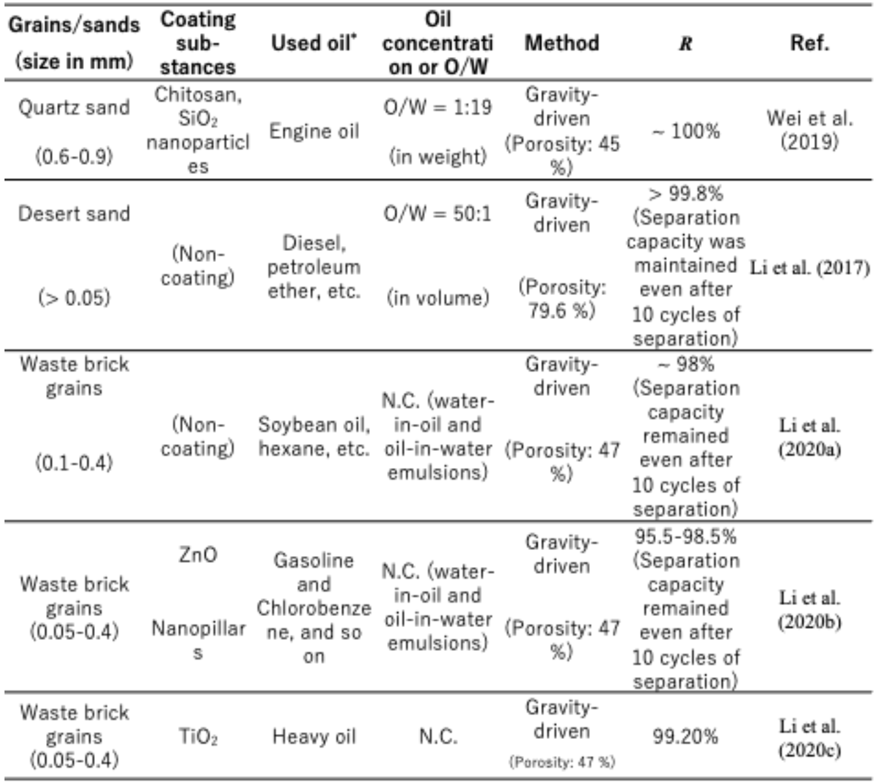

Grains/sands (size in mm)	Coating sub-stances	Used oil*	Oil concentration or O/W	Method	R	Ref.
Quartz sand (0.6-0.9)	Chitosan, SiO_2 nanoparticles	Engine oil	O/W = 1:19 (in weight)	Gravity-driven (Porosity: 45 %)	~ 100%	Wei et al. (2019)
Desert sand (> 0.05)	(Non-coating)	Diesel, petroleum ether, etc.	O/W = 50:1 (in volume)	Gravity-driven (Porosity: 79.6 %)	> 99.8% (Separation capacity was maintained even after 10 cycles of separation)	Li et al. (2017)
Waste brick grains (0.1-0.4)	(Non-coating)	Soybean oil, hexane, etc.	N.C. (water-in-oil and oil-in-water emulsions)	Gravity-driven (Porosity: 47 %)	~ 98% (Separation capacity remained even after 10 cycles of separation)	Li et al. (2020a)
Waste brick grains (0.05-0.4)	ZnO Nanopillars	Gasoline and Chlorobenzene, and so on	N.C. (water-in-oil and oil-in-water emulsions)	Gravity-driven (Porosity: 47 %)	95.5-98.5% (Separation capacity remained even after 10 cycles of separation)	Li et al. (2020b)
Waste brick grains (0.05-0.4)	TiO_2	Heavy oil	N.C.	Gravity-driven (Porosity: 47 %)	99.20%	Li et al. (2020c)

Figure 39. Relationship CA_{wa} or CA_{ow} to R in this study and previous study information.

Appendices

Figure 40 shows that XRD patterns for VN-AAC (Kumara et al. 2019) measured by X-Ray Diffraction (XRD-7000, Shimadzu Corporation, Japan). The component list identified based on the XRD patterns is Table 11. Table 12 shows Chemical compositions by Energy Dispersive X-ray fluorescence spectrometer (EDX-7000, Shimadzu Corporation, Japan) analysis of VN-AAC and JP Toyoura Sand (% by weight.).

Table 13-22 shows the filter sand for water supply standards in each country and compares them to the standards in Japan. Table 13 shows that appearance of the filter sand water supply standards in each country. This shows that the standards in each country are not uniform; Appearance seems to be common in that it appears to be strong. Table 14 shows that effective Diameter, D_{10} (mm) of the filter sand water supply standards in each country. This also differs among the various standards, but it is generally between D_{10} = 0.1-1.0. Table 15 shows that Uniformity coefficient, $U_c=D_{60}/D_{10}$ and Max. Diameter and Min. Diameter of the filter sand water supply standards in each country. This shows that for U_c, almost any standard can be applied with U_c = 1.7 or less. Regarding the maximum particle size, only JWWA A 103-2006 and TCXDVN 33:2006 have detailed specifications, while the others do not.

Table 16-17 shows that Wash Turbidity (degree), Specific Gravity and weight (g/cm^3) and Packed density of the filter sand water supply standards in each country. Wash Turbidity is a criterion adopted only in JWWA A 103-2006, and Specific Gravity is ambiguous among the standards, but JWWA A 103-2006 adopts a value of about 2.5. Only BS 12904-2005 shows the packing density.

Table 18 shows Loss on ignition (Loi) (%) and attrition rate or Friability (%) of standards. Loi should be less than 1% overall, and Friability should be less than 3%, although there is a range. Table 19 shows HCl solubility (%) of standards. This is adopted in many standards in various countries, with many standards adopting 5% or less. Table 20 shows SiO_2 (%), Mohs scale, Porosity (%) and Interstitial volume (Hydraulic Chracteristics) of the filter sand water supply standards in each country. Few standards have adopted this standard.

Table 21 shows Leachability and Chemical composition (%). Table 22 shows Thickness of Filter material layer (mm), Filtration speed in normal working (at least 12h) mode (m/h) and Permitted filtration speed in enhanced working (At least 6 h) mode (m/h). These are difficult to compare because of the few standards established.

Table 23 shows that Measurement data of the filter sand water supply standards. This shows that the Sand used in this study meets the standard. However, VN-AAC does not meet the standard for turbidity, etc., and this is an issue. Table 24 shows that Measurement data of the Column leaching test of filter sand water supply standards. From this, it appears that VN-AAC and Sand meet the criteria and are safe to use when water is flushed. They also contain very low levels of heavy metals.

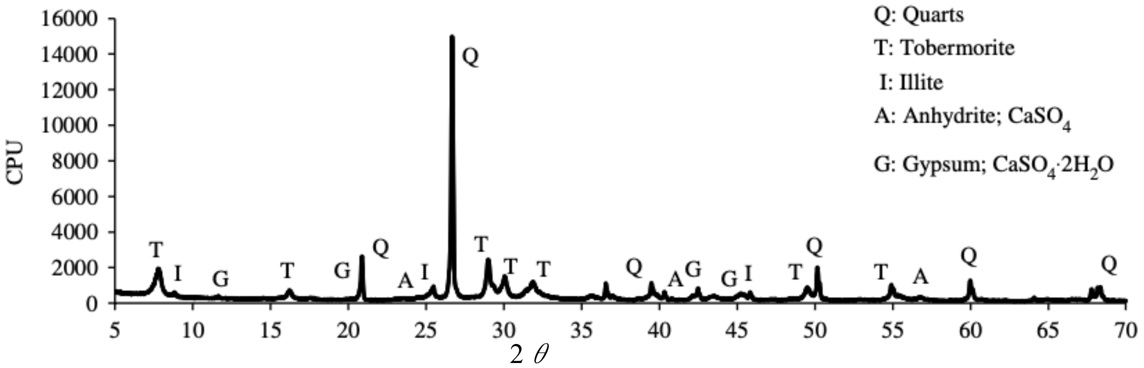

Figure 40. XRD patterns for VN-AAC (Kumara et al. 2019).

Table 11. Component list identified based on the XRD patterns (VN-AAC and JP Toyoura Sand).

Sample	Identified main components	Identified low abundance or unreliable components
VN-AAC	SiO_2 (Q: Quartz)	$Ca_5Si_6(O,OH,F)_{18}\cdot 5H_2O$ (T: Tobermorite) $(K,H_3O)Al_2Si_3AlO_{10}(OH)_2$ (I: Illite) $CaSO_4$ (A: Anhydrite) $CaSO_4 \cdot 2H_2O$ (G: Gypsum)
JP Toyoura Sand	SiO_2 (Q: Quartz)	$KAlSi_3O_8$ (Microcline) $(Na,Ca)Al(Si,Al)_3O_8$ (Albite)

Table 12. Chemical compositions (EDX analysis) of VN-AAC and JP Toyoura Sand (% by weight.).

Sample	SiO_2	CaO	Al_2O_3	Fe_2O_3	K_2O	SO_3	MgO	H_2O	Other
VN-AAC	55.18	28.89	2.76	1.72	0.87	1.77	0.63	7.63	0.55
JP Toyoura Sand	91.51	0.18	4.33	0.37	2.24	0.18	0	0.42	0.77

Table 13. Appearance of the filter sand water supply standards in each country.

Standard	**JWWA A 103-2006**			**BS 12904-2005**	**ANSI / AWWA B100-01**			**TCVN 9068 : 2012**			
	Sand for Rapid Filtration	Sand for Slow Filtration	Filtration gravel for water supply	Silica Sand and Silica Gravel	Silica Sand	Anthracite	High-density sand	Filter Gravel	Quartz Sand	Anthracite	Supporting gravels
Appearance	*1	*1	*2	*3	*4	*5	*6		*7	*8	*9

*1 Such as contaminants, flat or fragile sand, and low content iron sand.

*2 Hard and rounded, with little content of flats, impurities, clay, fragile particles, etc.

*3 Color: Grey/white, yellow or multicoloured granular material. Structure: Crystalline, with a smooth to rough texture. Shape: Spherical or angular

*4 Hard, durable, and dense grains of at least 85 percent siliceous material that will resist degradation during handling and use.

*5 Hard, durable anthracite coal particles of various sizes. Blending of non-anthracite material to meet any portion of this standard is not acceptable

*6 hard, durable, and dense grain garnet, ilmenite, hematite, magnetite, or associated minerals of those ores that will resist degradation during handling.

*7 Main component is silicate oxide, strong and hard, containing no clay

*8 hard, strong granular, has no sand or clay

*9 "Supporting gravels must be the granular that have polygons or globular shape; strong and hard enough to maintain the qualities during the transportation or construction; containing no clay, organic substrates or toxic substrates."

Table 14. Effective Diameter, D_{10} (mm) of the filter sand water supply standards in each country.

Standard	**JWWA A 103-2006**			**BS 12904-2005**	**ANSI / AWWA B100-01**				**TCVN 9068 : 2012**			**TCXDVN 33:2006**				
	Sand for Rapid Filtration	Sand for Slow Filtration	Filtration gravel for water supply	Silica Sand and Silica Gravel	Silica Sand	Anthracite	High-density sand	Filter Gravel	Quartz Sand	Anthracite	Supporting gravels	Quartz Sand: Quick filtering tank with one layer, filter material			Quick filtering tank with two filter material layers	
Effective Diameter, D_{10} (mm)	0.45 to 0.70	0.30 to 0.45	*10	Max. Deviation + 5(%)	0.35 to 0.65	0.6 to 1.6	0.18 to 0.6	*11			*12	0.6 to 0.65	0.75 to 0.8	0.9 to 1.00	0.6 to 0.65	0.9 to 1.1

*10 Shape of gravel particles (%): The shape of the gravel particles should be less than two by mass with a long diameter of 5 times more than the short diameter.

*11 The grains of each layer should be as uniform in size as possible, with the ratio of maximum particle size to minimum particle size not greater than 2. The minimum particle size of the top layer of fine gravel should be four to four-and-a-half times the effective size of the finest filter media to be retained. From layer to layer, the ratio of maximum particle size of the coarser layer should not be greater than four times the minimum particle size of the finer layer. The gravel of the bottom layer should be coarse enough to prevent its displacement by the jets of air or water emerging from the orifices of the underdrain system. The minimum particle size of the lowest layer should be at least two times the size of the underdrain openings.

*12 "Gravels which have broken surface or rifts must not exceed 25% of the sample total weight. The grain which have flat shape or too long (the length is greater than 5 times of the width) must not exceed 2% of the sample total weight."

Table 15. Continued.

Standard	**Indian Standard- IS : 8419 (Part I) - 1977**		**(Brandt et al. 2017)**		**WHO**
	Filter Sand	Filter Gravel	Typical Rapid Gravity Filters (Quartz Sands)	Slow Sand Filteration	Filter Sand
Effective Diameter, D_{10} (mm)	0.15-0.30	-	0.63-0.85 mm (Typical, Bed depth= 0.7 m Fine sand: 0.6 to 1.18 mm) 0.54-0.71 mm (Typical, Bed depth= 0.5 m Fine sand: 0.5 to 1.00 mm)	0.3	0.15-0.35

Table 15. Uniformity cofficient, $U_c=D_{60}/D_{10}$ and Max. Diamter and Min Diamter of the filter sand water supply standards in each country.

Standard	**JWWA A 103-2006**			**BS 12904-2005**	**ANSI / AWWA B100-01**				**TCXDVN 33:2006**					**Indian Standard - IS : 8419 (Part I) - 1977**	**(Brandt et al. 2017)**		**WHO**
	Sand for Rapid Filtration	Sand for Slow Filtration	Filtration gravel for water supply	Silica Sand and Silica Gravel	Silica Sand	Anthracite	High-density sand	Filter Gravel	Quartz Sand: Quick filtering tank with one layer, filter material			Quick filtering tank with two filter material layers		Filter Sand	Typical Rapid Gravity Filters (Quartz Sands)	Slow Sand Filtration	
Uniformity cofficient, $U_c=D_{60}/D_{10}$	<1.7	<2.0	*13	<1.5	1.7 or less	1.7 or less	2.2 or less	*11	1.5 to 1.7	1.3 to 1.5	1.2 to 1.4	1.5 to 1.7	1.5 to 1.7	3 to 5	1.5	2.36	1.5 to 3 (preferably < 2)
Max. Diamter (mm)	<2.0	<2.0							1.25	1.6	2	1.2	1.8				
Min. Diameter (mm)	>0.3	>0.18							0.5	0.7	0.8	0.5	0.8			0.4	0.21

*13 Particle size of mass ratio (%): The total particle size is the addition of the mass ratio of particles with diameters less than or equal to the design minimum diameter, and particles with diameters greater than or equal to the design maximum diameter for each layer of the filtered gravel shall be less than or equal to 15.

Table 16. Wash Turbidity (degree), Specific Gravity and weight (g/cm^3) of the filter sand water supply standards in each country.

Standard	**JWWA A 103-2006**			**ANSI / AWWA B100-01**				**TCVN 9068 : 2012**			**Indian Standard- IS : 8419 (Part I) - 1977**	**(Brandt et al. 2017)**
	Sand for Rapid Filtration	Sand for Slow Filtration	Filtration gravel for water supply	Silica Sand	Anthracite	High-density sand	Filter Gravel	Quartz Sand	Anthracite	Supporting gravels	Typical Rapid Gravity Filters (Quartz Sands)	Slow Sand Filtration
Wash Turbidity (degree)	<30	<30										
Specific Gravity (g/cm^3)	2.57 to 2.67	>2.5 (Surface dry and saturation)		> 2.5	> 1.4	> 3.8					2.6 to 2.7	
Specific weight (g/cm^3)	-	-						> 2.5	> 1.4	> 2.5		1.56

Table 17. Bulk Density - Loose (g/cm^3), Bulk Density - Packed (g/cm^3), Particle Density - Dry and wet (g/cm^3) and Absolute Density (g/cm^3) of the filter sand water supply standards in each country.

Standard	**BS 12904-2005**
	Silica Sand and Silica Gravel
Bulk Density - Loose (g/cm^3)	1.4 to 1.7
Bulk Density - Packed (g/cm^3)	1.5 to 1.9
Particle Density - Dry and wet (g/cm^3)	2.5 to 2.8
Absolute Density (g/cm^3)	2.5 to 2.8

Table 18. Loss on ignition (%) and attrition rate or Friability (%) of the filter sand water supply standards in each country.

Standard	**JWWA A 103-2006**		**TCVN 9068 : 2012**		**Indian Standard- IS : 8419 (Part I) - 1977**		**(Brandt et al. 2017)**
	Sand for Rapid Filtration	Sand for Slow Filtration	Quartz Sand	Anthracite	Filter Sand	Filter Gravel	Typical Rapid Gravity Filters (Quartz Sands)
Loss on ignition (%)	<1.3 (revised); previously, it was less than 0.75%		< 0.75		< 0.7%	< 0.7%	<2%
Attrition rate or Friability (%)	Less than 3.0 (The sand should be tested for friability to ensure that washing operations do not produce fines.)		< 15 % at 750 collision times for 15 min;	< 25 % at 1500 collision times for 30 min.			

Table 19. HCl solubility (%) of the filter sand water supply standards in each country.

Standard	**JWWA A 103-2006**			**BS 12904-2005**	**ANSI / AWWA B100-01**				**TCVN 9068 : 2012**			**Indian Standard- IS : 8419 (Part I) - 1977**		**(Brandt et al. 2017)**	**WHO**
	Sand for Rapid Filteration	Sand for Slow Filteration	Filtration gravel for water supply	Silica Sand and Silica Gravel	Silica Sand	Anthracite	High-density sand	Filter Gravel	Quartz Sand: Quick filtering tank with one layer, filter material	Quick filtering tank with two filter material layers	Supporting gravels	Filter Sand	Filter Gravel	Typical Rapid Gravity Filters (Quartz Sands)	Filter Sand
HCl solubility (%)	<3.5		<3.5	<2 (Type1,2) <5(Type3: d_{10}<2 mm) <10(Type4: d_{10}>2 mm)	<5				<5		<5 (2.5mm), <17.5 (2.5 to 25mm), <25 (bigger than 25mm)	<5 %	a) <5% b) 10 %	<2 %	<5 %

Table 20. SiO_2 (%), Mohs scale, Porosity (%) and Interstitial volume (Hydraulic Chracteristics) of the filter sand water supply standards in each country.

Standard	**BS 12904-2005**	**BS 12904-2005**	**ANSI / AWWA B100-01**				**TCVN 9068 : 2012**		
	Silica Sand and Silica Gravel	Silica	Silica Sand	Anthracite	High-density sand	Filter Gravel	Quartz Sand: Quick filtering tank with one layer, filter material	Quick filtering tank with two filter material layers	Supporting gravels
SiO_2 (%)	>96 (Type1) >80 (Type2) >80(Type3: d_{10}<2 mm) >80(Type3: d_{10}>2 mm)	Silica							
Mohs scale				> 2.7					
Porosity (%)								> 50%	
Interstitial volume (Hydraulic Chracteristics)		0.4 (V/V)							

Table 21. Leachability and Chemical composition (%) of the filter sand water supply standards in each country.

Standard		**JWWA A 103-2006**			**BS 12904-2005**		
		Sand for Rapid Filtration	Sand for Slow Filtration	Filtration gravel for water supply	Silica Sand and Silica Gravel		
Leachability	Taste	Not abnormal					
	Odor	Not abnormal					
	Chromaticity (degree)	<0.5					
	Turbidity (degree)	<0.2					
	Iron and its compounds (mg/L)	<0.03					
	Manganese and its compounds (mg/L)	<0.005					
Chemical composition (%)	Al_2O_3	-			<3 (Type1)	<13 (Type2)	<13 (Type3)
	Fe_2O_3				<2 (Type1)	<10 (Type2)	<2 (Type3)
	CaO				<1.5 (Type1)	<1 (Type2)	<5 (Type3)
	K_2O				<2 (Type1)	<4 (Type2)	<1 (Type3)
	Na_2O				<1.5 (Type1)	<2 (Type2)	<1 (Type3)

Table 22. Thickness of Filter material layer (mm), Filtration speed in normal working (at least 12h) mode (m/h) and Permitted filtration speed in enhanced working (At least 6 h) mode (m/h) of the filter sand water supply standards in each country.

Standard	**TCXDVN 33:2006**				
	Quartz Sand: Quick filtering tank with one layer, filter material			Quick filtering tank with two filter material layers	
Thickness of Filter material layer (mm)	700-800	1300-1500	1800-2000	Quartz sand 700-800	Anthracite coal 400-500
Filtration speed in normal working (at least 12h) mode (m/h)	5 to 6	6 to 8	8 to 10	7 to 10	7 to 10
Permitted filtration speed in enhanced working (At least 6 h) mode (m/h)	6 to7.5	7 to 9.5	10 to 12	8.5 to 12	8.5 to 12

Table 23. Measurement data of the filter sand water supply standards.

Sample	Particle size (mm)	Turbidity	G_s	LOI (%)	Attrition rate or Friability	HCl solubility (%)
VN-AAC	0.106-0.25	995	2.57	9.2	4.7	46.39
VN-AAC	0.25-0.85	937	2.55	9.5	4.7	49.5
VN-AAC	0.85-2.00	636	2.46	9.4	4.7	44.4
Slow sand	0.18-2.00	27	2.66	0.55	4.8	0.9
Rapid sand	0.30-2.00	20	2.63	0.49	0.9	0.6

Table 24. Measurement data of the Column leaching test of filter sand water supply standards.

Sample	Particle size (mm)	Taste	Smell	Color level	Turbidity	As (mg/L)	Cr^{6+} (mg/L)	Fe (mg/L)	Mn (mg/L)
VN-AAC	0.106-0.25	Unmeasureable	Chemical smell	1.0	ND	0.0031	0.0028	ND	ND
VN-AAC	0.25-0.85	Unmeasureable	Chemical smell	1.0	ND	0.0031	0.0028	ND	ND
VN-AAC	0.85-2.00	Unmeasureable	Chemical smell	0.4	ND	0.0023	0.0015	ND	ND
Slow sand	0.18-2.00	Not abnormal	Not abnormal	0.2	0.1	0.0001	ND	ND	ND
Rapid sand	0.30-2.00	No Problem	No Problem	ND	ND	ND	ND	ND	ND

REFERENCES

TCXDVN 33:2006 CẤP NƯỚC - MẠNG LƯỚI ĐƯỜNG ỐNG VÀ CÔNG TRÌNH TIÊU CHUẨN THIẾT K TIÊU CHUẨN THIẾT KẾ Water Supply - Distribution System and Facilities, (2006).

Decision No. 1216/2012/QD-TTg: Approving the Strategy of the National Environmental Protection until 2020 and Vision to 2030. (2012). Vietnam Retrieved from https://vanbanphapluat.co/decision-no-1216-qd-ttg-approving-the-strategy-for-protecting-the-national

TCVN 9068 : 2012 VẬT LIỆU LỌC DẠNG HẠT DÙNG TRONG XỬ LÝ NƯỚC SẠCH - YÊU CẦU KỸ THUẬT Granular filtering material for water purification - Specifications, (2012).

Decision No.609/2014/QD-TTg, Master Plan on Solid Waste Disposal of Hanoi Capital to 2030, with a Vision to 2050. (2014). Retrieved from https://thuvienphapluat.vn/van-ban/Xay-dung-Do-thi/Quyet-dinh-609-QD-TTg-nam-2014-Quy-hoach-xu-ly-chat-thai-ran-Ha-Noi-den-2030-tam-nhin-2050-227455.aspx

Circular No. 08/2017/TT-BXD, Construction Solid Waste Management; Vietnam. (2017). Vietnam Retrieved from https://thuvienphapluat. vn/van-ban/Xay-dung-Do-thi/Circular-08-2017-TT-BXD-construction-solid-waste-management-357117.aspx

Decision No.491/2018/QD-TTg, Approving Adjustments to National Strategy for General Management of Solid Waste to 2025 with Vision Towards 2050. (2018). Vietnam Retrieved from https://thuvienphapluat.vn/van-ban/Tai-nguyen-Moi-truong/Decision- 491-QD-TTg-approving-adjustments-to-national-strategy-for-general-management-solid-waste-387109.aspx

Agamuthu, P. (2008). Challenges in sustainable management of construction and demolition waste. *Waste Management & Research*, *26*(6), 491-492. https://doi.org/10.1177/0734242X08100096

Akhavan, B., Jarvis, K., & Majewski, P. (2013). Hydrophobic plasma polymer coated silica particles for petroleum hydrocarbon removal. *ACS Appl Mater Interfaces*, *5*(17), 8563-8571. https://doi.org/10.1021/am4020154

Alexanderson, J. (1979). Relations between structure and mechanical properties of autoclaved aerated concrete. *Cement and Concrete Research*, *9*(4), 507-514. https://doi.org/https://doi.org/10.1016/0008-8846(79)90049-8

ANSI/AWWA B100-09, Granular Filter Material, (2010).

Aroni, S. (2014). Autoclaved Aerated Concrete - Properties, Testing and Design. https://public.ebookcentral.proquest.com/choice/publicfullrecord.aspx?p=5378581

Asian Development Bank (ADB). (2000). *Environments in transition: Cambodia, Lao, Thailand, Vietnam. Manila: Asian Development Bank.*

Asian Development Bank (ADB), G. E. F. G., United Nation Environment Programme (UNEP),. (2006). *Vietnam National Environmental Performance Assessment (EPA) Report, National Performance Assessment and Subregional Strategic Environment Framework in the Greater Mekong Subregion*.

Atta, A. M., Abdullah, M. M. S., Al-Lohedan, H. A., & Mohamed, N. H. (2019). Novel Superhydrophobic Sand and Polyurethane Sponge Coated with Silica/Modified Asphaltene Nanoparticles for Rapid Oil Spill Cleanup. *Nanomaterials (Basel)*, *9*(2). https://doi.org/10.3390/nano9020187

Bachmann, J., Guggenberger, G., Baumgartl, T., Ellerbrock, R. H., Urbanek, E., Goebel, M. O., Kaiser, K., Horn, R., & Fischer, W. R. (2008). Physical carbon ‐ sequestration mechanisms under special consideration of soil wettability. *Journal of Plant Nutrition and Soil Science*, *171*(1), 14-26. https://doi.org/10.1002/jpln.200700054

Bachmann, J., Guggenberger, G., Baumgartl, T., Ellerbrock, R. H., Urbanek, E., Goebel, M. O., Kaiser, K., Horn, R., & Fischer, W. R. (2008). Physical carbon ‐ sequestration mechanisms under special consideration of soil wettability. *Journal of Plant Nutrition and Soil Science*, *171*(1), 14-26. https://doi.org/10.1002/jpln.200700054

Bardet, J. P., Jesmani, M., & Jabbari, N. (2014). Permeability and compressibility of wax-coated sands. *Géotechnique*, *64*(5), 341-350. https://doi.org/10.1680/geot.13.P.118

Barrett, E. P., Joyner, L. G., & Halenda, P. P. (1951). The Determination of Pore Volume and Area Distributions in Porous Substances. I. Computations from Nitrogen Isotherms. *Journal of the American Chemical Society*, *73*(1), 373-380. https://doi.org/10.1021/ja01145a126

Bigui, W., Cheng, Y., Jianlin, L., Gang, W., Liang, D., Xiaosan, S., Fuping, W., Hua, L., & Qing, C. (2019). Fabrication of superhydrophilic and underwater superoleophobic quartz sand filter for oil/water separation. *Separation and Purification Technology*, *229*. https://doi.org/10.1016/j.seppur.2019.115808

Bigui, W., Jianlin, L., Gang, W., & Qing, C. (2018). Filtration of oil from oily wastewater via hydrophobic modified quartz sand filter medium. *Journal of Water Reuse and Desalination*, *8*(4), 544-552. https://doi.org/10.2166/wrd.2018.052

Binh Dinh Provincial People’s Committee (PPC). (2016). *Environmental and social impact assessment report on coastal cities sustainable environment project (CCSEP): Quy Nhon City sub-project.* Washington, D.C. : World Bank Group.

Brandt, M. J., Johnson, K. M., Elphinston, A. J., & Ratnayaka, D. D. (2017). Chapter 9 - Water Filtration. In M. J. Brandt, K. M. Johnson, A. J. Elphinston, & D. D. Ratnayaka (Eds.), *Twort's Water Supply (Seventh Edition)* (pp. 367-406). Butterworth-Heinemann. https://doi.org/https://doi.org/10.1016/B978-0-08-100025-0.00009-0

BS EN 12904:2005 Products used for treatment of water intended for human consumption - Silica sand and silica gravel, (2005).

Brunauer, S., Emmett, P. H., & Teller, E. (1938). Adsorption of Gases in Multimolecular Layers. *Journal of the American Chemical Society*, *60*(2), 309-319. https://doi.org/10.1021/ja01269a023

Requirements for flltration equipment
part i filtration media-sand and gravel, (1977).

Celi, L., Schnitzer, M. I., & NÈgre, M. (1997). Analysis of carboxyl groups in soil humic acids by a wet chemical method, fourier-transform infrared spectrophotometry, and solution-state carbon-13 nuclear magnetic resonance. a comparative study. *Soil Science*, *162*, 189-197.

Chakrabarty, B., Ghoshal, A. K., & Purkait, M. K. (2008). Ultrafiltration of stable oil-in-water emulsion by polysulfone membrane. *Journal of Membrane Science*, *325*(1), 427-437. https://doi.org/10.1016/j.memsci.2008.08.007

Chanakya, H. N., Shwetmala, & Ramachandra, T. V. (2017). Nature and extent of unauthorized waste dump sites in and around Bangalore city. *Journal of Material Cycles and Waste Management*, *19*(1), 342-350. https://doi.org/10.1007/s10163-015-0423-6

Chen, L., Wu, Y., & Guo, Z. (2017). Superhydrophobic sand grains structured with aligned Cu(OH) 2 nano-needles for efficient oily water treatment. *Materials & Design*, *135*, 377-384. https://doi.org/10.1016/j.matdes.2017.09.047

Cheng, Y., Wang, L., Faustorilla, V., Megharaj, M., Naidu, R., & Chen, Z. (2017). Integrated electrochemical treatment systems for facilitating the bioremediation of oil spill contaminated soil. *Chemosphere*, *175*, 294-299. https://doi.org/10.1016/j.chemosphere.2017.02.079

da Paz, D. H. F., Lafayette, K. P. V., Holanda, M. J. d. O., Sobral, M. d. C. M., & Costa, L. A. R. d. C. (2020). Assessment of environmental impact risks arising from the illegal dumping of construction waste in Brazil. *Environment, Development and Sustainability*, *22*(3), 2289-2304. https://doi.org/10.1007/s10668-018-0289-6

Do Nam Thang, N. T. C. (2014). Recent development of water environmental management in Vietnam. Water Environment Partnership in Asia (WEPA). Seminar on current situation and future prospect of water environment governance in Asia,

Ellerbrock, R. H., Gerke, H. H., Bachmann, J., & Goebel, M.-O. (2005). Composition of Organic Matter Fractions for Explaining Wettability of Three Forest Soils. *Soil Science Society of America Journal*, *69*(1), 57-66. https://doi.org/https://doi.org/10.2136/sssaj2005.0057

Fan, J., Duan, J., Yu, Z., Wu, D., & Zhu, H. (2016). Oleophobicity of Chitosan/Micron-alumina-Coated Stainless Steel Mesh for Oil/Water Separation. *Water, Air, & Soil Pollution*, *227*(5). https://doi.org/10.1007/s11270-016-2861-8

Freundlich, H. (1922). *Kapillarchemie: eine Darstellung der Chemie der Kolloide und verwandter*

Gebiete. Akademische Verlagsgesellschaft. https://books.google.co.jp/books?id=5qOEAAAAIAAJ

Gerde, J. A., Hammond, E. G., Johnson, L. A., Su, C., Wang, T., & White, P. J. (2020). Soybean Oil. In *Bailey's Industrial Oil and Fat Products* (pp. 1-68). https://doi.org/https://doi.org/10.1002/047167849X.bio041.pub2

Giang, N. H., Tan, N. H., Quang, N. T., Hien, N. X., & Kawamoto, K. (2020). Sustainable management and technologies for recycled construction demolition waste in Vietnam. *IOP Conference Series: Materials Science and Engineering*, *869*(3), 032040. https://doi.org/10.1088/1757-899X/869/3/032040

Gong, Z., Alef, K., Wilke, B. M., & Li, P. (2007). Activated carbon adsorption of PAHs from vegetable oil used in soil remediation. *J Hazard Mater*, *143*(1-2), 372-378. https://doi.org/10.1016/j.jhazmat.2006.09.037

González-Peñaloza, F. A., Zavala, L. M., Jordán, A., Bellinfante, N., Bárcenas-Moreno, G., Mataix-Solera, J., Granged, A. J. P., Granja-Martins, F. M., & Neto-Paixão, H. M. (2013). Water repellency as conditioned by particle size and drying in hydrophobized sand. *Geoderma*, *209-210*, 31-40. https://doi.org/10.1016/j.geoderma.2013.05.022

Gupta, R. K., Dunderdale, G. J., England, M. W., & Hozumi, A. (2017). Oil/water separation techniques: a review of recent progresses and future directions. *Journal of Materials Chemistry A*, *5*(31), 16025-16058. https://doi.org/10.1039/c7ta02070h

Hassanshahian, M., Emtiazi, G., Caruso, G., & Cappello, S. (2014). Bioremediation (bioaugmentation/biostimulation) trials of oil polluted seawater: a mesocosm simulation study. *Mar Environ Res*, *95*, 28-38. https://doi.org/10.1016/j.marenvres.2013.12.010

Huang, J., & Yan, Z. (2018). Adsorption Mechanism of Oil by Resilient Graphene Aerogels from Oil-Water Emulsion. *Langmuir*, *34*(5), 1890-1898. https://doi.org/10.1021/acs.langmuir.7b03866

Huisman, L., & Wood, W. E. (1974). Slow sand filtration / L. Huisman, W. E. Wood. In. Geneva: World Health Organization.

Huu Tam, P. (2019). The Variation Trend of Environmental Quality at Corals in Coastal Areas of Khanh Hoa during 2010 - 2018. *VNU Journal of Science: Earth and Environmental Sciences; Vol 35 No 4*. https://doi.org/10.25073/2588-1094/vnuees.4385

Huynh, B. Q., Kwong, L. H., Kiang, M. V., Chin, E. T., Mohareb, A. M., Jumaan, A. O., Basu, S., Geldsetzer, P., Karaki, F. M., & Rehkopf, D. H. (2021). Public health impacts of an imminent Red Sea oil spill. *Nat Sustain*, *4*(12), 1084-1091. https://doi.org/10.1038/s41893-021-00774-8

Ibarra Torres, C. E., Serrano Quezada, T. E., Kharissova, O. V., Kharisov, B. I., & Gómez de la Fuente, M. I. (2021). Carbon-based aerogels and xerogels: Synthesis, properties, oil sorption capacities, and DFT simulations. *Journal of Environmental Chemical Engineering*, *9*(1).

https://doi.org/10.1016/j.jece.2020.104886

Institute for Global Environmental Strategies (IGES). (2007). Water Resources Management in Ho Chi Minh City, Sustainable Groundwater Management in Asian Cities. In *A final report of Research on Sustainable Water Management Policy* (pp. 69).

Integrated Waste Management Board, C. E. P. A. (2000). *Designing with Vision: A Technical Manual for Materials Choices in Sustainable Construction*. https://p2infohouse.org/ref/34/33883.pdf

Jafarinejad, S. (2017). 6 - Treatment of Oily Wastewater. In S. Jafarinejad (Ed.), *Petroleum Waste Treatment and Pollution Control* (pp. 185-267). Butterworth-Heinemann. https://doi.org/https://doi.org/10.1016/B978-0-12-809243-9.00006-7

Jain, S. N., Garud, V. B., Dawange, S. D., Sonawane, D. D., & Shaikh, E. R. (2020). Sesame (Sesamum indicum) oil cake—industrial waste biomass for sequestration of Basic Blue 26 from aqueous media. *Biomass Conversion and Biorefinery*, *12*(9), 3783-3793. https://doi.org/10.1007/s13399-020-00881-0

Japan International Cooperation Agency (JICA). (2013). *Project completion report on the project for strengthening capacity of water environmental management in Vietnam*.

Japan International Cooperation Agency (JICA). (2019). *Final Report on JICA survey on examination of monitoring methodology for indicator of SDG 6.3.1 in Vietnam.*

Japan Oilseed Processors Association. *Basic Knowledge on Vegetable Oil Vegetable Oils and JAS System*. https://www.oil.or.jp/en/kiso/jas.html

JWWA A 103-1:2006-2 Filter sand for water supply, 18p (2006). https://ci.nii.ac.jp/ncid/BB1361730X

Japanese Geotechnical Society (JGS). (2011). *Geotechnical Test : Basics and Guidance* (2nd edition ed.). Japanese Geotechnical Society (JGS). https://ci.nii.ac.jp/ncid/BB07983074

JIS Z 8801-1: 2019 Test sieves—Part 1: Test sieves of metal wire cloth, (2019).

Jing, H., Lu, S., Ji, L., Li, S., Zhu, B., Guo, J., Sun, J., Cai, L., & Wang, Y. (2022). Magnetic Wakame-Based Biochar/Ni Composites with Enhanced Adsorption Performance for Diesel. *Journal of Renewable Materials*, *10*(12), 3147-3165. https://doi.org/10.32604/jrm.2022.020215

Karatza, Z., Buckman, J., Medero, G. M., & Beckett, C. T. S. (2021). Evolution of meniscus structures in hydrophobic granular systems. *Journal of Hydrology*, *603*. https://doi.org/10.1016/j.jhydrol.2021.126954

Kikuma, J., Tsunashima, M., Ishikawa, T., Matsuno, S.-Y., Ogawa, A., Matsui, K., & Sato, M. (2010). In Situ Time-Resolved X-Ray Diffraction of Tobermorite Formation Process Under Autoclave Condition. *Journal of the American Ceramic Society*, *93*(9), 2667-2674. https://doi.org/10.1111/j.1551-2916.2010.03815.x

Kumara, G. M. P., Kawamoto, K., Saito, T., Hamamoto, S., & Asamoto, S. (2019). Evaluation of Autoclaved Aerated Concrete Fines for Removal of Cd(II) and Pb(II) from Wastewater. *Journal* *of Environmental Engineering*, *145*(11). https://doi.org/10.1061/(asce)ee.1943-7870.0001597

Langmuir, I. (1918). THE ADSORPTION OF GASES ON PLANE SURFACES OF GLASS, MICA AND PLATINUM. *Journal of the American Chemical Society*, *40*(9), 1361-1403. https://doi.org/10.1021/ja02242a004

Leelamanie, D. A. L., Karube, J., & Yoshida, A. (2008). Characterizing water repellency indices: Contact angle and water drop penetration time of hydrophobized sand. *Soil Science and Plant Nutrition*, *54*(2), 179-187. https://doi.org/10.1111/j.1747-0765.2007.00232.x

Li, Z., Wu, J., Yue, X., Qiu, F., Yang, D., & Zhang, T. (2020). Study on the application of waste bricks in emulsified oil-water separation. *Journal of Cleaner Production*, *251*. https://doi.org/10.1016/j.jclepro.2019.119609

Li, Z., Zhang, T., Wang, M., Qiu, F., Yue, X., & Yang, D. (2020). Hierarchical structurized waste brick with opposite wettability for on-demand oil/water separation. *Chemosphere*, *251*, 126348. https://doi.org/10.1016/j.chemosphere.2020.126348

Li, Z., Zhang, T., Wang, Y., Yue, X., Yang, D., & Qiu, F. (2020). Waste-to-resource strategy to fabricate functionalized material from waste brick. *Science of The Total Environment*, *703*. https://doi.org/10.1016/j.scitotenv.2019.135032

Liu, J., Zhu, X., Zhang, H., Wu, F., Wei, B., & Chang, Q. (2018). Superhydrophobic coating on quartz sand filter media for oily wastewater filtration. *Colloids and Surfaces A: Physicochemical and Engineering Aspects*, *553*, 509-514. https://doi.org/10.1016/j.colsurfa.2018.06.007

Liu, L., Wang, L., Song, W., Yang, L., Yin, L., Xia, S., Wang, H., Strong, P. J., & Song, Z. (2018). Crude oil removal from aqueous solution using raw and carbonized Xanthoceras sorbifolia shells. *Environ Sci Pollut Res Int*, *25*(29), 29325-29334. https://doi.org/10.1007/s11356-018-2895-0

Liu, P., Niu, L., Tao, X., Li, X., Zhang, Z., & Yu, L. (2018). Preparation of superhydrophobic-oleophilic quartz sand filter and its application in oil-water separation. *Applied Surface Science*, *447*, 656-663. https://doi.org/10.1016/j.apsusc.2018.04.030

Liu, W., Yang, G., Huang, M., Liang, J., Zeng, B., Fu, C., & Wu, H. (2020). Ultrarobust and Biomimetic Hierarchically Macroporous Ceramic Membrane for Oil–Water Separation Templated by Emulsion-Assisted Self-Assembly Method. *ACS Applied Materials & Interfaces*, *12*(31), 35555-35562. https://doi.org/10.1021/acsami.0c05294

Lockrey, S., Nguyen, H., Crossin, E., & Verghese, K. (2016). Recycling the construction and demolition waste in Vietnam: opportunities and challenges in practice. *Journal of Cleaner Production*, *133*, 757-766. https://doi.org/https://doi.org/10.1016/j.jclepro.2016.05.175

Lu, F., Chen, Y., Liu, N., Cao, Y., Xu, L., Wei, Y., & Feng, L. (2014). A fast and convenient cellulose hydrogel-coated colander for high-efficiency oil–water separation. *RSC Adv.*, *4*(61), 32544-

32548. https://doi.org/10.1039/c4ra04464a

Luu, N. C., Nguyen, L. H., Tran, T. V. N., Isobe, Y., Kawasaki, M., & Kawamoto, K. (2021). Construction and demolition waste illegal dumping: environmental, social and economic impacts assessment for a growing city. *Japanese Geotechnical Society Special Publication*, *9*(4), 148-155. https://doi.org/10.3208/jgssp.v09.cpeg133

Matsuno, A., & Kawamoto, K. (2022). Hydrophobicity/Oleophilicity of Autoclaved Aerated Concrete (AAC) Grains Coated with Oleic and Stearic Acids for Application as Oil/Water Separating Filtration and Adsorbent Materials in Vietnam. *Environments*, *9*(8), 101. https://www.mdpi.com/2076-3298/9/8/101

Matsuno, A., Shin, I., Trong Lam, N., Nguyen Tien, D., Van Tuan, N., Hoang Giang, N., & Ken, K. (2020). Comparison of macropore structures and networks of autoclaved aerated concrete blocks using micro-focus x-ray computed tomography. *GEOMATE Journal*, *19*(71), 160-165. https://geomatejournal.com/geomate/article/view/1019

Matsuno, A., Zafar Muhammad, J., Takeshi, S., Huyen Thi Thanh, D., Pham Thanh, H., Tran Thi Viet, N., & Ken, K. (2021). Oil/water separation techniques using hydrophobized/oleophilized grains: a review of recent studies. *GEOMATE Journal*, *20*(81), 28-34. https://geomatejournal.com/geomate/article/view/180

Medeiros, A. D. L. M. d., Silva Junior, C. J. G. d., Amorim, J. D. P. d., Durval, I. J. B., Costa, A. F. d. S., & Sarubbo, L. A. (2022). Oily Wastewater Treatment: Methods, Challenges, and Trends. *Processes*, *10*(4). https://doi.org/10.3390/pr10040743

Men, X., Ge, B., Li, P., Zhu, X., Shi, X., & Zhang, Z. (2016). Facile fabrication of superhydrophobic sand: Potential advantages for practical application in oil–water separation. *Journal of the Taiwan Institute of Chemical Engineers*, *60*, 651-655. https://doi.org/10.1016/j.jtice.2015.11.015

Ministry Of Natural Resources Environment Vietnam (MoNRE). (2006a). *Viet Nam National Environmental Performance Assessment (EPA) Report.*

Ministry Of Natural Resources Environment Vietnam (MoNRE). (2008). *NATIONAL STATE OF ENVIRONMENT 2008 VIETNAM CRAFT VILLAGE ENVIRONMENT.*

Ministry Of Natural Resources Environment Vietnam (MONRE). (2011). *Report on National Environment: Solid Waste; Ministry of Natural Resources and Environment: Hanoi.*

Ministry Of Natural Resources Environment Vietnam (MoNRE). (2020). *NATIONAL REPORT 2020 PROGRESS OF FIVE-YEAR–IMPLEMENTION OF SUSTAINABLE DEVELOPMENT GOALS.*

Ministry Of Natural Resources Environment Vietnam (MoNRE), World Bank, & DANIDA. (2006b). *Vietnam Environment Monitor 2006: WATER QUALITY IN VIET NAM with a focus on the Cau, Nhue-Day and Dong Nai River Basins.*

Mitra, D., Tai, M. H., Abdullah, E. B., Wang, C.-H., & Neoh, K. G. (2021). Facile fabrication of porous waste-derived carbon-polyethylene terephthalate composite sorbent for separation of free and emulsified oil from water. *Separation and Purification Technology*, *279*. https://doi.org/10.1016/j.seppur.2021.119664

Miyazaki, T., & Nishimura, T. (2011). *Soil Physics Experimental Methods*. University Of Tokyo Press. https://ci.nii.ac.jp/ncid/BB05251177

Mosayebi, E., Azizian, S., & Noei, N. (2020). Preparation of Robust Superhydrophobic Sand by Chemical Vapor Deposition of Polydimethylsiloxane for Oil/Water Separation [https://doi.org/10.1002/mame.202000425]. *Macromolecular Materials and Engineering*, *n/a*(n/a), 2000425. https://doi.org/https://doi.org/10.1002/mame.202000425

Murawski, S. A., Ainsworth, C. H., Gilbert, S., Hollander, D. J., Paris, C. B., Schlüter, M., & Wetzel, D. L. (2020). Introduction to the Volume. In S. A. Murawski, C. H. Ainsworth, S. Gilbert, D. J. Hollander, C. B. Paris, M. Schlüter, & D. L. Wetzel (Eds.), *Scenarios and Responses to Future Deep Oil Spills: Fighting the Next War* (pp. 4-15). Springer International Publishing. https://doi.org/10.1007/978-3-030-12963-7_1

News, A. B. (2020). *Thawing permafrost caused fuel spill in Russian Arctic 'Pandora's box' to open*.

Nghiem, H. T., Tran, V. C., Hoa, P. D., Kieu, T. S., & Giang, N. H. (2020). Flow of waste and a method for prediction of demolition waste generation from buildings – A case study in Hanoi, Vietnam. *IOP Conference Series: Materials Science and Engineering*, *869*(4), 042035. https://doi.org/10.1088/1757-899X/869/4/042035

Nguyen, H. G., Nguyen, D. T., Nghiem, H. T., Tran, V. C., Kato, A., Matsuno, A., Isobe, Y., Kawasaki, M., & Kawamoto, K. (2021). Current Management Condition and Waste Composition Characteristics of Construction and Demolition Waste Landfills in Hanoi of Vietnam. *Sustainability*, *13*(18), 10148. https://www.mdpi.com/2071-1050/13/18/10148

NGUYEN Hoang Anh. (2020). Wastewater management and treatment in urban areas in Viet Nam. 1st International Workshop on Water Environment Partnership in Asia (WEPA),

Nguyen Trong, L., Asamoto, S., & Matsui, K. (2018). Sorption isotherm and length change behavior of autoclaved aerated concrete. *Cement and Concrete Composites*, *94*, 136-144. https://doi.org/10.1016/j.cemconcomp.2018.09.003

Nguyen Van, T., Tong Ton, K., Dang Thi Thanh, H., Tran Thi Viet, N., Nguyen Hoang, G., Nguyen Tien, D., Yugo, I., Tomonori, I., & Ken, K. (2018). Current status of construction and demolition waste management in vietnam: challenges and opportunities. *GEOMATE Journal*, *15*(52), 23-29. https://geomatejournal.com/geomate/article/view/757

Oliveira, L., Saleem, J., Bazargan, A., Duarte, J., McKay, G., & Meili, L. (2021). Sorption as a rapidly response for oil spill accidents: A material and mechanistic approach. *J Hazard Mater*, *407*, 124842. https://doi.org/10.1016/j.jhazmat.2020.124842

Organization for Economic Co-Operation and Development Publications (OECD). (2000). *Guidelines for the testing of chemicals*.

Pacheco-Torgal, F. (2020). 1 - Introduction to advances in construction and demolition waste. In F. Pacheco-Torgal, Y. Ding, F. Colangelo, R. Tuladhar, & A. Koutamanis (Eds.), *Advances in Construction and Demolition Waste Recycling* (pp. 1-10). Woodhead Publishing. https://doi.org/https://doi.org/10.1016/B978-0-12-819055-5.00001-2

Parolo, M. E., Savini, M. C., & Loewy, R. M. (2017). Characterization of soil organic matter by FT-IR spectroscopy and its relationship with chlorpyrifos sorption. *J Environ Manage*, *196*, 316-322. https://doi.org/10.1016/j.jenvman.2017.03.018

Pintor, A. M. A., Vilar, V. J. P., Botelho, C. M. S., & Boaventura, R. A. R. (2016). Oil and grease removal from wastewaters: Sorption treatment as an alternative to state-of-the-art technologies. A critical review. *Chemical Engineering Journal*, *297*, 229-255. https://doi.org/10.1016/j.cej.2016.03.121

Pollution Control Department, V. P. (2009). *Report on project for building the wastewater pollution control action plan in Hanoi, Hai Phong and Ho Chi Minh city*.

Qu, M., Yuan, M., He, J., Xue, M., Ma, X., Hou, L., Zhang, T., Liu, X., & He, J. (2018). Substrate-versatile approach to multifunctional superamphiphobic coatings with mechanical durable property from quartz sand. *Surface and Coatings Technology*, *352*, 191-200. https://doi.org/10.1016/j.surfcoat.2018.08.018

Sachs, J., Kroll, C., Lafortune, G., Fuller, G., & Woelm, F. (2022). *Sustainable development report 2022*. Cambridge University Press.

Shi, G., Shen, Y., Mu, P., Wang, Q., Yang, Y., Ma, S., & Li, J. (2020). Effective separation of surfactant-stabilized crude oil-in-water emulsions by using waste brick powder-coated membranes under corrosive conditions. *Green Chemistry*, *22*(4), 1345-1352. https://doi.org/10.1039/c9gc04178h

Stewart, M., & Arnold, K. (2009). Chapter 1 - Crude Oil Treating Systems. In M. Stewart & K. Arnold (Eds.), *Emulsions and Oil Treating Equipment* (pp. 1-80). Gulf Professional Publishing. https://doi.org/https://doi.org/10.1016/B978-0-7506-8970-0.00001-3

Subedi, S., Kawamoto, K., Jayarathna, L., Vithanage, M., Moldrup, P., Wollesen de Jonge, L., & Komatsu, T. (2012). Characterizing Time-Dependent Contact Angles for Sands Hydrophobized with Oleic and Stearic Acids. *Vadose Zone Journal*, *11*(1). https://doi.org/10.2136/vzj2011.0055

Tada, S. (1983). Microstructural approach to properties of moist cellular concrete. *Autoclaved Aerated Concrete-Moisture and Properties*.

Tam, P. H. (2018). Coastal Seawater Quality from Data at South Vietnam Monitoring Stations during 2013 - 2017. *VNU Journal of Science: Earth and Environmental Sciences; Vol 34 No 2*.

https://doi.org/10.25073/2588-1094/vnuees.4250

Tarchitzky, J., Lerner, O., Shani, U., Arye, G., Lowengart-Aycicegi, A., Brener, A., & Chen, Y. (2007). Water distribution pattern in treated wastewater irrigated soils: hydrophobicity effect. *European Journal of Soil Science*, *58*(3), 573-588. https://doi.org/10.1111/j.1365-2389.2006.00845.x

Tarchitzky, J., Lerner, O., Shani, U., Arye, G., Lowengart-Aycicegi, A., Brener, A., & Chen, Y. (2007). Water distribution pattern in treated wastewater irrigated soils: hydrophobicity effect. *European Journal of Soil Science*, *58*(3), 573-588. https://doi.org/10.1111/j.1365-2389.2006.00845.x

Tasumi, M., & The Spectroscopical Society of Japan. (2012). *Infrared Spectroscopy measurement method : Basics and latest methods*. S.T. Japan. https://ci.nii.ac.jp/ncid/BB09055534

Thai, H. N., Kawamoto, K., Nguyen, H. G., Sakaki, T., Komatsu, T., & Moldrup, P. (2022). Measurements and Modeling of Thermal Conductivity of Recycled Aggregates from Concrete, Clay Brick, and Their Mixtures with Autoclaved Aerated Concrete Grains. *Sustainability*, *14*(4). https://doi.org/10.3390/su14042417

Thai, N. T. K. (2009). Hazardous industrial waste management in Vietnam: current status and future direction. *Journal of Material Cycles and Waste Management*, *11*(3), 258-262. https://doi.org/10.1007/s10163-009-0239-3

Thanh Giao, N., Kim Anh, P., & Thi Hong Nhien, H. (2021). Spatiotemporal Analysis of Surface Water Quality in Dong Thap Province, Vietnam Using Water Quality Index and Statistical Approaches. *Water*, *13*(3). https://doi.org/10.3390/w13030336

The Chemical Daily. (2010). *15710 chemical products*. The Chemical Daily Co., Ltd. https://ci.nii.ac.jp/ncid/BB00874434

trường, V. B. t. n. v. m., Resources, V. M. o. N., Environment, Bank, W., & DANIDA. (2003). *Vietnam Environment Monitor 2003: Water*. World Bank. https://books.google.co.jp/books?id=jhG7AAAAIAAJ

United Nations Statistics Division (UNSD). (2019). *Value Added by Economic Activity National Account Section*. https://unstats.un.org/unsd/snaama/Basic

United States. Environmental Protection Agency (EPA) Office of Wastewater Management. (2010). *National Pollutant Discharge Elimination System (NPDES) Permit Writers' Manual*. US Environmental Protection Agency, Office of Water.

van Boggelen, W., & van Boggelen, J. (2018). Sustainable building solutions with new generation autoclaved aerated concrete panel applications. *ce/papers*, *2*(4), 513-525. https://doi.org/10.1002/cepa.825

Vinh, L. T., & Tam, P. H. (2017). Water quality at Rach Gia monitoring station (1997-2015). *Vietnam Journal of Marine Science and Technology*, *17*(2), 222-231. https://doi.org/10.15625/1859-3097/7951

Voelkner, A., Holthusen, D., Ellerbrock, R. H., & Horn, R. (2015). Quantity of Hydrophobic Functional CH-Groups – Decisive for Soil Water Repellency Caused by Digestate Amendment. *International Agrophysics*, *29*(2), 247-255. https://doi.org/10.1515/intag-2015-0024

Walker, A. H. (2017). Chapter 1 - Oil Spills and Risk Perceptions. In M. Fingas (Ed.), *Oil Spill Science and Technology (Second Edition)* (pp. 1-70). Gulf Professional Publishing. https://doi.org/https://doi.org/10.1016/B978-0-12-809413-6.00001-1

Wang, B., Liang, W., Guo, Z., & Liu, W. (2015). Biomimetic super-lyophobic and super-lyophilic materials applied for oil/water separation: a new strategy beyond nature. *Chem Soc Rev*, *44*(1), 336-361. https://doi.org/10.1039/c4cs00220b

Wang, Z., Elimelech, M., & Lin, S. (2016). Environmental Applications of Interfacial Materials with Special Wettability. *Environ Sci Technol*, *50*(5), 2132-2150. https://doi.org/10.1021/acs.est.5b04351

Wijewardana, N. S., Kawamoto, K., Moldrup, P., Komatsu, T., Kurukulasuriya, L. C., & Priyankara, N. H. (2015). Characterization of water repellency for hydrophobized grains with different geometries and sizes. *Environmental Earth Sciences*, *74*(7), 5525-5539. https://doi.org/10.1007/s12665-015-4565-6

Wittmann, F. H. (1983). *Autoclaved aerated concrete moisture and properties*. Elsevier Scientific Publishing Co.

WWF. (2018). *WWF REPORT 2018 Textile and Garment Sector in Vietnam: Water Risks and Solutions*.

Xue, Z., Cao, Y., Liu, N., Feng, L., & Jiang, L. (2014). Special wettable materials for oil/water separation. *J. Mater. Chem. A*, *2*(8), 2445-2460. https://doi.org/10.1039/c3ta13397d

Yao, Q., Zhao, P., Li, R., Li, C., Luo, Y., Zhou, G., & Yang, M. (2017). Fabrication of recyclable carbonized asphalt-melamine sponges with high oil-absorption capability. *Journal of Chemical Technology & Biotechnology*, *92*(6), 1415-1420. https://doi.org/10.1002/jctb.5137

Yong, J., Chen, F., Yang, Q., Bian, H., Du, G., Shan, C., Huo, J., Fang, Y., & Hou, X. (2016). Oil‐Water Separation: A Gift from the Desert. *Advanced Materials Interfaces*, *3*(7). https://doi.org/10.1002/admi.201500650

Yong, J., Huo, J., Chen, F., Yang, Q., & Hou, X. (2018). Oil/water separation based on natural materials with super-wettability: recent advances. *Phys Chem Chem Phys*, *20*(39), 25140-25163. https://doi.org/10.1039/c8cp04009e

Yu, L., Han, M., & He, F. (2017). A review of treating oily wastewater. *Arabian Journal of Chemistry*, *10*, S1913-S1922. https://doi.org/10.1016/j.arabjc.2013.07.020

Zhang, S., Lu, F., Tao, L., Liu, N., Gao, C., Feng, L., & Wei, Y. (2013). Bio-inspired anti-oil-fouling chitosan-coated mesh for oil/water separation suitable for broad pH range and hyper-saline environments. *ACS Appl Mater Interfaces*, *5*(22), 11971-11976. https://doi.org/10.1021/am403203q

Zhang, Y., Zhang, Y., Cao, Q., Wang, C., Yang, C., Li, Y., & Zhou, J. (2020). Novel porous oil-water separation material with super-hydrophobicity and super-oleophilicity prepared from beeswax, lignin, and cotton. *Sci Total Environ*, *706*, 135807. https://doi.org/10.1016/j.scitotenv.2019.135807

Zhao, B., Ren, L., Du, Y., & Wang, J. (2020). Eco-friendly separation layers based on waste peanut shell for gravity-driven water-in-oil emulsion separation. *Journal of Cleaner Production*, *255*. https://doi.org/10.1016/j.jclepro.2020.120184